

**Lepton Flavor Violation
and
Physics beyond the Standard Model**

Ryuichiro Kitano

*A dissertation submitted in partial fulfillment of
the requirements for the degree of*

Doctor of Science

*Department of Particle and Nuclear Physics
School of Mathematical and Physical Science
The Graduate University for Advanced Studies*

2001

Abstract

We studied lepton flavor violation in physics beyond the standard model. Especially in the Randall-Sundrum type extra-dimension scenario, we showed that the $\mu \rightarrow e\gamma$ decay branching ratio becomes large. The loop diagrams mediated by Kaluza-Klein modes of the bulk neutrinos, which are introduced so as to generate tiny neutrino masses, are large and we obtained a severe constraint on the mass of the lowest Kaluza-Klein mode i.e. $m_{\text{KK}} \geq 25\text{TeV}$. For the τ lepton physics, we analyzed P and CP violation of τ decays in model independent way. We calculated the differential cross sections of the processes in which one of the pair created τ particles at an e^+e^- collider decays into lepton flavor violating final states e.g. $\tau \rightarrow \mu\gamma$, $\tau \rightarrow 3\mu$, $\tau \rightarrow \mu ee$. Using the correlations between angular distributions of both sides of τ decays, we can obtain information on parity and CP violations of lepton flavor non-conserving interactions. We also studied the muon-electron conversion process in nuclei. With values in this thesis, we can calculate the $\mu - e$ conversion rate in any models for each nucleus. We find that the conversion branching ratio has a tendency that it is larger in the nuclei with moderate atomic number than that in light or heavy nuclei.

Contents

1	Introduction	5
2	Lepton Flavor Violation (Overview)	11
2.1	LFV and physics beyond the standard model	11
2.1.1	What is LFV?	11
2.1.2	LFV in SUSY models	14
2.1.3	LFV in models with extra-dimensions	19
2.2	Studies of LFV processes	21
2.2.1	Model discrimination by angular distribution of LFV decay	21
2.2.2	$\mu - e$ conversion in nuclei	22
2.2.3	Collider signals	23
2.3	Summary	24
3	LFV in the Randall-Sundrum model with bulk neutrinos	29
3.1	Randall-Sundrum model and bulk neutrinos	29
3.2	LFV mediated by Kaluza-Klein modes	32
3.3	Summary	36
4	P and T odd asymmetries in LFV τ decays	37
4.1	General formula for spin correlation	37
4.2	Parity asymmetry in $\tau \rightarrow \mu\gamma$ decay	40
4.3	P and T asymmetries in LFV three body τ decays	49

4.4	$\tau \rightarrow \mu\nu\bar{\nu}\gamma$ process and background suppressions	57
4.5	Summary and Discussion	59
5	Nucleus dependence of muon-electron conversion ratio	61
5.1	Calculation of conversion rate	61
5.2	Nucleus dependence of conversion rate	66
5.3	Calculation in typical cases	74
5.4	Summary	76
6	Conclusions	81
	Acknowledgments	83
A	The Minimal Supersymmetric Standard Model	85
A.1	Notation	85
A.2	SUSY Lagrangian	86
A.3	Particle content	86
A.4	Soft SUSY breaking terms	87
A.5	Renormalization group equations	88
A.6	The mass matrices	91
A.7	The vertices	94
B	The minimal SU(5) SUSY GUT	99
C	The derivation of the general formulae for the spin correlation	105
D	The kinematical functions in LFV τ decays	107

Chapter 1

Introduction

Now theorists are getting into the second phase of the particle physics. The modern particle physics have begun with a powerful tool “quantum field theory” which describes motions, creations, and annihilations of particles and is a consistent theory based on the Lorentz symmetry, the gauge symmetry, and the quantum theory. The prediction of the quantum field theory is verified with a great accuracy, for example in QED processes such as the anomalous magnetic moment of the electron [1, 2]. As an application of the quantum field theory, the standard model has been proposed [3] It is a simple and beautiful model which describes the interactions between the quarks, leptons, and gauge bosons with the gauge group of $SU(3)_C \times SU(2)_L \times U(1)_Y$. The properties of the gauge interactions are successfully confirmed by the LEP experiments [4]. The flavor structure and the CP violation effect in the quark sector are consistently included in the standard model [6, 7] and investigated in experiments [2, 5]. The determination of the mixing and CP phase parameters is one of the important subjects now. This is the first phase of the particle physics including the construction and the test of the standard model.

However, on the other side of such great progress, the standard model can be effective only below the TeV energy range by a theoretical reason. In the standard model, there is a dimensionful parameter which is the mass parameter of the Higgs particle m_H^2 . For the consistency of the theory, the parameter should be of the order of 100 GeV. In the quantum field theory, the values of such parameters are the sum of the bare value defined

at some scale and the quantum corrections. If we take a cut-off scale Λ below which the standard model is good description, the quantum correction to m_H^2 is of the order of Λ^2 . It follows that the bare value should be also of the order of Λ^2 and the m_H is obtained by the subtraction of $m_H^2 = O(\Lambda^2) - O(\Lambda^2)$. From the naturalness point of view, the scale Λ should be at most a few TeV.

We need, therefore, a new theory describing the physics beyond TeV energy region which might be a theory beyond the quantum field theory. Seeking the new physics is the work in the second phase of the particle physics. The condition for being a candidate of the new theory is that the theory is free from a quantum correction of the order of $\tilde{\Lambda}^2$ to the m_H^2 parameter, where $\tilde{\Lambda}$ is the cut-off scale of the new theory. Among models in the quantum field theory, supersymmetry (SUSY) is one of the candidates in which the quantum corrections are almost canceled between boson and fermion loop diagrams and the remained contributions are of order $\log \tilde{\Lambda}^2$ [8]. The cut-off scale of the standard model $\Lambda \sim \text{TeV}$ is identified to the SUSY breaking scale. Interestingly, if the supersymmetric world is realized beyond TeV energy region, the three coupling constants of the $SU(3)_C$, $SU(2)_L$, and $U(1)_Y$ gauge interaction coincide each other at the energy of 10^{16} GeV [9]. This fact strongly supports the Grand Unified Theory (GUT) in which the gauge interactions are unified to a large simple gauge group such as $SU(5)$ [10] so that the quantization of the electric charges of the quarks and leptons are naturally explained. Models with extra-dimensions are also candidates in which the TeV scale is the fundamental scale of the gravitational interaction [11, 12]. These theories are out of the applicable range of the quantum field theory. It is supposed that the standard model particles and interactions are confined in a four dimensional brane in the higher dimensional space. The weakness of the gravity we feel is explained by the large volume of the extra-dimensional space which dilutes the graviton wave function [11], or the localization of the graviton wave function away from our brane by the warped geometry of the fifth dimension [12]. The use of the extra-dimensions provides us many interesting theoretical applications such as self-tuning mechanism of the cosmological constant of our universe [13] and very small

neutrino masses [14, 15]. In such theories, the theory describing the beyond TeV region should include quantum gravity which might be string theories [16] or something unknown theories. We escape from the condition of no $\tilde{\Lambda}^2$ correction with the less knowledge of quantum gravity.

Anyway, the current status of the theoretical particle physics is that we recognize the necessity of the physics beyond the standard model and several attractive models such as SUSY and extra-dimension have been already proposed. One of the important theme now is, therefore, discrimination of the models which appear in high energy. The study of lepton flavor violation (LFV) is one of the most effective methods for this purpose. In the standard model, lepton flavor is approximately conserved because of the smallness of the neutrino masses and the expected branching fractions of LFV processes, e.g. $\mu \rightarrow e\gamma$, $\tau \rightarrow \mu\gamma$, $\mu - e$ conversion in nuclei, are too small to be observable [17, 18]. However, interestingly many new physics include extensions of the lepton sector and such extensions may easily break the symmetry. Therefore, if a LFV process is observed, this is purely the effect of the physics beyond the standard model and the observed quantities such as the branching ratio, angular distribution, etc. have important information on the physics beyond the standard model.

SUSY and extra-dimensional models both include the extension of the lepton sector. In SUSY models, the prediction of the branching fraction of the LFV processes can be close to the current experimental upper bound. In this case, the flavor mixing in the slepton mass matrix is a new source of LFV. Even in the minimal supergravity scenario [19], in which the slepton mass matrix is proportional to the unit matrix at the Planck scale, the renormalization effects due to LFV interactions can induce sizable slepton mixings [20]. For example, such LFV Yukawa interactions exist in SUSY GUT [21–23], SUSY model with right-handed neutrinos [24, 25], and SUSY models with exotic vectorlike leptons [26]. There is another interesting possibility in models with extra dimensions, where the neutrino masses and mixings are obtained from the Yukawa interaction between the ordinary left-handed leptons and the gauge-singlet neutrinos which propagate in the bulk

of extra dimensions [14, 15]. This Yukawa interaction breaks the lepton flavor conservation and the Kaluza-Klein (KK) modes of the bulk neutrinos enhance $\mu \rightarrow e\gamma$ decay, $\tau \rightarrow \mu\gamma$ decay, etc. through the loop diagrams [27, 28].

In the side of experiments, the status of the current and near future experiments for $\mu \rightarrow e\gamma$ and $\mu - e$ conversion search are both prospective. The expected reach of the branching ratios covers wide range of the parameters in models of physics beyond the standard model. The MEGA collaboration has already given an upper bound for the $\mu \rightarrow e\gamma$ decay branching ratio of 1.2×10^{-11} [29] and the new experiments at PSI [30] and JHF [31] are proposed with a sensitivity of 10^{-14} and 10^{-15} , respectively. For the $\mu - e$ conversion, an upper bound for the conversion branching ratio, which is conversion rate divided by the ordinary muon capture rate, in Ti nuclei is 6.1×10^{-13} [32] reported by the SINDRUM II experiment at PSI and now SINDRUM II is running with Au targets. The MECO experiment at Brookhaven [33] and the PRISM experiment at JHF [31] are planned with a sensitivity of 10^{-17} using Al nuclei and 10^{-18} , respectively. In the τ decay, the search for the LFV processes have been done in B-factories. Especially in the $\tau \rightarrow \mu\gamma$ decay, the CLEO collaboration have accomplished to obtain the upper limit of $B(\tau \rightarrow \mu\gamma) < 1.1 \times 10^{-6}$ [34], and the on going experiment at KEKB (the Belle collaboration) have obtained the upper limit of 1.0×10^{-6} from the present data [35]. These values also give severe constraints for the parameters in the models of physics beyond the standard model.

In this thesis, we studied the physics of LFV in detail. This study is useful to both the current experiments of the LFV search and discrimination of the models after the discovery. The theoretical side of LFV physics is reviewed in the next chapter. Especially the branching fraction of the $\mu \rightarrow e\gamma$ decay is calculated in SUSY GUT models and SUSY models with right-handed neutrinos, in which we scan a wide range of the parameter space. LFV in extra-dimension models and the parity violation of the $\mu \rightarrow e\gamma$ decay are also reviewed.

The remained part of this thesis is organized by our original works concerning LFV.

In Chapter 3, we consider a new possibility of LFV in the Randall-Sundrum (RS) type extra-dimension scenario [28]. In the extra-dimension scenario, the introduction of the bulk neutrinos is necessary in order to obtain the tiny neutrino masses [14, 15]. The introduction of bulk fermions in the RS background leads to the existence of the KK modes whose masses are at the electroweak scale in four dimensional effective theory. The effect of the KK modes on the low energy phenomenology is not negligible. We show that the experimental bound of $B(\mu \rightarrow e\gamma)$ gives severe constraints on the mixing between the bulk fermions and neutrinos. If the Yukawa coupling is $O(1)$, the KK modes should be heavier than 25 TeV which means the fine-tuning of the Higgs mass parameter is necessary to reproduce the correct vacuum expectation value (VEV).

In Chapter 4, we discuss the LFV processes of τ decays such as $\tau \rightarrow \mu\gamma$, $\tau \rightarrow 3\mu$, $\tau \rightarrow \mu ee$, taking into account P and T odd asymmetries, based on the work by Y. Okada and the present author [36]. In the $\tau^+\tau^-$ pair production at e^+e^- collision, we can extract information on the spin of the decaying τ particle from the angular distribution of the τ decay products in the opposite side. Using this technique, we can obtain the P and T odd asymmetry defined in the rest frame of τ . The method of the spin correlation has been developed since the days before the discovery of τ particle [37]. There have been many works on spin correlation method in search for anomalous coupling involving τ [38]. We have applied the formalism in order to obtain information on LFV interactions under P and T transformations. We also calculate angular correlation of the process where one of the τ 's decays through $\tau \rightarrow l\nu\bar{\nu}\gamma$ mode. This mode is a background process to the $\tau \rightarrow l\gamma$ search if the neutrinos carry little energy. We show that the angular correlation is useful to identify the background process and the background suppression is effective for $\tau^- \rightarrow \mu_L^- \gamma$ ($\tau^+ \rightarrow \mu_R^+ \gamma$) search.

In Chapter 5, the $\mu - e$ conversion rates in various nuclei are precisely calculated, which is based on the collaboration with M. Koike and Y. Okada [39]. With the values listed in this chapter, one can calculate the accurate conversion ratio in any models. We solve the Dirac equations numerically for the initial state muon and the final state electron

in the Coulomb force, and perform the overlap integrals between the wave functions and the nucleon densities. The results indicate that the conversion branching ratio is larger in the nuclei with moderate numbers of Z than that in the light or heavy nuclei if there is no accidental cancellation between the parameters of the models. Our calculation is useful to distinguishing models of physics beyond the standard model since each model may predict different Z dependences of the conversion ratio. The summary of this thesis is given in Chapter 6.

Chapter 2

Lepton Flavor Violation (Overview)

We review the LFV physics from the theoretical point of view.

2.1 LFV and physics beyond the standard model

2.1.1 What is LFV?

Lepton flavor is a quantum number assigned in each generation of leptons. For example, the electron number one is assigned for the electron and the electron neutrino, and zero for the other leptons i.e. μ , τ , ν_μ , and ν_τ . These quantum numbers are conserved in the standard model if we do not consider the neutrino masses. The Lagrangian for the lepton sector is given by

$$\begin{aligned} \mathcal{L} = & i \sum_{i=e,\mu,\tau} \bar{l}_i \gamma^\mu (\partial_\mu + \frac{i}{2} g_Y B_\mu - \frac{i}{2} g_2 \sigma^a A_\mu^a) P_L l_i + i \sum_{i=e,\mu,\tau} \bar{e}_{Ri} \gamma^\mu (\partial_\mu + i g_Y B_\mu) P_R e_{Ri} \\ & - \sum_{i,j=e,\mu,\tau} f_e^{ij} \{ (\bar{l}_i h) e_{Rj} + \text{h.c.} \} , \end{aligned} \quad (2.1)$$

where the fields l_i and e_{Ri} are the $SU(2)_L$ doublet left-handed lepton fields and the right-handed lepton fields, respectively. B_μ and A_μ^a are the gauge fields of the $U(1)_Y$ and $SU(2)_L$ gauge group, and g_Y and g_2 are the corresponding coupling constants, respectively. This Lagrangian includes all the renormalizable terms allowed by the gauge symmetry of $SU(2)_L$ and $U(1)_Y$. The terms in the second line describe the Yukawa interactions between

the $SU(2)_L$ doublet Higgs field h and lepton fields. The essential point is that we can diagonalize the Yukawa matrix f_e^{ij} by the redefinition of the lepton fields l and e_R . In the basis of the diagonal Yukawa matrix ($f_e^{ij} = f_e^i \delta_{ij}$), there is no interaction term of the inter generation transition so that lepton flavor is conserved. In other words, this Lagrangian possesses a global $U(1)$ symmetry automatically within the particle content and the gauge symmetries of the standard model. As a consequence, the branching ratio of $\mu \rightarrow e\gamma$, $\mu \rightarrow 3e$, $\tau \rightarrow \mu\gamma$, etc. are predicted to be zero exactly because the quantum numbers of the initial and final state are different.

This situation slightly changes when we consider the neutrino masses. In the Lagrangian (2.1), we cannot obtain non-vanishing neutrino masses while the charged leptons become massive by the condensation of the Higgs field. It is thus necessary to extend this minimal standard model. First, we consider the case where the neutrinos have Dirac mass terms which come from the newly introduced Yukawa interaction terms $f_\nu^{ij}(\bar{l}_i h)\nu_{Rj} + \text{h.c.}$ in the Lagrangian. Here ν_{Ri} is the additional gauge singlet field called the right-handed neutrino. These terms are gauge invariant and generate the mass terms of the neutrinos through the $SU(2)_L \times U(1)_Y$ breaking effect. In this case, lepton flavor is no longer conserved since the Yukawa matrices f_ν and f_e cannot be diagonalized simultaneously. However, the effect on LFV in the charged lepton sector is negligible because of the smallness of the neutrino masses [17, 18]. The data from Super-Kamiokande shows that the neutrino masses are at most a few eV [40]. It follows that the Yukawa coupling f_ν is small of order 10^{-12} and the prediction to the branching ratio of the $\mu \rightarrow e\gamma$ decay is at most 10^{-50} [17] which is much smaller than the current experimental upper bound of 1.2×10^{-11} . In the case of the Majorana masses for the neutrinos, the additional terms in the Lagrangian are $\lambda_{ij}(\bar{l}_i h)(l_j h^\dagger) + \text{h.c.}$, where the parameters λ_{ij} have mass dimension of -1 and are of the order of $10^{-14} \text{ GeV}^{-1}$ in order to fit the neutrino masses. These small values of λ_{ij} are naturally explained by the seesaw mechanism [41], in which the $\bar{l}h l h^\dagger$ terms are obtained by integrating out the heavy right-handed neutrinos. Again the LFV effect by the introduction of these terms is negligible because of the small parameters λ_{ij} .

The contribution to the $B(\mu \rightarrow e\gamma)$ is calculated to be at most 10^{-40} [18].

The standard model forbids LFV processes such as $\mu \rightarrow e\gamma$ by symmetry, and the extension of the neutrino mass inclusion does not change this situation so much. However, the importance of LFV is not the verification of the standard model. As we mentioned in the introduction, the LFV processes are very sensitive to physics beyond the standard model which is required from the theoretical point of view. The SUSY theory is one of the most promising candidates describing beyond TeV scale. Since SUSY is a symmetry under the transformation of the boson into the fermion and vice versa, we need superpartners of different statistics for each particles in the standard model. By the symmetry, the properties of the particles and newly introduced their superpartners are almost the same, for example, the same strength of the interactions, the same masses, and the same charges. The minimal embedding of the standard model into the SUSY model is easily done by adding superpartners in the spectrum and making interaction terms (See Appendix A). In the lepton sector, corresponding to the leptons, we introduce the scalar leptons (sleptons) which have the same quantum numbers. In this stage, there is no additional LFV effect to the (non SUSY) standard model since the properties of the slepton interactions are almost the same as the lepton ones as we mentioned above. The interesting point is that the SUSY must be slightly broken because of the fact of non-observation of any superpartners which have the same masses as the known particles. The SUSY breaking terms which are introduced in the Lagrangian can be a new source of LFV as we see later.

Models with extra-dimensions are also interesting candidates for physics beyond the standard model. In such theories, the small neutrino masses are naturally explained by the introduction of the bulk neutrinos instead of the seesaw mechanism which does not work in extra-dimensional theories [14, 15]. The bulk neutrinos are gauge singlet fermion fields and can propagate out of our four-dimensional world. As in the standard model, we introduce the LFV Yukawa interactions between the bulk neutrinos and ordinary leptons in order to obtain the neutrino masses. In the case of the standard model, the effects on the charged lepton are much suppressed because of the smallness of the coupling constants.

However, the situation dramatically changes in the extra-dimensional scenario. In the words of four dimensional effective theory, the existence of the KK modes enhance LFV in the charged lepton sector [27, 28].

Interesting points are not only that there is a large possibility to observe the LFV processes in near future, but also we can extract information on the physics beyond the standard model including SUSY and extra-dimensional models by the analysis of the LFV processes.

2.1.2 LFV in SUSY models

Now we review LFV in SUSY models. As mentioned before, the SUSY invariant Lagrangian does not have LFV terms, namely the SUSY Lagrangian only contains the flavor diagonal terms. LFV comes from the SUSY breaking terms for the slepton fields which are given as follows:

$$\mathcal{L}_{\text{soft}} = -(\tilde{m}_{\tilde{l}}^2)_{ij} \tilde{l}_i^\dagger \tilde{l}_j - (\tilde{m}_{\tilde{e}^c}^2)_{ij} \tilde{e}_i^{c\dagger} \tilde{e}_j^c - (A_e^{ij} H_1 \cdot \tilde{e}_j^c \tilde{l}_i + \text{h.c.}) . \quad (2.2)$$

The indices i, j represent the generation ($i, j = e, \mu, \tau$) and the fields \tilde{l} , \tilde{e}^c , and H_1 are the left-handed sleptons, the right-handed sleptons, and the Higgs field, respectively. (The notation of e^c represents the charge conjugation of e_R .) The source of LFV is the off-diagonal components of the soft mass terms $(\tilde{m}_{\tilde{l}}^2)_{ij}$ and $(\tilde{m}_{\tilde{e}^c}^2)_{ij}$, and the coupling constants of the scalar three point interactions A_e^{ij} .

The terms in eq.(2.2) break SUSY softly by giving the different masses for the bosons and fermions, but, successfully, do not introduce the radiative correction to the Higgs mass parameter of the order of square of the cut-off scale [8]. One of the most interesting scenarios for the nature of the soft terms in eq.(2.2) is the supergravity scenario in which we feel the SUSY breaking only through the gravitational interaction [19]. We do not need a complicated mechanism in this scenario because all the particles have couplings to the gravity. In the minimal version of this scenario, the soft terms in eq.(2.2) are still flavor diagonal and moreover the same for all the scalar particles since the gravitational interaction is uniform for any particles. However, if there is a LFV interaction in the theory

describing between the Planck ($M_P \sim 10^{18}$ GeV) and TeV scale, the renormalization effects induce the off-diagonal terms in the low energy effective Lagrangian.

The first example for such a LFV interaction is in SU(5) GUT models [21–23]. The superpotential, which describes the supersymmetric interactions including Yukawa interactions and scalar potentials, for the matter part of the SU(5) SUSY GUT is given by

$$W = \frac{1}{8} \epsilon_{abcde} (\tilde{y}_u)_{ij} T_i^{ab} T_j^{cd} H^e + (\tilde{y}_d)_{ij} \bar{F}_{ja} T_i^{ab} \bar{H}_b, \quad (2.3)$$

where T and \bar{F} are the matter superfields of $\mathbf{10}$ and $\bar{\mathbf{5}}$ representation of SU(5), respectively, and H and \bar{H} are the Higgs superfields of the $\mathbf{5}$ and $\bar{\mathbf{5}}$ representation. The indices i, j represent the generation ($i, j = 1, 2, 3$), and a, b, c, d, e are the SU(5) indices ($a, b, c, d, e = 1 - 5$). The decomposition of the superfields of T and \bar{F} into the standard model gauge group is shown in Appendix B. The important point is that the superpotential contains LFV terms as follows:

$$W_{\text{LFV}} = -V_{\text{CKM}}^{ji} f_u^j E_i^c U_j^c H_C + f_d^i L_i Q_i \bar{H}_C, \quad (2.4)$$

in the basis where the lepton Yukawa matrix is diagonalized. The coupling constants are determined so that they reproduce the masses and mixing of the quarks. The matrix V_{CKM} is the Cabibbo-Kobayashi-Maskawa matrix [6, 7], and f_u and f_d are the diagonalized up-type and down-type Yukawa matrix, respectively. The superfields E^c , L , U^c , and Q are the right-handed leptons, the left-handed leptons, the right-handed up-type quarks, and the left-handed quarks, respectively. The colored Higgs fields H_C and \bar{H}_C are super heavy fields whose masses are the GUT scale ($M_{\text{GUT}} \sim 10^{16}$ GeV). It follows that these interaction terms are effective in physics beyond the GUT scale. However, the running effect from the Planck scale to the GUT scale induces off-diagonal components of the soft masses for the slepton through the loop diagrams. Especially, from the fact that the Yukawa coupling constant for the top quark f_u^3 is as large as nearly unity, the first terms in eq.(2.4) give sizable contributions to the soft masses of the right-handed sleptons $\tilde{m}_{\tilde{e}^c}$. Figure 2.1 shows one of the loop diagrams which induces the off-diagonal components of

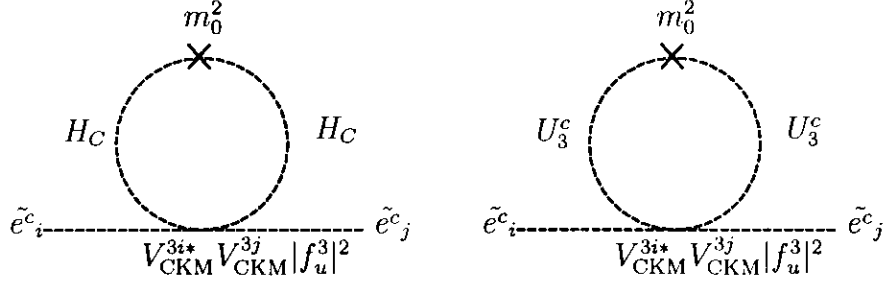


Figure 2.1: The loop diagrams for the off-diagonal components of the right-handed slepton masses in SU(5) SUSY GUT are shown.

soft masses. Approximately, the off-diagonal components are evaluated to be

$$(\tilde{m}_{\tilde{e}^c})_{ij} \simeq -\frac{3}{8\pi} V_{\text{CKM}}^{3i*} V_{\text{CKM}}^{3j} |f_u^3|^2 (3 + |a_0|^2) m_0^2 \log \frac{M_{\text{Pl}}}{M_{\text{GUT}}}, \quad (2.5)$$

where a_0 and m_0 are the universal coupling constant of the scalar three point interactions and universal masses for the scalar particles, respectively. The renormalization equations for the coupling constants and the SUSY breaking parameters in SU(5) SUSY GUT are listed in Appendix B.

Now we evaluate the LFV processes, especially the branching ratio of the $\mu \rightarrow e\gamma$ decay, in SU(5) SUSY GUT models with the minimal supergravity scenario. The effective Lagrangian for the $\mu \rightarrow e\gamma$ decay is given by

$$\mathcal{L} = -\frac{4G_{\text{F}}}{\sqrt{2}} \{m_\mu A_R \bar{\mu} \sigma^{\mu\nu} P_L e F_{\mu\nu} + m_\mu A_L \bar{\mu} \sigma^{\mu\nu} P_R e F_{\mu\nu}\} + \text{h.c.}, \quad (2.6)$$

where G_{F} and m_μ are the Fermi constant and the muon mass, respectively, and $P_{L,R}$ are the projection operators of the chirality. The dimensionless coupling constants $A_{L,R}$ are calculated by the loop diagrams mediated by the neutralinos and charginos as shown in Figure 2.2. The neutralinos and charginos are the fermionic superpartners of the Higgs fields and the gauge bosons. The interaction vertices and mass matrices are listed in Appendix A. With the notation of Appendix A, the coefficients $A_{L,R}$ are calculated as follows [25]:

$$A_R = -\frac{\sqrt{2}}{8m_\mu G_{\text{F}}} (g_R^{(c)*} + g_R^{(n)*}), \quad A_L = A_R|_{R \leftrightarrow L}, \quad (2.7)$$

where the chargino contributions $g_{L,R}^{(c)}$ and the neutralino contributions $g_{L,R}^{(n)}$ are given by

$$g_R^{(c)} = \sum_{A=1,2} \sum_{X=1-3} \frac{-e}{2(4\pi)^2} \times \left[C_{1AX}^{L(e)*} C_{2AX}^{L(e)} \frac{m_\mu}{m_{\tilde{\nu}_X}^2} \frac{-2 - 3x_{AX}^{(c)} + 6x_{AX}^{(c)2} - x_{AX}^{(c)3} - 6x_{AX}^{(c)} \log x_{AX}^{(c)}}{6(1 - x_{AX}^{(c)})^4} + C_{1AX}^{L(e)*} C_{2AX}^{R(e)} \frac{m_{\tilde{\chi}_A^-}}{m_{\tilde{\nu}_X}^2} \frac{3 - 4x_{AX}^{(c)} + x_{AX}^{(c)2} + 2 \log x_{AX}^{(c)}}{(1 - x_{AX}^{(c)})^3} \right], \quad (2.8)$$

$$g_L^{(c)} = g_R^{(c)}|_{L \rightarrow R}, \quad (2.9)$$

and

$$g_R^{(n)} = \sum_{A=1-4} \sum_{X=1-6} \frac{-e}{2(4\pi)^2} \times \left[N_{1AX}^{L(e)*} N_{2AX}^{L(e)} \frac{m_\mu}{m_{\tilde{l}_X}^2} \frac{1 - 6x_{AX}^{(n)} + 3x_{AX}^{(n)2} + 2x_{AX}^{(n)3} - 6x_{AX}^{(n)2} \log x_{AX}^{(n)}}{6(1 - x_{AX}^{(n)})^4} + N_{1AX}^{L(e)*} N_{2AX}^{R(e)} \frac{m_{\tilde{\chi}_A^0}}{m_{\tilde{l}_X}^2} \frac{1 - x_{AX}^{(n)} + 2x_{AX}^{(n)} \log x_{AX}^{(n)}}{(1 - x_{AX}^{(n)})^3} \right], \quad (2.10)$$

$$g_L^{(n)} = g_R^{(n)}|_{L \rightarrow R}. \quad (2.11)$$

Here e (> 0) is the positron charge, and $m_{\tilde{\nu}_X}$, $m_{\tilde{\chi}_A^-}$, $m_{\tilde{l}_X}$, and $m_{\tilde{\chi}_A^0}$ are the masses of the sneutrinos, charginos, charged sleptons, and neutralinos, respectively, and $x_{AX}^{(c)}$ and $x_{AX}^{(n)}$ are defined by $x_{AX}^{(c)} \equiv m_{\tilde{\chi}_A^-}^2/m_{\tilde{\nu}_X}^2$ and $x_{AX}^{(n)} \equiv m_{\tilde{\chi}_A^0}^2/m_{\tilde{l}_X}^2$, respectively.

With the coefficients $A_{L,R}$, the branching ratio is given by

$$B(\mu \rightarrow e\gamma) = 384\pi^2(|A_R|^2 + |A_L|^2). \quad (2.12)$$

We plot $B(\mu \rightarrow e\gamma)$ in Figure 2.3. The horizontal and the vertical axis represent the universal scalar mass m_0 and the gaugino mass $M_{1/2}$ at the Planck scale. We can see in the figures that there are parameter ranges where the branching ratio reaches 10^{-15} . Especially, $B(\mu \rightarrow e\gamma)$ enhances for large $\tan\beta$ which is the ratio of the two VEVs of the

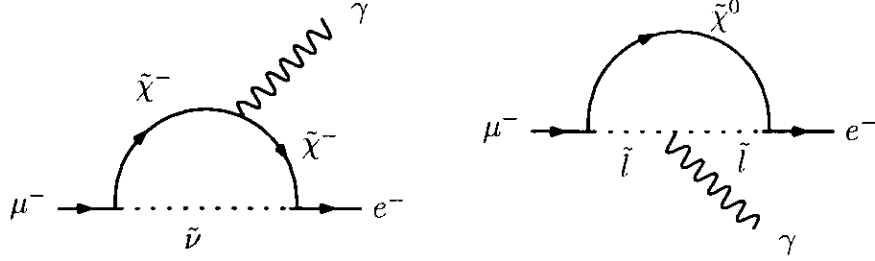


Figure 2.2: The Feynman diagrams for the $\mu \rightarrow e\gamma$ decay in SUSY models are shown.

Higgs fields. The region below the thick line is excluded by the mass bound for the Higgs mass i.e. $m_h > 113.5$ GeV [42]. In the bottom-right area of the figures, $B(\mu \rightarrow e\gamma)$ is very small because of the cancellation between the diagrams [23]. This is one of the typical features in SU(5) SUSY GUT.

Another contribution in SUSY models comes from the effect of the Yukawa interactions between the left-handed lepton doublets and the right-handed neutrinos [24], which are introduced in order to account for the non-vanishing neutrino masses by the seesaw mechanism. The LFV part of the superpotential is given by

$$W_{\text{LFV}} = f_\nu^{ij} H_2 \cdot N_i^c L_j + \frac{1}{2} M_N^{ij} N_i^c N_j^c, \quad (2.13)$$

where N^c are the right-handed neutrino superfields. The neutrino mass matrix is obtained from these terms as follows:

$$m_{\nu ij} = -(f_\nu^T M_N^{-1} f_\nu)_{ij} v_2^2, \quad (2.14)$$

where v_2 is the VEV of the neutral component of the Higgs field H_2 . If we assume the Yukawa coupling constants f_ν to be of order unity, the order of the masses for the right-handed neutrinos M_N are determined as large as 10^{14} GeV by substituting the neutrino masses m_ν . Thus, the LFV interactions in eq.(2.13) give the radiative correction to the the generation mixing of the left-handed sleptons beyond the scale of M_N (See Figure 2.4). An approximate formula for the off-diagonal components of the left-handed slepton

$(\tilde{m}_l^2)_{ij}$ is given by

$$(\tilde{m}_l^2)_{ij} \simeq -\frac{1}{8\pi^2} f_\nu^{ki*} f_\nu^{kj} (3 + |a_0|^2) m_0^2 \log \frac{M_{\text{GUT}}}{M_N}, \quad (2.15)$$

where we put the initial condition of the universal scalar mass at the scale of M_{GUT} . If we assume the right-handed mass matrix M_N is proportional to the unit matrix, i.e. $M_N = \text{diag.}(m_N, m_N, m_N)$, the Yukawa matrix f_ν can be determined as

$$f_\nu^{ij} = \sqrt{\frac{m_N m_\nu^i}{v_2^2}} U_{\text{MNS}}^{ij}, \quad (2.16)$$

where m_ν^i and U_{MNS}^{ij} are the neutrino masses and the Maki-Nakagawa-Sakata (MNS) matrix [43], respectively.

Now we show $B(\mu \rightarrow e\gamma)$ in this model in Figure 2.5, where we choose the large angle MSW solution to the solar neutrino anomaly [44] in the parameters of the neutrino masses and mixing, and take $m_N = 10^{14}$ GeV. For the U_{MNS}^{e3} component of the MNS matrix, which we know only the upper bound of $\lesssim 0.1$ [45], we take the maximum value of 0.1. In this set of the parameters, $B(\mu \rightarrow e\gamma)$ exceeds the current experimental bound of 1.2×10^{-11} in a wide range of the $m_0 - M_{1/2}$ plane, so that the $\mu \rightarrow e\gamma$ experiments have already given a severe constraint on the SUSY models. The parameter region below the thick line is excluded by the constraint of the Higgs mass ($m_h > 113.5$ GeV). Also, the top-left region is excluded by the condition that the lightest superparticle should be neutral from a cosmological reason. In this case the lightest superparticle is scalar τ , and one of the neutralinos is the lightest in the other region.

2.1.3 LFV in models with extra-dimensions

Not only in SUSY models, the LFV processes are also enhanced in models with extra-dimensions [27, 28].

Recently, it was pointed out that the existence of extra-dimensions could be a solution of the hierarchy problem [11, 12]. In the RS model, the electroweak scale is generated from the Planck scale parameters through the non-factorizable metric of the extra-dimension.

In these models, however, it is not easy to explain small neutrino masses suggested by the neutrino oscillation data. In four dimensional theory, the seesaw mechanism is an elegant way of providing such tiny neutrino masses [41]. However, the RS scenario is incompatible with an intermediate scale such as the right-handed Majorana mass scale because all the dimensionful parameters on our brane are suppressed by the exponential factor to electroweak scale. Recently a new mechanism for generating tiny neutrino masses was proposed by Grossman and Neubert [15]. They introduce bulk fermion fields which couple to the lepton doublets with Dirac Yukawa couplings in the same way as right-handed neutrinos. In this scenario, the neutrino Dirac Yukawa couplings are exponentially suppressed in four dimensions because the zero mode wave functions of the bulk fermions are localized on another brane and the tiny Dirac mass terms for neutrinos are generated.

The introduction of bulk fermions in the RS background leads to the existence of KK modes whose masses are at the electroweak scale in four dimensional theory, and the neutrino Dirac Yukawa couplings for these KK modes are not suppressed. Therefore sizable effects may arise in the phenomenology at the electroweak scale [46–48] because of the large mixing between KK modes and neutrinos.

LFV processes reflect such effects. As we see in the next chapter, the effect of the KK modes of the bulk neutrinos on the LFV processes is large through the mediation of the loop diagrams. This model is, therefore, severely constrained.

There is another scenario of the extra-dimension which is so-called the large extra-dimensions [11]. In this scenario, the weakness of the gravity is explained by the wide spreaded wave function of the graviton over the large extra dimensions. The smallness of the neutrino masses can be explained in the same way as gravity. In this scenario, the masses of the KK modes of the neutrinos are of the order of $1/R$ where the R is the large radius of the extra-dimension. It means that the KK modes are light typically of eV order. It follows that the number of the KK modes which mediate the loop diagrams of $\mu \rightarrow e\gamma$ is enormous of order millions, so that this type of models is also severely constrained. The estimation in ref. [27] shows that the fundamental scale of the gravity, which should be of

at most TeV from the naturalness point of view, must be larger than 100 TeV when the existence of two extra-dimensions is assumed.

2.2 Studies of LFV processes

In this section, we review the studies of the LFV processes. The model independent analysis of each LFV process gives a method to distinguish models of physics beyond the standard model.

2.2.1 Model discrimination by angular distribution of LFV decay

For the decay processes, the angular distribution of the particles in the final state have information on the LFV interactions. In the $\mu \rightarrow e\gamma$ decay, the parity breaking quantities of the LFV interactions are obtained by using the decay of the polarized muon [49]. The angular distribution of the $\mu \rightarrow e\gamma$ decay is given by

$$\frac{dB(\mu^+ \rightarrow e^+\gamma)}{d\cos\theta_e} = 384\pi^2(|A_L|^2 + |A_R|^2) [1 + P_\mu A_{\mu \rightarrow e\gamma} \cos\theta_e] \frac{d\cos\theta_e}{2}, \quad (2.17)$$

where

$$A_{\mu \rightarrow e\gamma} = \frac{|A_L|^2 - |A_R|^2}{|A_L|^2 + |A_R|^2}. \quad (2.18)$$

$A_{L,R}$ are the same quantities defined in eq.(2.6), and θ_e is the angle between the direction of the muon polarization and the electron momentum. P_μ is the magnitude of the muon polarization. By using this distribution, we can distinguish the models which have a different parity violating quantity of $A_{\mu \rightarrow e\gamma}$. Interestingly, the models we reviewed in the previous section have characteristic values. In the SU(5) SUSY GUT model, LFV originates from the right-handed slepton mixing. This implies that $A_R \simeq 0$, namely $A_{\mu \rightarrow e\gamma} = 1$. In contrast, SUSY models with right-handed neutrinos predict $A_{\mu \rightarrow e\gamma} = -1$, since the effect of the right-handed neutrinos appears only in left-handed slepton mixing. As we see in the next chapter, the prediction of the models with extra-dimensions is also

$A_{\mu \rightarrow e\gamma} = -1$. This fact of characteristic values of $A_{\mu \rightarrow e\gamma}$ shows that the measurement of this quantity is indeed important.

For the three body decays of the muon of $\mu \rightarrow 3e$, we can define the T-odd quantities. They are also important to extract information on the CP violating phases in the LFV interactions [49].

In the LFV τ decay, such as $\tau \rightarrow \mu\gamma$, $\tau \rightarrow e\gamma$, $\tau \rightarrow 3\mu$, etc. , we can also define the P and T-odd quantities in the same way [36]. In experiments, τ 's are created in e^+e^- colliders by the pair production of the QED process. In this case, the polarization of the τ can be measured by the analysis of the τ decay in the other side. The detailed analysis are given in Chapter 4.

2.2.2 $\mu - e$ conversion in nuclei

The $\mu - e$ conversion in nuclei is one of the most prospective processes for the discovery in the current and the near future experimental circumstance. In this process, the nucleus dependence of the conversion ratio is important for discrimination of the models and also for the planning of experiments. In order to know that the precise calculation is necessary.

There have been several calculations of conversion rate. Weinberg and Feinberg have calculated in the case where the conversion occurs through the photonic interactions ($\mu - e - \gamma$ vertex) [50]. In this calculation, they used several approximations which the muon wave function is taken to be constant in nuclei and plane wave is used for the outgoing electron. The plane wave treatment of the electron is a good approximation only for the light nuclei because the Coulomb distortion effect on the electron wave function is large for heavy targets. Shanker improved these points by solving the Dirac equations for the muon and electron wave functions in the electric potential of the nuclei [51]. The calculation was carried out about all the interactions including the photonic and four-fermi operators in the effective Lagrangian, but the treatment of the photonic dipole operator was incomplete because he used an approximate value for the off-shellness of the photon ($q^2 = -m_\mu^2$) and non-relativistic approximation in the amplitude level. Recently,

Czarnecki *et al.* presented calculation in which the off-shell photon is correctly treated as an electric field in the nuclei and listed the value of the conversion rate for Al, Ti, and Pb targets in the case where the photonic dipole operators are dominated [52]. Kosmas also calculated the conversion rate by solving the Schrödinger equation for the muon wave function and pointed out that the binding energy of the muon is important [53].

In Chapter 5, we complete the calculation of the $\mu - e$ conversion rate in the nuclei with wide range of atomic numbers by the method of Czarnecki *et al.* We take into account all the operators for the $\mu - e$ transition.

2.2.3 Collider signals

If we assume SUSY, the LFV decays of the SUSY particles are also interesting signals. The SUSY particles are expected to be discovered in the experiment of the Large Hadron Collider (LHC) at CERN. Agash *et al.* studied the LFV $\tilde{\chi}_2^0$ decays, mainly $\tilde{\chi}_2^0 \tilde{\chi}_2^0 \rightarrow e\mu\mu\mu + X$, and pointed out the possibility of the LFV discovery by using the parameter point of so-called Point 5 i.e. $m_0 = 100$, $M_{1/2} = 300$, $a_0 = 3$, and $\tan\beta = 2.1$ [54]. Recently, Hinchliffe *et al.* considered the $\tilde{\chi}_2^0 \rightarrow \tilde{\tau}_1\tau \rightarrow \tau\mu\tilde{\chi}_1^0$ mode and concluded that it is also observable in a wide parameter range [55].

Hisano, Nojiri, and the present author considered another possibility of the $\mu - e$ transition mode of $\tilde{\chi}_2^0 \rightarrow \tilde{l}_R l \rightarrow e\mu\tilde{\chi}_1^0$, where l (\tilde{l}_R) stands for the electron or the muon (right-handed selectron and smuon) [56]. The reach in the parameter space of the SUSY models is shown in Figure 2.6. The slepton mixing is taken to be $\sin 2\theta = 0.5$ and $\Delta m = 1$ GeV for the right-handed sleptons. The bottom-right region is not allowed kinematically and the top-right region is suppressed statistically by the domination of $\tilde{\chi}_2^0 \rightarrow h\tilde{\chi}_1^0$ mode. The top-left region is also suppressed by the $\tilde{\chi}^0 \rightarrow \tilde{l}_L l$ modes. In this analysis, we investigate the parameter point of $\mu = M_2$, where μ and M_2 are the mass parameters of the Higgsino and the SU(2) gaugino, respectively, in addition to the point where the minimal supergravity relation $\mu \simeq 1.5M_2$ is satisfied.

2.3 Summary

We reviewed LFV in models of physics beyond the standard model, and the studies of the LFV processes for the purpose of the extraction of information on the nature of LFV.

In SUSY models, LFV originates from the slepton mixing. $B(\mu \rightarrow e\gamma)$ is calculated in the wide range of the SUSY parameters and plotted. LFV in models with extra-dimensions is also sizable. We investigate this point in detail in the next chapter.

For the LFV decays of the muon and τ , P and T-odd asymmetry are the useful information on the high-energy models. The use of the polarized muon enables us to measure such quantities in the muon decay. In the τ decay, we do not necessitate an additional experimental set-up in the experiment at e^+e^- colliders, since the angular distribution of the decay products from the other side τ have information on the spin of τ which decays into LFV final states. The detailed analysis are given in Chapter 4.

Although the $\mu - e$ conversion in nuclei is extremely important, the complete calculation have not done yet. We, thus, calculated the conversion ratio taking into account the effects of the relativistic wave functions, Coulomb force, and binding energy. The method and the results are shown in Chapter 5.

The collider reach of the discovery at LHC assuming the SUSY model is plotted. This signal also gives independent information on LFV.

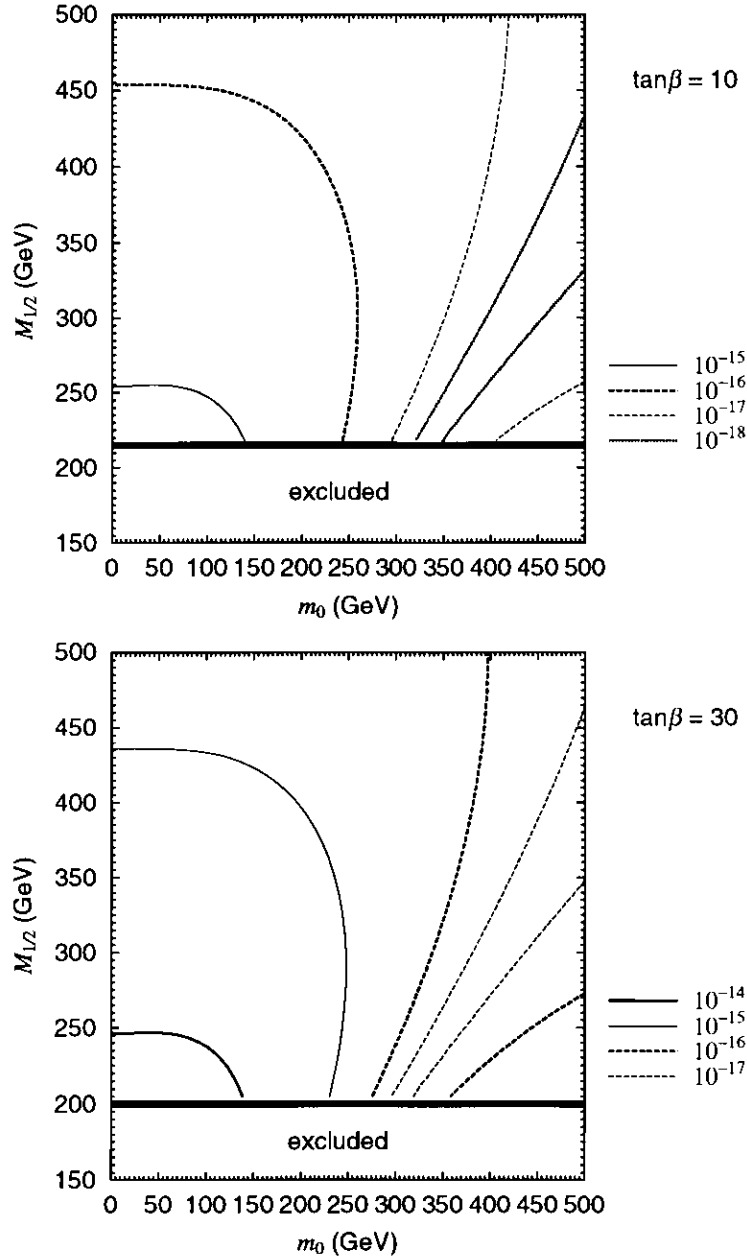


Figure 2.3: The branching ratio of the $\mu \rightarrow e\gamma$ decay in SU(5) SUSY GUT are shown. The first and second figure show the case where $\tan\beta = 10$ and $\tan\beta = 30$, respectively. We take $a_0 = 0$ and $\mu > 0$.

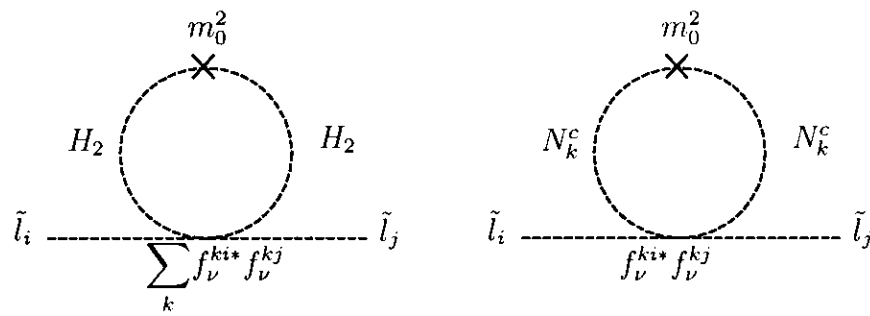


Figure 2.4: The loop diagrams for the off-diagonal components of the right-handed slepton masses in SUSY models with the right-handed neutrinos are shown.

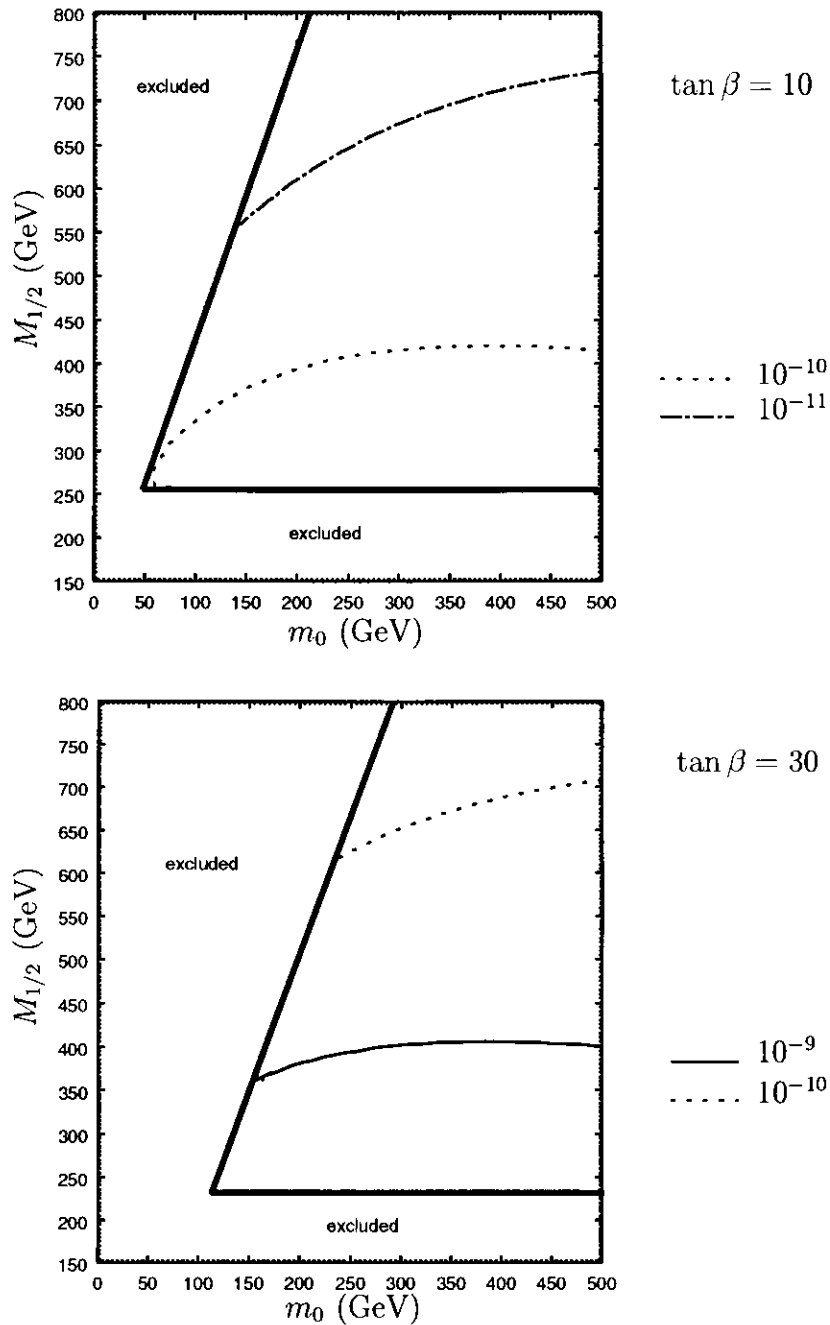


Figure 2.5: The branching ratio of the $\mu \rightarrow e\gamma$ decay in SUSY models with right-handed neutrinos are shown. We take a parameter set of the large angle MSW solution to the solar neutrino anomaly. The first and second figure show the case where $\tan \beta = 10$ and $\tan \beta = 30$, respectively. We take $a_0 = 0$, $\mu > 0$, and the right-handed neutrino masses M_N to be 10^{14} GeV.

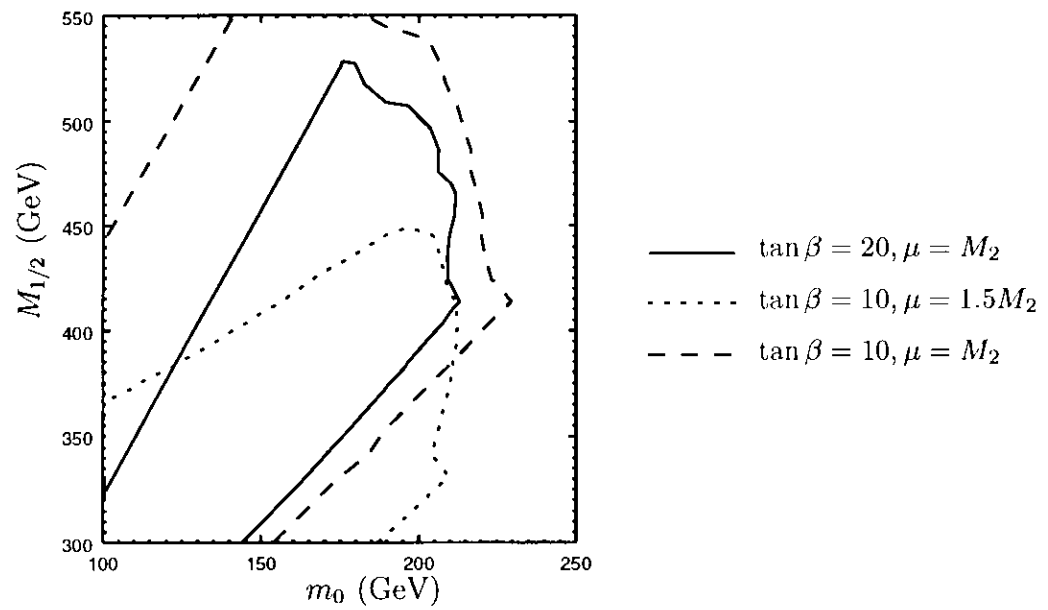


Figure 2.6: The 5σ line for the discovery of the LFV neutralino decay is shown. The LFV parameters for the right-handed sleptons are taken to be $\sin 2\theta = 0.5$ and $\Delta m = 1$ GeV.

Chapter 3

LFV in the Randall-Sundrum model with bulk neutrinos

In this chapter, LFV in the Randall-Sundrum model with bulk neutrinos is considered [28]. Grossman and Neubert recently proposed that the existence of tiny neutrino masses and large mixing could be explained by the presence of the bulk neutrinos in the Randall-Sundrum background [15]. Since the zero mode wave functions of the bulk neutrinos are localized on Planck brane, the Dirac Yukawa couplings on our brane are exponentially suppressed enough to generate tiny neutrino masses. However, the existence of Kaluza-Klein modes of these bulk neutrinos enhance LFV processes such as $\mu \rightarrow e\gamma$, from which lower bounds on their masses can be derived. We find that the first KK mode must be heavier than 25 TeV if all the neutrino Yukawa couplings are of order unity, which requires a fine-tuning for the Higgs mass parameter.

3.1 Randall-Sundrum model and bulk neutrinos

The RS model is a five dimensional theory in which the fifth dimension is compactified to S_1/\mathbf{Z}_2 and two 3-branes are located at two orbifold fixed points. The five dimensional metric is given as

$$ds^2 = e^{-2kr_c|\phi|} \eta_{\mu\nu} dx^\mu dx^\nu - r_c^2 d\phi^2, \quad (3.1)$$

where k is a parameter of the order of the fundamental scale M , r_c is the compactification radius which is also of the order of M^{-1} and ϕ is the coordinate of the fifth dimension which is defined on $[0, \pi]$. The standard model fields are confined on the brane at $\phi = \pi$. In this set-up, the Planck scale M_{Pl} and the VEV for the Higgs field v in the four dimensional effective theory are given as

$$M_{\text{Pl}}^2 = \frac{M^3}{k}(1 - e^{-2kr_c\pi}), \quad v = e^{-kr_c\pi} v_0, \quad (3.2)$$

where v_0 is the VEV for the Higgs field in the five dimensional theory. We can see from eq.(3.2) that if we consider $M, k, 1/r_c$ and v_0 as parameters of the order of 10^{19} GeV, all the dimensionful parameters on weak brane such as v can be taken of the order of 100 GeV for $kr_c \sim 12$ while keeping M_{Pl} close to 10^{19} GeV.

The action of the bulk fermion in the RS set-up is given by [15]

$$S = \int d^4x \int_0^\pi d\phi \sqrt{G} \left\{ \frac{i}{2} \bar{\Psi} \hat{\gamma}^A \partial_A \Psi - \frac{i}{2} (\partial_A \bar{\Psi}) \hat{\gamma}^A \Psi - m \operatorname{sgn}(\phi) \bar{\Psi} \Psi \right\}. \quad (3.3)$$

The Majorana mass term is omitted by imposing lepton number conservation. Kaluza-Klein decomposition of Ψ reduces this action to the usual four dimensional Dirac action which is given by

$$S = \sum_n \int d^4x \{ \bar{\psi}_n(x) i \not{\partial} \psi_n(x) - m_n \bar{\psi}_n(x) \psi_n(x) \}, \quad (3.4)$$

where $\psi \equiv \psi^L + \psi^R$, and $\psi^{L,R}$ is defined as

$$\Psi_{L,R}(x, \phi) \equiv \frac{1}{2}(1 \mp \gamma_5) \Psi = \frac{e^{2kr_c|\phi|}}{\sqrt{r_c}} \sum_n \psi_n^{L,R}(x) \hat{f}_n^{L,R}(\phi). \quad (3.5)$$

The wave functions $\hat{f}_n^{L,R}$ and the masses of KK modes m_n are expressed by the following parameters:

$$\epsilon = e^{-kr_c\pi}, \quad t = \epsilon e^{kr_c|\phi|}, \quad \nu = \frac{m}{k}, \quad (3.6)$$

where the parameter ϵ should be fixed as $\epsilon \sim 10^{-16}$ i.e. $kr_c \sim 12$ in order to produce the hierarchy between the Planck scale and the electroweak scale. The parameter $t \in [\epsilon, 1]$ is

the redefined spatial coordinate of the fifth dimension; $t = \epsilon$ is the location of the Planck brane and $t = 1$ is that of our brane. By rescaling the function as $\hat{f}_n^{L,R}(\phi) \rightarrow \sqrt{k\tau_c\epsilon} f_n^{L,R}(t)$, the wave functions and the masses are explicitly given as

$$f_0^L(t) = 0, \quad f_0^R(t) = \sqrt{\frac{1-2\nu}{1-\epsilon^{1-2\nu}}} t^{-\nu}, \quad (3.7)$$

$$f_n^{L,R}(t) = \frac{\sqrt{2t}}{J_{\nu+\frac{1}{2}}(x_n)} J_{\nu\mp\frac{1}{2}}(x_n t) \quad (n \neq 0, \nu > \frac{1}{2}), \quad (3.8)$$

$$m_n = \epsilon k x_n, \quad (3.9)$$

where x_n is the solution of $J_{\nu-\frac{1}{2}}(x_n) = 0$. For $\epsilon \sim 10^{-16}$, the masses of the KK modes m_n are of the order of the electroweak scale. The zero mode wave function (there is a zero mode f_0^R since $x_0 = 0$.) on our brane is very suppressed such as $f_0^R(1) \propto \epsilon^{\nu-\frac{1}{2}}$ for $\nu > 1/2$. This smallness is the origin of the tiny neutrino masses. The wave functions of KK modes are not suppressed ($f_n^R(1) = \sqrt{2}$) and this gives large coupling constants which violate lepton flavor conservation.

We can construct the gauge invariant interaction terms between the lepton doublets $L_0^i = (\nu_{0L}^i, e_{0L}^i)$ ($i = e, \mu, \tau$) and the two kinds of bulk fermions Ψ^α ($\alpha = 1, 2$) as

$$S_Y = - \int d^4x e^{-4k\tau_c\pi} \left\{ \hat{y}_{i\alpha} \bar{L}_0^i(x) \tilde{H}_0(x) \Psi_R^\alpha(x, \pi) + \text{h.c.} \right\}, \quad (3.10)$$

where $\tilde{H}_0 \equiv i\sigma_2 H_0^* = (H_0^{0*}, H_0^-)$ is the Higgs field. At least two kinds of bulk fermions are necessary to give masses for two neutrinos. The couplings $\hat{y}_{i\alpha}$ are dimensionful parameters which are naturally of the order of $M_{\text{Pl}}^{-1/2}$. In four dimensional effective theory, this action is written in terms of ψ as

$$S_Y = - \sum_{n \geq 0} \int d^4x \left\{ y_n^{i\alpha} \bar{L}^i(x) \tilde{H}(x) \psi_{n,\alpha}^R(x) + \text{h.c.} \right\}, \quad (3.11)$$

where the lepton doublets L and the Higgs doublet $\tilde{H} \equiv i\sigma_2 H^*$ are properly rescaled to give canonical kinetic terms in four dimensions. The relation of $\hat{y}_{i\alpha}$ and $y_n^{i\alpha}$ is

$$y_n^{i\alpha} = \sqrt{k} \hat{y}_{i\alpha} f_n^R(1) \equiv z_{i\alpha} f_n^R(1). \quad (3.12)$$

Here we take that $z_{i\alpha}$ to be parameters of order unity. From eq.(3.4) and eq.(3.11), the mass matrix for neutrinos is given by

$$M = \begin{matrix} & \psi_{0,\alpha}^R & \psi_{1,\alpha}^R & \cdots & \psi_{n,\alpha}^R & \cdots \\ \nu_L^i & \left(\begin{array}{cccc} \psi_{0,\alpha}^R & \psi_{1,\alpha}^R & \cdots & \psi_{n,\alpha}^R & \cdots \\ \psi_{1,\alpha}^L & 0 & m_{1,\alpha} & 0 & 0 & 0 \\ \vdots & 0 & 0 & \ddots & 0 & 0 \\ \psi_{n,\alpha}^L & 0 & 0 & 0 & m_{n,\alpha} & 0 \\ \vdots & 0 & 0 & 0 & 0 & \ddots \end{array} \right) & \end{matrix}, \quad (3.13)$$

where $m_{n,\alpha}$ (from eq.(3.4)) is the mass of the n -th KK mode for Ψ^α . For appropriate choices of ν ($\nu \sim 1$), $y_0^{i\alpha} (\equiv z_{i\alpha} f_0^R(1))$ becomes small enough to explain the tiny neutrino masses. In four dimensional effective theory, this model also contains a series of vector-like neutrinos which may lead to sizable LFV [57].

The 3×2 submatrix for the light neutrinos is written as

$$M_{\text{sub}} = \begin{pmatrix} \sqrt{2\nu_1 - 1}\epsilon^{\nu_1 - \frac{1}{2}} z_{e1} v & \sqrt{2\nu_2 - 1}\epsilon^{\nu_2 - \frac{1}{2}} z_{e2} v \\ \sqrt{2\nu_1 - 1}\epsilon^{\nu_1 - \frac{1}{2}} z_{\mu 1} v & \sqrt{2\nu_2 - 1}\epsilon^{\nu_2 - \frac{1}{2}} z_{\mu 2} v \\ \sqrt{2\nu_1 - 1}\epsilon^{\nu_1 - \frac{1}{2}} z_{\tau 1} v & \sqrt{2\nu_2 - 1}\epsilon^{\nu_2 - \frac{1}{2}} z_{\tau 2} v \end{pmatrix}, \quad (3.14)$$

where $\nu_\alpha = m_\alpha/k$ ($\alpha = 1, 2$) and m_α is the mass of the bulk fermions (see eq.(3.3)). We take here $m_1 > m_2$. Since this matrix is 3×2 , one of the three light neutrinos remains massless.

3.2 LFV mediated by Kaluza-Klein modes

Now we discuss the lepton flavor violating processes such as $\mu \rightarrow e\gamma$, $\tau \rightarrow \mu\gamma$ and $\tau \rightarrow e\gamma$. The experimental bounds for these processes give severe constraints on the mass of the KK modes and/or couplings $z_{i\alpha}$.

The four dimensional gauge and Yukawa interaction terms relevant to $\mu \rightarrow e\gamma$, $\tau \rightarrow \mu\gamma$

and $\tau \rightarrow e\gamma$ process are given by

$$\begin{aligned}\mathcal{L}^{\text{gauge}} &= \sum_{i=e,\mu,\tau} \frac{g}{\sqrt{2}} W_\mu^\dagger \bar{e}_L^i \gamma^\mu P_L \nu_L^i + \text{h.c.} \\ &= \sum_{i=e,\mu,\tau} \sum_{A=1}^{2N+3} \frac{g}{\sqrt{2}} U_{iA} W_\mu^\dagger \bar{e}_L^i \gamma^\mu P_L \psi_\nu^A + \text{h.c.} ,\end{aligned}\tag{3.15}$$

$$\begin{aligned}\mathcal{L}^{\text{Yukawa}} &= \sum_{n=0}^N \sum_{i=e,\mu,\tau} \sum_{\alpha=1,2} y_n^{i\alpha} \bar{e}_L^i H^- P_R \psi_{n,\alpha}^R - \sum_{i=e,\mu,\tau} f^i \bar{\nu}_L^i H^+ P_R e_R^i + \text{h.c.} \\ &= \sum_{n=0}^N \sum_{i=e,\mu,\tau} \sum_{\alpha=1,2} \sum_{A=1}^N y_n^{i\alpha} V_{(n,\alpha)A} \bar{e}_L^i H^- P_R \psi_\nu^A \\ &\quad - \sum_{i=e,\mu,\tau} \sum_{A=1}^N f^i U_{iA}^* \bar{\psi}_\nu^A H^+ P_R e_R^i + \text{h.c.} ,\end{aligned}\tag{3.16}$$

where the indices i, A, n, α represent the flavor, the mass eigenstates of neutrinos, the KK excitations and the species of the bulk fermions, respectively. Here the left-handed mixing matrix U and the right-handed mixing matrix V are defined as the matrices which diagonalize MM^\dagger and $M^\dagger M$, respectively. To cut-off the infinite KK modes we introduce N and consider up to N -th KK mode. Then U and V are $(2N+3) \times (2N+3)$, $(2N+2) \times (2N+2)$ matrices respectively. The coupling f^i is the lepton Dirac Yukawa coupling of the i -th generation and $y_n^{i\alpha}$ are neutrino Dirac Yukawa couplings defined in eq.(3.11). The field ψ_ν^A represents the A -th mass eigenstate of the neutrinos.

We first calculate $B(\mu \rightarrow e\gamma)$. $B(\tau \rightarrow \mu\gamma)$ and $B(\tau \rightarrow e\gamma)$ can be calculated in the same way. Neglecting the mass of the electron, A_L and A_R in eq.(2.6) can be expressed as

$$A_L = 0 ,\tag{3.17}$$

$$A_R = \frac{e}{4\sqrt{2}} \sum_A U_{eA} U_{\mu A}^* \times \frac{1}{24(1 - \xi_A)^4} (10 - 43\xi_A + 78\xi_A^2 - 49\xi_A^3 + 4\xi_A^4 + 18\xi_A^3 \log \xi_A) , \quad (3.18)$$

$$(\xi_A \equiv m_A^2/M_W^2)$$

where M_W is W boson mass and m_A is the mass of the A -th mass eigenstates of neutrinos. Notice that this model predicts $\mu^- \rightarrow e_L^- \gamma$ (or $\mu^+ \rightarrow e_R^+ \gamma$) decay. If all the neutrino masses are small, this amplitude is suppressed by the GIM mechanism [58]. However, due to the existence of heavy neutrinos, the GIM cancellation does not work and A_R is estimated approximately as

$$A_R \simeq \frac{1}{(4\pi)^2} \frac{e}{4\sqrt{2}G_F} \sum_{n=1}^N \left(\frac{z_{e1}z_{\mu 1}}{m_{n,1}^2} + \frac{z_{e2}z_{\mu 2}}{m_{n,2}^2} \right) . \quad (3.19)$$

and from eq.(3.9), this is written as

$$A_R \simeq \frac{1}{(4\pi)^2} \frac{e}{4\sqrt{2}G_F} \frac{1}{(\epsilon k)^2} (z_{e1}z_{\mu 1}C_1(N) + z_{e2}z_{\mu 2}C_2(N)) , \quad (3.20)$$

$$C_\alpha(N) = \sum_{n=1}^N \frac{1}{x_{n,\alpha}^2} , \quad (\alpha = 1, 2) , \quad (3.21)$$

where $x_{n,\alpha}$ are the solutions for $J_{\nu_\alpha - \frac{1}{2}}(x_{n,\alpha}) = 0$. The functions $C_\alpha(N)$ are slowly increasing functions of N , and therefore the cut off dependence of $\text{Br}(\mu \rightarrow e\gamma)$ is small. In the limit of $N \rightarrow \infty$, $C_\alpha(N) \rightarrow (2(2\nu_\alpha + 1))^{-1}$.

The branching ratio is given by eq.(3.20) as

$$B(\mu \rightarrow e\gamma) \simeq 0.0037 \left(\frac{v}{\epsilon k} \right)^4 |z_{e1}z_{\mu 1}C_1(N) + z_{e2}z_{\mu 2}C_2(N)|^2 . \quad (3.22)$$

The same calculation for $\tau \rightarrow \mu\gamma$ and $\tau \rightarrow e\gamma$ gives

$$B(\tau \rightarrow \mu\gamma) \simeq 0.00065 \left(\frac{v}{\epsilon k} \right)^4 |z_{\mu 1}z_{\tau 1}C_1(N) + z_{\mu 2}z_{\tau 2}C_2(N)|^2 , \quad (3.23)$$

$$B(\tau \rightarrow e\gamma) \simeq 0.00065 \left(\frac{v}{\epsilon k} \right)^4 |z_{e1}z_{\tau 1}C_1(N) + z_{e2}z_{\tau 2}C_2(N)|^2 . \quad (3.24)$$

The present experimental bounds are $B(\mu \rightarrow e\gamma) < 1.2 \times 10^{-11}$ [29], $B(\tau \rightarrow \mu\gamma) < 1.0 \times 10^{-6}$ [35] and $B(\tau \rightarrow e\gamma) < 2.7 \times 10^{-6}$ [59]. If all $z_{i\alpha}$ are of order unity, the dimensionless combination $v/\epsilon k$ must satisfy

$$\frac{v}{\epsilon k} \lesssim 0.02, \quad (3.25)$$

from the constraint from $B(\mu \rightarrow e\gamma)$. In eq.(3.25), we use $C_\alpha(N) \sim (2(2\nu_\alpha + 1))^{-1}$ and $\nu_\alpha \sim 1$ which is a reasonable region for producing light neutrino masses. The parameter $x_{1,\alpha}$ is roughly estimated to be $x_{1,\alpha} \sim 3$ for $\nu_\alpha \sim 1$, so that we can derive the following bound for the lowest KK mode m_{KK} from eq.(3.9) and eq.(3.25):

$$m_{\text{KK}} \gtrsim 25 \text{ TeV}. \quad (3.26)$$

Since this value is two order of magnitude larger than the Higgs VEV, a fine-tuning of 10^{-2} is necessary.

An individual constraint on $z_{i\alpha}$ can be obtained by considering the neutrino oscillation data. To reproduce the mixing angle $\sin^2 2\theta_{12} \sim 10^{-2}$ for the small angle MSW solution, $\sin^2 2\theta_{12} \sim 1$ for the large angle MSW solution, $\sin^2 2\theta_{23} \sim 1$ to explain the atmospheric neutrino anomaly [40] and $\sin^2 2\theta_{13} \lesssim 0.1$ from the CHOOZ experiment [45], the structure of the Yukawa couplings are roughly given by

$$|z_{e1}| \sim x|z_{\mu1}| \sim x|z_{\tau1}|, \quad (3.27)$$

$$|z_{e2}| \ll |z_{\mu2}| \sim |z_{\tau2}|, \quad (3.28)$$

where $x \sim 14, 1/28$ for the small angle MSW solution and $x \sim 0.7$ for the large angle MSW solution [15]. Therefore the restrictions on z_{i1} are given as

$$\frac{v|z_{e1}|}{\epsilon k} \lesssim 0.08, \quad \frac{v|z_{\mu1}|}{\epsilon k} \sim \frac{v|z_{\tau1}|}{\epsilon k} \lesssim 0.006 \quad (x = 14) \quad (3.29)$$

$$\frac{v|z_{e1}|}{\epsilon k} \lesssim 0.004, \quad \frac{v|z_{\mu1}|}{\epsilon k} \sim \frac{v|z_{\tau1}|}{\epsilon k} \lesssim 0.1 \quad (x = \frac{1}{28}) \quad (3.30)$$

$$\frac{v|z_{e1}|}{\epsilon k} \sim \frac{v|z_{\mu1}|}{\epsilon k} \sim \frac{v|z_{\tau1}|}{\epsilon k} \lesssim 0.02 \quad (x = 0.7). \quad (3.31)$$

Since we only know the upper bound on the mixing angle $\sin^2 2\theta_{13}$, typically we take $\sin^2 2\theta_{13} = 0.05$. Then the constraints on z_{i2} are given by

$$\frac{v|z_{e2}|}{\epsilon k} \lesssim 0.009, \quad \frac{v|z_{\mu 2}|}{\epsilon k} \sim \frac{v|z_{\tau 2}|}{\epsilon k} \lesssim 0.05. \quad (3.32)$$

In ref. [15], the constraint $v|z_{i\alpha}|/\epsilon k \lesssim 0.1$ was derived from the invisible decay width of the Z^0 boson i.e. the deviation from unitarity of the MNS matrix which is 3×3 submatrix of the matrix U [43]. We can find more severe constraints from considering LFV. The smallness of $v|z_{i\alpha}|/\epsilon k$ means that the five dimensional Yukawa couplings $\hat{y}_{i\alpha}$ or the five dimensional VEV of the Higgs field v_0 should be much smaller than $M_{\text{Pl}}^{-1/2}$ or M_{Pl} , respectively, which is the only natural scale of the original parameters. In this sense, the bounds in eq.(3.29–3.32) are considered to be somewhat unnatural.

3.3 Summary

We have considered LFV processes in the context of the small extra-dimension scenario. The neutrino mass and mixing needs right-handed neutrinos, but naive introduction of the right-handed neutrino does not provide tiny neutrino masses. Grossman and Neubert then proposed the existence of right-handed neutrinos which live in bulk and couple to the lepton doublets and we saw that this model lead to small Dirac neutrino mass terms. The neutrino mass and mixing causes LFV. The KK modes of the right-handed neutrinos enhance the branching ratio of these processes. We calculated the $B(\mu \rightarrow e\gamma)$, $B(\tau \rightarrow \mu\gamma)$ and $B(\tau \rightarrow e\gamma)$ and found that $B(\mu \rightarrow e\gamma)$ gives severe constraints on the neutrino Yukawa couplings $\hat{y}_{i\alpha}$ and/or the Higgs mass parameter v_0 in the five dimensional theory.

Chapter 4

P and T odd asymmetries in LFV τ decays

We calculated the differential cross sections of the processes in which one of the pair created τ particles at an e^+e^- collider decays into LFV final states e.g. $\tau \rightarrow \mu\gamma$, $\tau \rightarrow 3\mu$, $\tau \rightarrow \mu ee$ [36]. Using the correlations between angular distributions of both sides of τ decays, we can obtain information on parity and CP violations of lepton flavor non-conserving interactions. The formulae derived here are useful in distinguishing different models, since each model of physics beyond the standard model predicts different angular correlations. We also calculate angular distributions of the major background process to $\tau \rightarrow l\gamma$ search, namely $\tau \rightarrow l\nu\bar{\nu}\gamma$, and discuss usefulness of the angular correlation for background suppression.

4.1 General formula for spin correlation

In this section, we present general formulae used in the calculation of differential cross sections and spin correlations.

We calculate differential cross sections of $e^+e^- \rightarrow \tau^+\tau^- \rightarrow f_B f_A$, where f_B (f_A) represents the decay products of τ^+ (τ^-). If the intermediate states were spinless particles, the cross section is simply a product of a production cross section and decay branching ratios. However, in the case of spin 1/2 particles, we have to take into account spin correlation

between two intermediate particles. If we take $\tau^+ \rightarrow f_B$ to be a LFV decay mode, we can measure P and T violation of LFV interactions by using the angular correlations of decay products of τ^+ and τ^- .

The differential cross section of $e^+e^- \rightarrow \tau^+\tau^- \rightarrow f_B f_A$ is given by

$$d\sigma = d\sigma^P dB^{\tau^- \rightarrow f_A} dB^{\tau^+ \rightarrow f_B} + \sum_{a,b=1}^3 d\Sigma_{ab}^P dR_a^{\tau^- \rightarrow f_A} dR_b^{\tau^+ \rightarrow f_B}, \quad (4.1)$$

and

$$d\sigma^P = \frac{d^3 p_A}{(2\pi)^3 2p_A^0} \frac{d^3 p_B}{(2\pi)^3 2p_B^0} \frac{1}{2s} (2\pi)^4 \delta^4(p_A + p_B - p_{e^+} - p_{e^-}) \alpha^P, \quad (4.2)$$

$$dB^{\tau^- \rightarrow f_A} = \frac{1}{\Gamma} \frac{d^3 q_1}{(2\pi)^3 2q_1^0} \cdots \frac{d^3 q_n}{(2\pi)^3 2q_n^0} \frac{1}{2m_\tau} (2\pi)^4 \delta^4\left(\sum_{i=1}^n q_i - p_A\right) \alpha^{D-}, \quad (4.3)$$

$$dB^{\tau^+ \rightarrow f_B} = \frac{1}{\Gamma} \frac{d^3 q_{n+1}}{(2\pi)^3 2q_{n+1}^0} \cdots \frac{d^3 q_{n+m}}{(2\pi)^3 2q_{n+m}^0} \frac{1}{2m_\tau} (2\pi)^4 \delta^4\left(\sum_{i=n+1}^{n+m} q_i - p_B\right) \alpha^{D+}, \quad (4.4)$$

$$d\Sigma_{ab}^P = \frac{d^3 p_A}{(2\pi)^3 2p_A^0} \frac{d^3 p_B}{(2\pi)^3 2p_B^0} \frac{1}{2s} (2\pi)^4 \delta^4(p_A + p_B - p_{e^+} - p_{e^-}) \rho^P, \quad (4.5)$$

$$dR_a^{\tau^- \rightarrow f_A} = \frac{1}{\Gamma} \frac{d^3 q_1}{(2\pi)^3 2q_1^0} \cdots \frac{d^3 q_n}{(2\pi)^3 2q_n^0} \frac{1}{2m_\tau} (2\pi)^4 \delta^4\left(\sum_{i=1}^n q_i - p_A\right) \rho_a^{D-}, \quad (4.6)$$

$$dR_b^{\tau^+ \rightarrow f_B} = \frac{1}{\Gamma} \frac{d^3 q_{n+1}}{(2\pi)^3 2q_{n+1}^0} \cdots \frac{d^3 q_{n+m}}{(2\pi)^3 2q_{n+m}^0} \frac{1}{2m_\tau} (2\pi)^4 \delta^4\left(\sum_{i=n+1}^{n+m} q_i - p_B\right) \rho_b^{D+}, \quad (4.7)$$

where we assume that f_A is a n body system and f_B is a m body system. p_{e^+} (p_{e^-}) is e^+ (e^-) four momentum, p_B (p_A) is τ^+ (τ^-) four momentum, and q_i 's are momenta of final state particles. s is determined as $s = (p_{e^+} + p_{e^-})^2$. Γ and m_τ are the width and the mass

of the τ , respectively. In order to define α^P , α^{D-} , α^{D+} , ρ_{ab}^P , ρ_a^{D-} , and ρ_b^{D+} , we first write down the invariant amplitude of $e^+e^- \rightarrow \tau^+\tau^- \rightarrow f_B f_A$ as follows:

$$M = \frac{e^2}{s} \bar{A}(\not{p}_A + m_\tau)\gamma^\mu(\not{p}_B - m_\tau)B \bar{v}_{e^+}\gamma_\mu u_{e^-} \\ \times \frac{1}{p_A^2 - (m_\tau - \frac{i\Gamma}{2})^2} \frac{1}{p_B^2 - (m_\tau - \frac{i\Gamma}{2})^2}, \quad (4.8)$$

where v_{e^+} (u_{e^-}) is the wave function of positron (electron) and A and B are spinors which include wave functions of final states and interaction vertices. By using the Bouchiat-Michel formulae [60] and the narrow width approximation, α^P , α^{D-} , α^{D+} , ρ_{ab}^P , ρ_a^{D-} , and ρ_b^{D+} are given by

$$\alpha^P = \frac{1}{4} \frac{e^4}{s^2} \text{Tr}[(\not{p}_A + m_\tau)\gamma^\mu(\not{p}_B - m_\tau)\gamma^\nu] \text{Tr}[\not{p}_{e^+}\gamma_\mu\not{p}_{e^-}\gamma_\nu], \quad (4.9)$$

$$\alpha^{D-} = \frac{1}{2} \{\bar{A}(\not{p}_A + m_\tau)A\}, \quad (4.10)$$

$$\alpha^{D+} = \frac{1}{2} \{\bar{B}(\not{p}_B - m_\tau)B\}, \quad (4.11)$$

$$\rho_{ab}^P = \frac{1}{4} \frac{e^4}{s^2} \text{Tr}[\gamma_5 \beta_A^a (\not{p}_A + m_\tau)\gamma^\mu \gamma_5 \beta_B^b (\not{p}_B - m_\tau)\gamma^\nu] \text{Tr}[\not{p}_{e^+}\gamma_\mu\not{p}_{e^-}\gamma_\nu], \quad (4.12)$$

$$\rho_a^{D-} = \frac{1}{2} \{\bar{A} \gamma_5 \beta_A^a (\not{p}_A + m_\tau)A\}, \quad (4.13)$$

$$\rho_b^{D+} = \frac{1}{2} \{\bar{B} \gamma_5 \beta_B^b (\not{p}_B - m_\tau)B\}, \quad (4.14)$$

where the spins of the final state fermions are summed over, and four vectors $(s_A^a)^\mu$ and $(s_B^b)^\nu$ ($a, b = 1, 2, 3$) are a set of vectors which satisfy following equations.

$$p_A \cdot s_A^a = p_B \cdot s_B^b = 0, \quad (4.15)$$

$$s_A^a \cdot s_A^b = s_B^a \cdot s_B^b = -\delta^{ab}, \quad (4.16)$$

$$\sum_{a=1}^3 (s_A^a)_\mu (s_A^a)_\nu = -g_{\mu\nu} + \frac{p_{A\mu} p_{A\nu}}{m_\tau^2}, \quad \sum_{b=1}^3 (s_B^b)_\mu (s_B^b)_\nu = -g_{\mu\nu} + \frac{p_{B\mu} p_{B\nu}}{m_\tau^2}. \quad (4.17)$$

The derivation of the above result is shown in Appendix C. Notice that $d\sigma^P$, $dB^{\tau^- \rightarrow f_A}$, and $dB^{\tau^+ \rightarrow f_B}$ in eq.(4.1) are the $\tau^+\tau^-$ production cross section and τ decay branching ratios, in which spins of τ 's are averaged, and $d\Sigma_{ab}^P$, $DR_a^{\tau^- \rightarrow f_A}$, and $DR_b^{\tau^+ \rightarrow f_B}$ represent the spin correlation effects of this process.

In above formulae, it is assumed that the τ pair production occurs through the photon exchange. It is straightforward to include the contribution from the Z boson exchange and the $\gamma - Z$ interference. If we consider the e^+e^- center of mass energy to be in the range of the $\tau^+\tau^-$ threshold energy considered in the τ -charm factory or the $\Upsilon(4S)$ resonance energy where e^+e^- B-factories are operated, these effects only contribute to the production cross section at the level of $O(10^{-4})$ of the photon exchanging diagram.

4.2 Parity asymmetry in $\tau \rightarrow \mu\gamma$ decay

Let us calculate the cross section of $e^+e^- \rightarrow \tau^+\tau^- \rightarrow \mu^+\gamma + f_A$ processes. For f_A , we consider hadronic and leptonic modes such as $(\pi\nu, \rho\nu, a_1\nu, \text{ and } l\bar{\nu}\nu)$. Below we neglect the muon mass compared to τ mass, and therefore all formulae can be applied also to the $\tau \rightarrow e\gamma$ process. The effective Lagrangian for $\tau^+ \rightarrow \mu^+\gamma$ decay is given by

$$\mathcal{L} = -\frac{4G_F}{\sqrt{2}} \{m_\tau A_R^\tau \bar{\tau} \sigma^{\mu\nu} P_L \mu F_{\mu\nu} + m_\tau A_L^\tau \bar{\tau} \sigma^{\mu\nu} P_R \mu F_{\mu\nu} + \text{h.c.}\} , \quad (4.18)$$

where G_F is the Fermi coupling constant, $P_L = (1 - \gamma_5)/2$, and $P_R = (1 + \gamma_5)/2$. Here, we use the conventions $\sigma^{\mu\nu} = \frac{i}{2}[\gamma^\mu, \gamma^\nu]$, $F_{\mu\nu} = \partial_\mu A_\nu - \partial_\nu A_\mu$, and $D_\mu = \partial_\mu + ieA_\mu$ for the electrons where $e(> 0)$ is the positron charge. The operator with the coupling constant A_R^τ (A_L^τ) induces the $\tau^+ \rightarrow \mu_R^+\gamma$ ($\tau^+ \rightarrow \mu_L^+\gamma$) decay. As mentioned in Chapter 2, each model of the physics beyond the standard model predicts a different ratio of A_L^τ and A_R^τ . For example, the SU(5) SUSY GUT in the minimal supergravity scenario predicts that only A_L^τ has a non-vanishing value for small and intermediate values of $\tan\beta$. Therefore the separate determination of A_L^τ and A_R^τ provides us important information on the origin of LFV. For this purpose, we need information about the τ polarization. This can be done by observing angular distributions of final state of τ decay in the opposite side in the

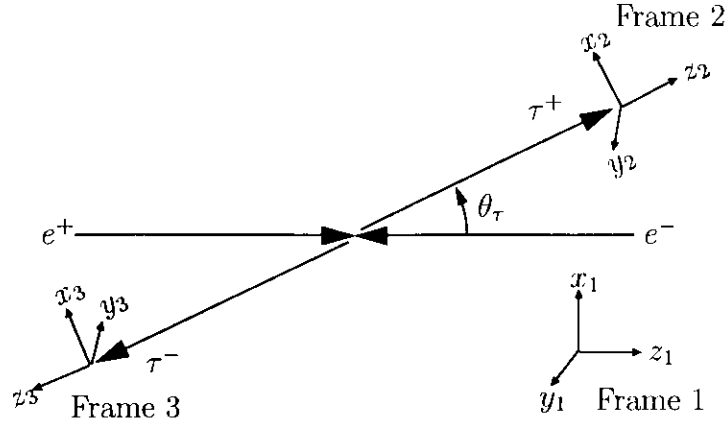


Figure 4.1: The coordinate systems. The plane determined by e^+e^- and $\tau^+\tau^-$ momentum vectors corresponds to the xz -planes in each of three coordinate systems.

modes of $\tau \rightarrow \pi\nu$, $\tau \rightarrow \rho\nu$, $\tau \rightarrow a_1\nu$, and $\tau \rightarrow l\bar{\nu}l$, because these processes proceed due to the $V - A$ interaction and therefore have a specific angular distribution with respect to polarization of τ . Using $\tau^+ - \tau^-$ spin correlation, we can determine $|A_L^\tau|^2$ and $|A_R^\tau|^2$, separately.

We first define three coordinate systems (Fig.4.1). The first coordinate system (Frame 1) is the center of mass frame of the e^+e^- collision in which the z axis is taken to be the e^+ momentum direction. The second one (Frame 2) is the rest frame of the τ^+ , and the third one (Frame 3) is the rest frame of the τ^- . More explicitly, the relation of a four vector in the three systems are given as follows:

$$\begin{aligned} \xi_1^\mu &= \begin{pmatrix} 1 & 0 & 0 & 0 \\ 0 & \cos\theta_\tau & 0 & \sin\theta_\tau \\ 0 & 0 & 1 & 0 \\ 0 & -\sin\theta_\tau & 0 & \cos\theta_\tau \end{pmatrix} \begin{pmatrix} \gamma & 0 & 0 & \gamma\beta_\tau \\ 0 & 1 & 0 & 0 \\ 0 & 0 & 1 & 0 \\ \gamma\beta_\tau & 0 & 0 & \gamma \end{pmatrix} \xi_2^\mu \\ &= \begin{pmatrix} 1 & 0 & 0 & 0 \\ 0 & 1 & 0 & 0 \\ 0 & 0 & -1 & 0 \\ 0 & 0 & 0 & -1 \end{pmatrix} \begin{pmatrix} 1 & 0 & 0 & 0 \\ 0 & \cos\theta_\tau & 0 & -\sin\theta_\tau \\ 0 & 0 & 1 & 0 \\ 0 & \sin\theta_\tau & 0 & \cos\theta_\tau \end{pmatrix} \begin{pmatrix} \gamma & 0 & 0 & \gamma\beta_\tau \\ 0 & 1 & 0 & 0 \\ 0 & 0 & 1 & 0 \\ \gamma\beta_\tau & 0 & 0 & \gamma \end{pmatrix} \xi_3^\mu \end{aligned} \quad (4.19)$$

where $\gamma = \sqrt{s}/(2m_\tau)$ and $\beta_\tau = \sqrt{1 - 4m_\tau^2/s}$, and the four vectors ξ_{1-3} are defined in

Frame 1-3, respectively. We calculate the production process in Frame 1, and the τ^+ (τ^-) decay in Frame 2 (Frame 3). In the calculations, we choose the spin vectors $(s_A^a)^\mu$, $(s_B^a)^\mu$ as follows:

$$(s_A^a)^\mu = \begin{pmatrix} 0 \\ \delta_{a\mu} \end{pmatrix} \quad (\text{in Frame 3}) , \quad (4.20)$$

$$(s_B^b)^\mu = \begin{pmatrix} 0 \\ \delta_{b\mu} \end{pmatrix} \quad (\text{in Frame 2}) . \quad (4.21)$$

The production cross section and spin dependence term are obtained from eq.(4.9) and eq.(4.12) as follows:

$$\begin{aligned} d\sigma^P &= \frac{d\Omega_\tau}{4\pi} \frac{\pi\alpha^2}{s} \sqrt{1 - \frac{4m_\tau^2}{s}} \left\{ \left(1 + \frac{4m_\tau^2}{s}\right) + \left(1 - \frac{4m_\tau^2}{s}\right) \cos^2 \theta_\tau \right\} , \quad (4.22) \\ d\Sigma_{ab}^P &= \frac{d\Omega_\tau}{4\pi} \frac{\pi\alpha^2}{s} \sqrt{1 - \frac{4m_\tau^2}{s}} \\ &\times \begin{pmatrix} \left(1 + \frac{4m_\tau^2}{s}\right) \sin^2 \theta_\tau & 0 & -\frac{2m_\tau}{\sqrt{s}} \sin 2\theta_\tau \\ 0 & \left(1 - \frac{4m_\tau^2}{s}\right) \sin^2 \theta_\tau & 0 \\ \frac{2m_\tau}{\sqrt{s}} \sin 2\theta_\tau & 0 & -\left(1 - \frac{4m_\tau^2}{s}\right) - \left(1 + \frac{4m_\tau^2}{s}\right) \cos^2 \theta_\tau \end{pmatrix} , \quad (4.23) \end{aligned}$$

where θ_τ is the angle between the e^+ and τ^+ directions in the Frame 1, and $d\Omega_\tau$ is a solid angle element of τ^+ , $d\Omega_\tau = d\cos\theta_\tau d\phi_\tau$.

For decay processes, we take $\tau^+ \rightarrow \mu^+\gamma$ for the τ^+ side and hadronic ($\tau^- \rightarrow \pi^-\nu$, $\tau^- \rightarrow \rho^-\nu$, and $\tau^- \rightarrow a_1^-\nu$) and leptonic ($\tau^- \rightarrow l^-\bar{\nu}l$) decays for the τ^- side. $dB^{\tau^+ \rightarrow \mu^+\gamma}$ and $dR_b^{\tau^+ \rightarrow \mu^+\gamma}$ (see eq.(4.1)) can be calculated from eq.(4.11) and eq.(4.14) in which the spinor B is given by

$$B = \frac{8i}{\sqrt{2}} G_F m_\tau \sigma^{\mu\nu} (q_\gamma)_\mu (A_R^\tau P_L + A_L^\tau P_R) \epsilon_\nu^* v(q_\mu) , \quad (4.24)$$

where ϵ_ν is the polarization vector of the photon and $(q_\gamma)_\mu$ is the momentum of the photon and $v(q_\mu)$ is the wave function of the muon. These quantities are given as follows:

$$dB^{\tau^+ \rightarrow \mu^+\gamma} = \frac{d\Omega_\mu}{4\pi} \frac{1}{\Gamma} \frac{2}{\pi} G_F^2 m_\tau^5 (|A_L^\tau|^2 + |A_R^\tau|^2) , \quad (4.25)$$

$$dR_b^{\tau^+ \rightarrow \mu^+ \gamma} = \frac{d\Omega_\mu}{4\pi} \frac{1}{\Gamma} \frac{2}{\pi} G_F^2 m_\tau^5 (|A_L^\tau|^2 - |A_R^\tau|^2) \begin{pmatrix} \sin \theta_\mu \cos \phi_\mu \\ \sin \theta_\mu \sin \phi_\mu \\ \cos \theta_\mu \end{pmatrix}, \quad (4.26)$$

where (θ_μ, ϕ_μ) are angles in the polar coordinate for a unit vector of the muon momentum direction in Frame 2. The three components in eq.(4.26) corresponds to $b = 1, 2$, and 3.

Next, we list dB and dR for the τ^- decay in each mode of $\tau^- \rightarrow \pi^- \nu$, $\tau^- \rightarrow \rho^- \nu$, $\tau^- \rightarrow a_1^- \nu$, and $\tau^- \rightarrow l^- \bar{\nu} \nu$. For $\tau^- \rightarrow \pi^- \nu$ decay, the spinor A in eqs.(4.10) and (4.13) is given by

$$A = 2iV_{ud}f_\pi G_F \not{q}_\pi P_L u(q_\nu), \quad (4.27)$$

where f_π is the pion decay constant, q_π is the momentum of the pion, and $u(q_\nu)$ is the neutrino wave function. Then, $dB^{\tau^- \rightarrow \pi^- \nu}$ and $dR_a^{\tau^- \rightarrow \pi^- \nu}$ are given by

$$dB^{\tau^- \rightarrow \pi^- \nu} = \frac{d\Omega_\pi}{4\pi} \frac{1}{\Gamma} \frac{1}{8\pi} |V_{ud}|^2 f_\pi^2 G_F^2 m_\tau^3, \quad (4.28)$$

$$dR_a^{\tau^- \rightarrow \pi^- \nu} = dB^{\tau^- \rightarrow \pi^- \nu} \begin{pmatrix} \sin \theta_\pi \cos \phi_\pi \\ \sin \theta_\pi \sin \phi_\pi \\ \cos \theta_\pi \end{pmatrix}, \quad (4.29)$$

where (θ_π, ϕ_π) are the polar angles of π^- momentum in Frame 3 and $d\Omega_\pi = d\cos \theta_\pi d\phi_\pi$ (we use a similar notation in the following expressions). Here we neglect the mass of the pion. As before three elements in eq.(4.29) corresponds to $a = 1, 2$, and 3. Similar results can be obtained for the vector mesons. The spinor A for $\tau \rightarrow \rho\nu$, $\tau \rightarrow a_1\nu$ is given by

$$A = -2V_{ud}g_V G_F \not{\epsilon}_V P_L u(q_\nu), \quad (4.30)$$

where g_V and ϵ_V are the decay constant and polarization vector of the corresponding vector mesons, respectively. From this expression, we can obtain dB and dR for the longitudinally polarized vector mesons e.g. $\tau^- \rightarrow \rho^-(L)\nu$ and $\tau^- \rightarrow a_1^-(L)\nu$ as follows:

$$dB^{\tau^- \rightarrow V(L)^- \nu} = \frac{d\Omega_V}{4\pi} \frac{1}{\Gamma} \frac{1}{8\pi} |V_{ud}|^2 \left(\frac{g_V}{m_V^2} \right)^2 G_F^2 m_\tau^3 m_V^2 \left(1 - \frac{m_V^2}{m_\tau^2} \right), \quad (4.31)$$

$$dR_a^{\tau^- \rightarrow V(L)^- \nu} = dB^{\tau^- \rightarrow V(L)^- \nu} \begin{pmatrix} \sin \theta_V \cos \phi_V \\ \sin \theta_V \sin \phi_V \\ \cos \theta_V \end{pmatrix}, \quad (4.32)$$

where m_V and (θ_V, ϕ_V) are the mass, and polar angles of the corresponding vector meson, respectively. For the transversely polarized vector mesons, the spin dependence terms have a minus sign contrary to the case of the pion and longitudinally polarized vector mesons.

$$dB^{\tau^- \rightarrow V(T)^- \nu} = \frac{d\Omega_V}{4\pi} \frac{1}{\Gamma} \frac{1}{8\pi} |V_{ud}|^2 \left(\frac{g_V}{m_V^2} \right)^2 G_F^2 m_\tau^3 m_V^2 \left(1 - \frac{m_V^2}{m_\tau^2} \right) \frac{2m_V^2}{m_\tau^2}, \quad (4.33)$$

$$dR_a^{\tau^- \rightarrow V(T)^- \nu} = dB^{\tau^- \rightarrow V(T)^- \nu} \begin{pmatrix} -\sin \theta_V \cos \phi_V \\ -\sin \theta_V \sin \phi_V \\ -\cos \theta_V \end{pmatrix}. \quad (4.34)$$

For leptonic decays, after integrating over the phase space of the neutrinos, the branching ratio and the spin dependence term are given by

$$dB^{\tau^- \rightarrow l^- \bar{\nu} \nu} = \frac{d\Omega_l}{4\pi} dx \frac{1}{\Gamma} \frac{G_F^2 m_\tau^5}{192\pi^3} 2x^2(3-2x), \quad (4.35)$$

$$dR_a^{\tau^- \rightarrow l^- \bar{\nu} \nu} = \frac{d\Omega_l}{4\pi} dx \frac{1}{\Gamma} \frac{G_F^2 m_\tau^5}{192\pi^3} 2x^2(1-2x) \begin{pmatrix} \sin \theta_l \cos \phi_l \\ \sin \theta_l \sin \phi_l \\ \cos \theta_l \end{pmatrix}, \quad (4.36)$$

where we neglect the masses of the leptons (e and μ) and x is the lepton energy normalized by the maximum energy $m_\tau/2$ i.e. $x = 2E_l/m_\tau$, and (θ_l, ϕ_l) are the polar angles of the lepton in Frame 3.

Substituting these results into the formula in eq.(4.1), we obtain the differential cross sections of each processes. For example, the differential cross section of $e^+e^- \rightarrow \tau^+\tau^- \rightarrow$

$\mu^+\gamma + \pi^-\nu$ process is given by

$$\begin{aligned}
& d\sigma(e^+e^- \rightarrow \tau^+\tau^- \rightarrow \mu^+\gamma + \pi^-\nu) \\
&= \frac{\sigma(e^+e^- \rightarrow \tau^+\tau^-)}{\frac{4}{3}\left(1 + \frac{2m_\tau^2}{s}\right)} B(\tau^- \rightarrow \pi^-\nu) B(\tau^+ \rightarrow \mu^+\gamma) \frac{d\Omega_\tau}{4\pi} \frac{d\Omega_\gamma}{4\pi} \frac{d\Omega_\pi}{4\pi} \\
&\times \left[\left(1 + \frac{4m_\tau^2}{s}\right) + \left(1 - \frac{4m_\tau^2}{s}\right) \cos^2 \theta_\tau \right. \\
&\quad \left. + A_P \left(\sin \theta_\pi \cos \phi_\pi \quad \sin \theta_\pi \sin \phi_\pi \quad \cos \theta_\pi \right) \right. \\
&\quad \times \begin{pmatrix} \left(1 + \frac{4m_\tau^2}{s}\right) \sin^2 \theta_\tau & 0 & -\frac{2m_\tau}{\sqrt{s}} \sin 2\theta_\tau \\ 0 & \left(1 - \frac{4m_\tau^2}{s}\right) \sin^2 \theta_\tau & 0 \\ \frac{2m_\tau}{\sqrt{s}} \sin 2\theta_\tau & 0 & -\left(1 - \frac{4m_\tau^2}{s}\right) - \left(1 + \frac{4m_\tau^2}{s}\right) \cos^2 \theta_\tau \end{pmatrix} \\
&\quad \left. \times \begin{pmatrix} \sin \theta_\mu \cos \phi_\mu \\ \sin \theta_\mu \sin \phi_\mu \\ \cos \theta_\mu \end{pmatrix} \right] , \tag{4.37}
\end{aligned}$$

where

$$\sigma(e^+e^- \rightarrow \tau^+\tau^-) = \frac{4\pi\alpha^2}{3s} \sqrt{1 - \frac{4m_\tau^2}{s}} \left(1 + \frac{2m_\tau^2}{s}\right) \tag{4.38}$$

is the $\tau^+\tau^-$ production cross section. The branching ratio of $\tau^- \rightarrow \pi^-\nu$ and $\tau^+ \rightarrow \mu^+\gamma$ is given by

$$B(\tau^- \rightarrow \pi^-\nu) = \frac{1}{\Gamma} \frac{1}{8\pi} |V_{ud}|^2 f_\pi^2 G_F^2 m_\tau^3 , \tag{4.39}$$

$$B(\tau^+ \rightarrow \mu^+\gamma) = \frac{1}{\Gamma} \frac{2}{\pi} G_F^2 m_\tau^5 (|A_L^\tau|^2 + |A_R^\tau|^2) , \tag{4.40}$$

and the asymmetry parameter A_P is defined as follows:

$$A_P \equiv \frac{|A_L^\tau|^2 - |A_R^\tau|^2}{|A_L^\tau|^2 + |A_R^\tau|^2} . \tag{4.41}$$

We can see that the measurement of angular correlation of the pion and muon momentum enables us to determine the parameter A_P , so that we can obtain $|A_L^\tau|^2$ and $|A_R^\tau|^2$ separately.

A simpler expressions can be obtained if we integrate over the angle θ_τ , ϕ_τ , ϕ_π , and ϕ_γ in eq.(4.37). The differential cross section is given by

$$\begin{aligned} d\sigma(e^+e^- \rightarrow \tau^+\tau^- \rightarrow \mu^+\gamma + \pi^-\nu) \\ = \sigma(e^+e^- \rightarrow \tau^+\tau^-)B(\tau^+ \rightarrow \mu^+\gamma)B(\tau^- \rightarrow \pi^-\nu)\frac{d\cos\theta_\mu}{2}\frac{d\cos\theta_\pi}{2} \\ \times \left(1 - \frac{s-2m_\tau^2}{s+2m_\tau^2} A_P \cos\theta_\mu \cos\theta_\pi\right). \end{aligned} \quad (4.42)$$

Notice that angular distribution in the rest frames of τ^+ and τ^- can be easily converted to the energy distribution in the center of mass frame of the e^+e^- collision. We obtain

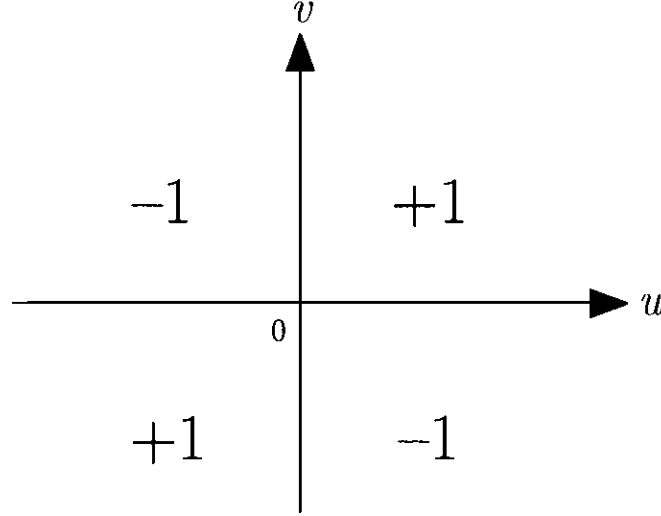
$$\begin{aligned} d\sigma(e^+e^- \rightarrow \tau^+\tau^- \rightarrow \mu^+\gamma + \pi^-\nu) \\ = \sigma(e^+e^- \rightarrow \tau^+\tau^-)B(\tau^+ \rightarrow \mu^+\gamma)B(\tau^- \rightarrow \pi^-\nu)\frac{s}{s-4m_\tau^2} dz_\mu dz_\pi \\ \times \left(1 - \frac{s(s-2m_\tau^2)}{(s-4m_\tau^2)(s+2m_\tau^2)} A_P (2z_\mu - 1)(2z_\pi - 1)\right), \end{aligned} \quad (4.43)$$

where $z_\mu = E_\mu/E_\tau$ ($z_\pi = E_\pi/E_\tau$), and E_μ , E_π , and $E_\tau = \sqrt{s}/2$ are the energies of the muon, pion, and τ in the center of mass frame, respectively.

The angular (or energy) distributions in eq.(4.42) (eq.(4.43)) can be understood as follows. Because of the helicity conservation of the $\tau^+\tau^-$ production process, the helicities of τ^+ and τ^- are correlated, namely $\tau_L^+\tau_R^-$ or $\tau_R^+\tau_L^-$ is produced. This means that two τ spins are parallel in the limit of $\sqrt{s} \gg m_\tau$. In the decay process, the π^- tends to be emitted to the spin direction of τ^- for $\tau^- \rightarrow \pi^-\nu$, because of the $V-A$ interaction. On the other hand, for $\tau^+ \rightarrow \mu^+\gamma$ decay, the muon tends to be emitted to the same direction of the τ^+ spin if $A_P > 0$. Therefore the differential branching ratio is enhanced (suppressed) if the sign of $\cos\theta_\mu \cos\theta_\pi$ is negative (positive). In other words, pion and muon energies in the center of mass frame of the e^+e^- collision have a negative correlation if $A_P > 0$. If $A_P < 0$, we have an opposite correlation.

We can define an asymmetry $A^{\mu^+\gamma, \pi^-\nu}$ by the following asymmetric integrations

$$\begin{aligned} A^{\mu^+\gamma, \pi^-\nu} &= \frac{\int d\cos\theta_\mu d\cos\theta_\pi w(\cos\theta_\mu, \cos\theta_\pi) \frac{d^2\sigma}{d\cos\theta_\mu d\cos\theta_\pi}}{\sigma(e^+e^- \rightarrow \tau^+\tau^-)B(\tau^+ \rightarrow \mu^+\gamma)B(\tau^- \rightarrow \pi^-\nu)} \\ &= \frac{N^{++} + N^{--} - N^{+-} - N^{-+}}{N^{++} + N^{--} + N^{+-} + N^{-+}}, \end{aligned} \quad (4.44)$$

Figure 4.2: The weight function $w(u, v)$.

where the weight function $w(u, v)$ is defined by

$$w(u, v) = \frac{uv}{|uv|}, \quad (4.45)$$

and shown in Fig.4.2. In the second line, $N^{\pm\pm}$ are the event numbers where the first \pm represent the sign of $\cos\theta_\mu$ and the second one is that of $\cos\theta_\pi$, respectively. $A^{\mu^+\gamma,\pi^-\nu}$ is related to the parameter A_P by

$$A^{\mu^+\gamma,\pi^-\nu} = -\frac{s - 2m_\tau^2}{4(s + 2m_\tau^2)} A_P. \quad (4.46)$$

In Fig.4.3, \sqrt{s} dependence of $A^{\mu^+\gamma,\pi^-\nu}$ is shown for $A_P = -1$. We can see that the asymmetry is already close to the maximal value at the B-factory energy.

It is straightforward to extend the above formula to other cases. We only present here formulae corresponding to eq.(4.42) for different decay modes of τ^- .

$$\begin{aligned} d\sigma(e^+e^- \rightarrow \tau^+\tau^- \rightarrow \mu^+\gamma + V^-\nu) \\ = \sigma(e^+e^- \rightarrow \tau^+\tau^-)B(\tau^+ \rightarrow \mu^+\gamma)B(\tau^- \rightarrow V^-\nu)\frac{d\cos\theta_\mu}{2}\frac{d\cos\theta_V}{2} \\ \times \left(1 \pm \frac{s - 2m_\tau^2}{s + 2m_\tau^2} A_P \cos\theta_\mu \cos\theta_V \right), \end{aligned} \quad (4.47)$$

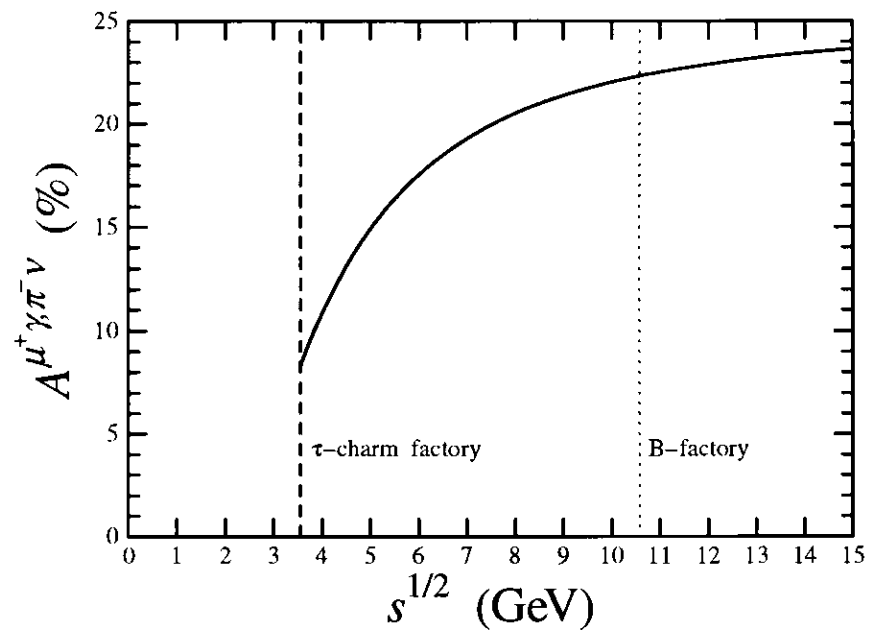


Figure 4.3: The observable asymmetry $A^{\mu^+\gamma\pi^-\nu}$ vs \sqrt{s} for $A_P = -1$. The dashed line represents the \sqrt{s} of τ -charm factory and the dotted line represents that of B-factory.

where + corresponds to the vector mesons with transverse polarization $V = \rho(T)$, $a_1(T)$ and - corresponds to those with longitudinal polarization $V = \rho(L)$, $a_1(L)$. For leptonic decay, we obtain

$$\begin{aligned} d\sigma(e^+e^- \rightarrow \tau^+\tau^- \rightarrow \mu^+\gamma + l^-\bar{\nu}l) \\ = \sigma(e^+e^- \rightarrow \tau^+\tau^-)B(\tau^+ \rightarrow \mu^+\gamma)B(\tau^- \rightarrow l^-\bar{\nu}l)\frac{d\cos\theta_\mu}{2}\frac{d\cos\theta_l}{2}dx2x^2 \\ \times \left\{ 3 - 2x - \frac{s - 2m_\tau^2}{s + 2m_\tau^2}(1 - 2x)A_P \cos\theta_\mu \cos\theta_l \right\}. \end{aligned} \quad (4.48)$$

The measurement of the polarization of the vector mesons can be done by the analysis of the distribution of the two (or three) pions from the ρ (a_1) meson decay [61].

In the case of τ^- decays into $\mu^-\gamma$ and τ^+ decays via $V - A$ interaction, the $dR_a^{\tau^- \rightarrow fA}$ and $dR_b^{\tau^+ \rightarrow fB}$ acquire extra minus signs. For example,

$$dR_a^{\tau^- \rightarrow \mu^-\gamma} = -\frac{d\Omega'_\mu}{4\pi} \frac{1}{\Gamma} \frac{2}{\pi} G_F^2 m_\tau^5 (|A_L^\tau|^2 - |A_R^\tau|^2) \begin{pmatrix} \sin\theta'_\mu \cos\phi'_\mu \\ \sin\theta'_\mu \sin\phi'_\mu \\ \cos\theta'_\mu \end{pmatrix}, \quad (4.49)$$

$$dR_b^{\tau^+ \rightarrow \pi^+\bar{\nu}} = -\frac{d\Omega'_\pi}{4\pi} \frac{1}{\Gamma} \frac{1}{8\pi} |V_{ud}|^2 f_\pi^2 G_F^2 m_\tau^3 \begin{pmatrix} \sin\theta'_\pi \cos\phi'_\pi \\ \sin\theta'_\pi \sin\phi'_\pi \\ \cos\theta'_\pi \end{pmatrix}, \quad (4.50)$$

where (θ'_μ, ϕ'_μ) ((θ'_π, ϕ'_π)) are the polar angle of the muon (pion) momentum in Frame 3 (Frame 2). The formula in eq.(4.42) can be applied to the $\tau^- \rightarrow \mu^-\gamma$ case by the replacement of (θ_μ, θ_π) by $(\theta'_\mu, \theta'_\pi)$, and therefore same angular and energy correlation holds as in the $\tau^+ \rightarrow \mu^+\gamma$ case. In a similar way, we can obtain the formulae corresponds to eqs.(4.47) and (4.48) for the $\tau^- \rightarrow \mu^-\gamma$ case by replacement of (θ_V, θ_l) by (θ'_V, θ'_l) , where θ'_V (θ'_l) is the angle between the vector meson (lepton) momentum and τ^+ direction in Frame 2.

4.3 P and T asymmetries in LFV three body τ decays

In this section, we consider LFV three body decays i.e. $\tau \rightarrow 3\mu$, $\tau \rightarrow 3e$, $\tau \rightarrow \mu ee$, and $\tau \rightarrow e\mu\mu$. Within the approximation that the muon and electron masses are neglected,

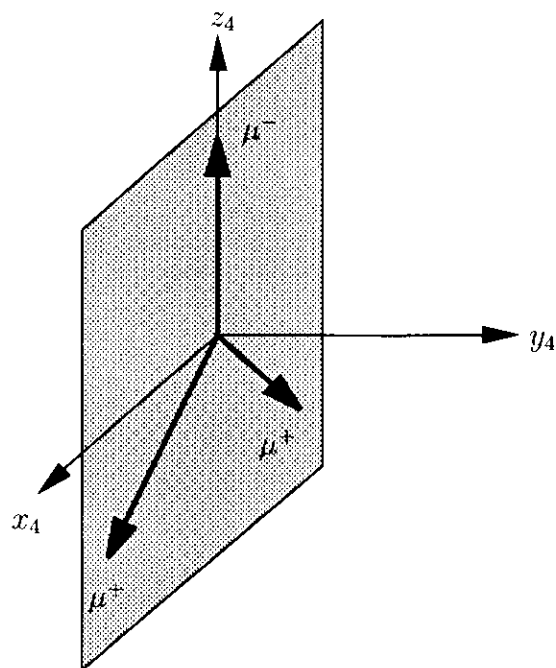


Figure 4.4: The coordinate system in the $\tau \rightarrow 3\mu$ calculation.

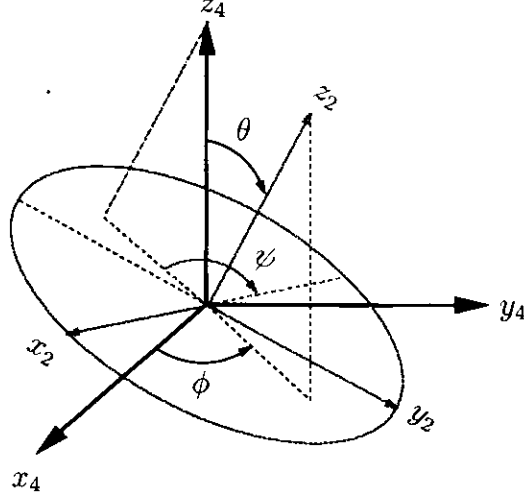


Figure 4.5: The relation between Frame 2 and Frame 4.

$\tau \rightarrow 3\mu$ and $\tau \rightarrow 3e$ (or $\tau \rightarrow \mu ee$ and $\tau \rightarrow e\mu\mu$) give the same formula, so that we only consider $\tau \rightarrow 3\mu$ and $\tau \rightarrow \mu ee$ processes. In these processes, we can define the P odd as well as T odd asymmetries of τ decays.

For $\tau^+ \rightarrow \mu^+\mu^+\mu^-$ decay, the effective Lagrangian is given by

$$\begin{aligned}
\mathcal{L} = & -\frac{4G_F}{\sqrt{2}} \{ m_\tau A_R^\tau \bar{\tau} \sigma^{\mu\nu} P_L \mu F_{\mu\nu} + m_\tau A_L^\tau \bar{\tau} \sigma^{\mu\nu} P_R \mu F_{\mu\nu} \\
& + g_1 (\bar{\tau} P_L \mu) (\bar{\mu} P_L \mu) + g_2 (\bar{\tau} P_R \mu) (\bar{\mu} P_R \mu) \\
& + g_3 (\bar{\tau} \gamma^\mu P_R \mu) (\bar{\mu} \gamma_\mu P_R \mu) + g_4 (\bar{\tau} \gamma^\mu P_L \mu) (\bar{\mu} \gamma_\mu P_L \mu) \\
& + g_5 (\bar{\tau} \gamma^\mu P_R \mu) (\bar{\mu} \gamma_\mu P_L \mu) + g_6 (\bar{\tau} \gamma^\mu P_L \mu) (\bar{\mu} \gamma_\mu P_R \mu) + \text{h.c.} \} . \quad (4.51)
\end{aligned}$$

With this Lagrangian in eq.(4.51), we can calculate the differential branching ratio $dB^{\tau^+ \rightarrow 3\mu}$ and the spin dependence term $dR_b^{\tau^+ \rightarrow 3\mu}$ in eq.(4.1). In order to calculate these quantities we first define the Lorentz frame (Frame 4) for the three body decays [49]. Frame 4 is the rest frame of τ^+ and we take z-direction to be μ^- momentum direction, and xz -plane

to be the decay plane. The x -direction is determined so that the x -component of the momentum for the μ^+ with larger energy is positive. The coordinate system are shown in Fig.4.4. Any four vector in Frame 4 is related to that in Frame 2 by the Euler rotation with three angles (θ, ϕ, ψ) as follows (Fig.4.5):

$$\xi_4^\mu = \begin{pmatrix} 1 & 0 & 0 & 0 \\ 0 & \cos \phi & -\sin \phi & 0 \\ 0 & \sin \phi & \cos \phi & 0 \\ 0 & 0 & 0 & 1 \end{pmatrix} \begin{pmatrix} 1 & 0 & 0 & 0 \\ 0 & \cos \theta & 0 & \sin \theta \\ 0 & 0 & 1 & 0 \\ 0 & -\sin \theta & 0 & \cos \theta \end{pmatrix} \begin{pmatrix} 1 & 0 & 0 & 0 \\ 0 & \cos \psi & -\sin \psi & 0 \\ 0 & \sin \psi & \cos \psi & 0 \\ 0 & 0 & 0 & 1 \end{pmatrix} \xi_2^\mu, \quad (4.52)$$

where

$$0 \leq \theta \leq \pi, \quad 0 \leq \phi \leq 2\pi, \quad 0 \leq \psi \leq 2\pi. \quad (4.53)$$

We also define the energy variables $x_1 = 2E_1/m_\tau$ and $x_2 = 2E_2/m_\tau$ where E_1 (E_2) is the energy of μ^+ with a larger (smaller) energy in the rest frame of τ^+ .

With these angles and energy variables, the branching ratio and spin dependence term can be expressed as follows:

$$dB^{\tau^+ \rightarrow 3\mu} = \frac{1}{\Gamma} \frac{m_\tau^5 G_F^2}{256\pi^5} dx_1 dx_2 d\cos\theta d\phi d\psi X, \quad (4.54)$$

$$dR_b^{\tau^+ \rightarrow 3\mu} = \frac{1}{\Gamma} \frac{m_\tau^5 G_F^2}{256\pi^5} dx_1 dx_2 d\cos\theta d\phi d\psi \times \begin{pmatrix} -Y s_\theta c_\psi + Z(c_\theta c_\phi c_\psi - s_\phi s_\psi) + W(c_\theta s_\phi c_\psi + c_\phi s_\psi) \\ Y s_\theta s_\psi + Z(-c_\theta c_\phi s_\psi - s_\phi c_\psi) + W(-c_\theta s_\phi s_\psi + c_\phi c_\psi) \\ Y c_\theta + Z s_\theta c_\phi + W s_\theta s_\phi \end{pmatrix}, \quad (4.55)$$

where s_θ (s_ϕ , s_ψ) and c_θ (c_ϕ , c_ψ) represent $\sin\theta$ ($\sin\phi$, $\sin\psi$) and $\cos\theta$ ($\cos\phi$, $\cos\psi$), respectively. The functions X , Y , Z , and W are defined as follows:

$$X = \left(\frac{|g_1|^2}{16} + \frac{|g_2|^2}{16} + |g_3|^2 + |g_4|^2 \right) \alpha_1(x_1, x_2) + (|g_5|^2 + |g_6|^2) \alpha_2(x_1, x_2) \\ + (|eA_R^\tau|^2 + |eA_L^\tau|^2) \alpha_3(x_1, x_2) - \text{Re}(eA_R^\tau g_4^* + eA_L^\tau g_3^*) \alpha_4(x_1, x_2) \\ - \text{Re}(eA_R^\tau g_6^* + eA_L^\tau g_5^*) \alpha_5(x_1, x_2), \quad (4.56)$$

$$\begin{aligned}
Y &= \left(\frac{|g_1|^2}{16} - \frac{|g_2|^2}{16} + |g_3|^2 - |g_4|^2 \right) \alpha_1(x_1, x_2) + \text{Re}(eA_R^\tau g_4^* - eA_L^\tau g_3^*) \alpha_4(x_1, x_2) \\
&\quad - \text{Re}(eA_R^\tau g_6^* - eA_L^\tau g_5^*) \alpha_5(x_1, x_2) + (|g_5|^2 - |g_6|^2) \beta_1(x_1, x_2) \\
&\quad + (|eA_R^\tau|^2 - |eA_L^\tau|^2) \beta_2(x_1, x_2) , \tag{4.57}
\end{aligned}$$

$$\begin{aligned}
Z &= (|g_5|^2 - |g_6|^2) \gamma_1(x_1, x_2) + (|eA_R^\tau|^2 - |eA_L^\tau|^2) \gamma_2(x_1, x_2) \\
&\quad - \text{Re}(eA_R^\tau g_4^* - eA_L^\tau g_3^*) \gamma_3(x_1, x_2) + \text{Re}(eA_R^\tau g_6^* - eA_L^\tau g_5^*) \gamma_4(x_1, x_2) , \tag{4.58}
\end{aligned}$$

$$W = -\text{Im}(eA_R^\tau g_4^* + eA_L^\tau g_3^*) \gamma_3(x_1, x_2) + \text{Im}(eA_R^\tau g_6^* + eA_L^\tau g_5^*) \gamma_4(x_1, x_2) , \tag{4.59}$$

where e (> 0) is the positron charge and functions α_{1-5} , β_{1-2} , and γ_{1-4} are given in Appendix D. Notice that the Y and Z terms represent P odd quantities with respect to the τ^+ spin in the rest frame of τ^+ and the W term represents a T odd quantity. These are the same as P and T odd terms considered in the differential decay width of $\mu^+ \rightarrow e^+ e^+ e^-$ [49].

The differential cross section is obtained by substituting this into eq.(4.1). In the case that the opposite side τ decays into $\pi^- \nu$, we obtain after integrating over ϕ_π , ψ , θ_τ , and ϕ_τ

$$\begin{aligned}
&d\sigma(e^+ e^- \rightarrow \tau^+ \tau^- \rightarrow \mu^+ \mu^+ \mu^- + \pi^- \nu) \\
&= \sigma(e^+ e^- \rightarrow \tau^+ \tau^-) B(\tau^- \rightarrow \pi^- \nu) \left(\frac{m_\tau^5 G_F^2}{128\pi^4} / \Gamma \right) \frac{d \cos \theta_\pi}{2} dx_1 dx_2 d \cos \theta d \phi \\
&\quad \times \left[X - \frac{s - 2m_\tau^2}{s + 2m_\tau^2} \{ Y \cos \theta + Z \sin \theta \cos \phi + W \sin \theta \sin \phi \} \cos \theta_\pi \right] . \tag{4.60}
\end{aligned}$$

The terms X , Y , Z , and W can be extracted by the following (asymmetric) integrations.

$$\begin{aligned}
&\int d \cos \theta d \phi d \cos \theta_\pi \frac{d^5 \sigma}{dx_1 dx_2 d \cos \theta d \phi d \cos \theta_\pi} \\
&\times \left\{ \sigma(e^+ e^- \rightarrow \tau^+ \tau^-) B(\tau^- \rightarrow \pi^- \nu) \left(\frac{m_\tau^5 G_F^2}{32\pi^3} / \Gamma \right) \right\}^{-1} = X , \tag{4.61}
\end{aligned}$$

$$\begin{aligned}
&\int d \cos \theta d \cos \theta_\pi w(\cos \theta, \cos \theta_\pi) \frac{d^4 \sigma}{dx_1 dx_2 d \cos \theta d \cos \theta_\pi} \\
&\times \left\{ \sigma(e^+ e^- \rightarrow \tau^+ \tau^-) B(\tau^- \rightarrow \pi^- \nu) \left(\frac{m_\tau^5 G_F^2}{32\pi^3} / \Gamma \right) \right\}^{-1} = -\frac{(s - 2m_\tau^2)}{4(s + 2m_\tau^2)} Y , \tag{4.62}
\end{aligned}$$

$$\int d\phi d\cos\theta_\pi w(\cos\phi, \cos\theta_\pi) \frac{d^4\sigma}{dx_1 dx_2 d\phi d\cos\theta_\pi} \times \left\{ \sigma(e^+e^- \rightarrow \tau^+\tau^-) B(\tau^- \rightarrow \pi^-\nu) \left(\frac{m_\tau^5 G_F^2}{32\pi^3} / \Gamma \right) \right\}^{-1} = -\frac{(s-2m_\tau^2)}{4(s+2m_\tau^2)} Z, \quad (4.63)$$

$$\int d\phi d\cos\theta_\pi w(\sin\phi, \cos\theta_\pi) \frac{d^4\sigma}{dx_1 dx_2 d\phi d\cos\theta_\pi} \times \left\{ \sigma(e^+e^- \rightarrow \tau^+\tau^-) B(\tau^- \rightarrow \pi^-\nu) \left(\frac{m_\tau^5 G_F^2}{32\pi^3} / \Gamma \right) \right\}^{-1} = -\frac{(s-2m_\tau^2)}{4(s+2m_\tau^2)} W. \quad (4.64)$$

Notice that the function W represents CP violating LFV interaction. We can see that this is induced by the relative phase between the photon-penguin coupling constants (A_L^τ and A_R^τ) and the four-fermion coupling constants ($g_3 - g_6$).

A similar formula can be obtained for the $\tau^+ \rightarrow \mu^+e^+e^-$ decay. The effective Lagrangian for the $\tau^+ \rightarrow \mu^+e^+e^-$ is given by

$$\begin{aligned} \mathcal{L} = & -\frac{4G_F}{\sqrt{2}} \{ m_\tau A_R^\tau \bar{\tau} \sigma^{\mu\nu} P_L \mu F_{\mu\nu} + m_\tau A_L^\tau \bar{\tau} \sigma^{\mu\nu} P_R \mu F_{\mu\nu} \\ & + \lambda_1 (\bar{\tau} P_L \mu) (\bar{e} P_L e) + \lambda_2 (\bar{\tau} P_L \mu) (\bar{e} P_R e) \\ & + \lambda_3 (\bar{\tau} P_R \mu) (\bar{e} P_L e) + \lambda_4 (\bar{\tau} P_R \mu) (\bar{e} P_R e) \\ & + \lambda_5 (\bar{\tau} \gamma^\mu P_L \mu) (\bar{e} \gamma_\mu P_L e) + \lambda_6 (\bar{\tau} \gamma^\mu P_L \mu) (\bar{e} \gamma_\mu P_R e) \\ & + \lambda_7 (\bar{\tau} \gamma^\mu P_R \mu) (\bar{e} \gamma_\mu P_L e) + \lambda_8 (\bar{\tau} \gamma^\mu P_R \mu) (\bar{e} \gamma_\mu P_R e) \\ & + \lambda_9 (\bar{\tau} \sigma^{\mu\nu} P_L \mu) (\bar{e} \sigma_{\mu\nu} e) + \lambda_{10} (\bar{\tau} \sigma^{\mu\nu} P_R \mu) (\bar{e} \sigma_{\mu\nu} e) + \text{h.c.} \} . \quad (4.65) \end{aligned}$$

In this calculation, we define Frame 4' which is almost the same as Frame 4 in the $\tau^+ \rightarrow \mu^+\mu^+\mu^-$ case. The definition is obtained by the replacement of μ^- of $\tau^+ \rightarrow \mu^+\mu^+\mu^-$ by e^- of $\tau^+ \rightarrow \mu^+e^+e^-$, the μ^+ with a larger energy of $\tau^+ \rightarrow \mu^+\mu^+\mu^-$ by μ^+ of $\tau^+ \rightarrow \mu^+e^+e^-$, and μ^+ with a smaller energy of $\tau^+ \rightarrow \mu^+\mu^+\mu^-$ by e^+ of $\tau^+ \rightarrow \mu^+e^+e^-$. If we take the definition of (θ, ϕ, ψ) in such a way that the same relation is satisfied as in eq.(4.52), the branching ratio and the spin dependence term are given by

$$dB^{\tau^+ \rightarrow \mu^+e^+e^-} = \frac{1}{\Gamma} \frac{m_\tau^5 G_F^2}{256\pi^5} dx_1 dx_2 d\cos\theta d\phi d\psi X', \quad (4.66)$$

$$dR_b^{\tau^+ \rightarrow \mu^+ e^+ e^-} = \frac{1}{\Gamma} \frac{m_\tau^5 G_F^2}{256\pi^5} dx_1 dx_2 d\cos\theta d\phi d\psi$$

$$\times \begin{pmatrix} -Y' s_\theta c_\psi + Z'(c_\theta c_\phi c_\psi - s_\phi s_\psi) + W'(c_\theta s_\phi c_\psi + c_\phi s_\psi) \\ Y' s_\theta s_\psi + Z'(-c_\theta c_\phi s_\psi - s_\phi c_\psi) + W'(-c_\theta s_\phi s_\psi + c_\phi c_\psi) \\ Y' c_\theta + Z' s_\theta c_\phi + W' s_\theta s_\phi \end{pmatrix}, \quad (4.67)$$

where the functions X' , Y' , Z' , and W' are given by

$$X' = (|eA_R^\tau|^2 + |eA_L^\tau|^2) A_1(x_1, x_2) + \text{Re}(eA_R^\tau \lambda_5^* + eA_L^\tau \lambda_8^*) A_2(x_1, x_2)$$

$$+ \text{Re}(eA_R^\tau \lambda_6^* + eA_L^\tau \lambda_7^*) A_3(x_2) + (|\lambda_1|^2 + |\lambda_2|^2 + |\lambda_3|^2 + |\lambda_4|^2) A_4(x_1)$$

$$+ (|\lambda_5|^2 + |\lambda_8|^2) A_5(x_1, x_2) + (|\lambda_6|^2 + |\lambda_7|^2) A_6(x_2)$$

$$+ (|\lambda_9|^2 + |\lambda_{10}|^2) A_7(x_1, x_2) + \text{Re}(\lambda_1 \lambda_9^* + \lambda_4 \lambda_{10}^*) A_8(x_1, x_2), \quad (4.68)$$

$$Y' = -\text{Re}(eA_R^\tau \lambda_5^* - eA_L^\tau \lambda_8^*) A_2(x_1, x_2) + \text{Re}(eA_R^\tau \lambda_6^* - eA_L^\tau \lambda_7^*) A_3(x_1, x_2)$$

$$- (|\lambda_5|^2 - |\lambda_8|^2) A_5(x_1, x_2) + (|eA_R^\tau|^2 - |eA_L^\tau|^2) B_1(x_1, x_2)$$

$$+ (|\lambda_1|^2 + |\lambda_2|^2 - |\lambda_3|^2 - |\lambda_4|^2) B_2(x_1, x_2) + (|\lambda_6|^2 - |\lambda_7|^2) B_3(x_1, x_2)$$

$$+ (|\lambda_9|^2 - |\lambda_{10}|^2) B_4(x_1, x_2) + \text{Re}(\lambda_1 \lambda_9^* - \lambda_4 \lambda_{10}^*) B_5(x_1, x_2), \quad (4.69)$$

$$Z' = (|eA_R^\tau|^2 - |eA_L^\tau|^2) C_1(x_1, x_2) + \text{Re}(eA_R^\tau \lambda_5^* - eA_L^\tau \lambda_8^*) C_2(x_1, x_2)$$

$$+ \text{Re}(eA_R^\tau \lambda_6^* - eA_L^\tau \lambda_7^*) C_3(x_1, x_2) + (|\lambda_1|^2 + |\lambda_2|^2 - |\lambda_3|^2 - |\lambda_4|^2) C_4(x_1, x_2)$$

$$+ \{|\lambda_6|^2 - |\lambda_7|^2 + \text{Re}(-2\lambda_1 \lambda_9^* + 2\lambda_4 \lambda_{10}^*)\} C_5(x_1, x_2)$$

$$+ (|\lambda_9|^2 - |\lambda_{10}|^2) C_6(x_1, x_2), \quad (4.70)$$

$$W' = \text{Im}(eA_R^\tau \lambda_5^* + eA_L^\tau \lambda_8^*) C_2(x_1, x_2) + \text{Im}(eA_R^\tau \lambda_6^* + eA_L^\tau \lambda_7^*) C_3(x_1, x_2)$$

$$+ \text{Im}(\lambda_1 \lambda_9^* + \lambda_4 \lambda_{10}^*) C_7(x_1, x_2). \quad (4.71)$$

The functions A_{1-7} , B_{1-4} , C_{1-6} are given in Appendix D. The X' , Y' , Z' , and W' can be extracted in the same way as in eqs.(4.61)-(4.64).

Next we consider the decay mode of $\tau^+ \rightarrow \mu^- e^+ e^+$. This case is different from above in the point that both $\tau \rightarrow e$ and $\mu \rightarrow e$ transitions are necessary. The effective Lagrangian for this process is given by

$$\begin{aligned} \mathcal{L} = & -\frac{4G_F}{\sqrt{2}} \{g'_1(\bar{\tau}P_L e)(\bar{\mu}P_L e) + g'_2(\bar{\tau}P_R e)(\bar{\mu}P_R e) \\ & + g'_3(\bar{\tau}\gamma^\mu P_R e)(\bar{\mu}\gamma_\mu P_R e) + g'_4(\bar{\tau}\gamma^\mu P_L e)(\bar{\mu}\gamma_\mu P_L e) \\ & + g'_5(\bar{\tau}\gamma^\mu P_R e)(\bar{\mu}\gamma_\mu P_L e) + g'_6(\bar{\tau}\gamma^\mu P_L e)(\bar{\mu}\gamma_\mu P_R e) + \text{h.c.}\} . \end{aligned} \quad (4.72)$$

If we take a coordinate system similar to Frame 4, in which the larger (smaller) energy μ^+ is replaced by the larger (smaller) energy e^+ , $dB^{\tau^+ \rightarrow \mu^- e^+ e^+}$ and $dR_b^{\tau^+ \rightarrow \mu^- e^+ e^+}$ are given by

$$dB^{\tau^+ \rightarrow \mu^- e^+ e^+} = \frac{1}{\Gamma} \frac{m_\tau^5 G_F^2}{256\pi^5} dx_1 dx_2 d\cos\theta d\phi d\psi X'' , \quad (4.73)$$

$$\begin{aligned} dR_b^{\tau^+ \rightarrow \mu^+ e^+ e^-} = & \frac{1}{\Gamma} \frac{m_\tau^5 G_F^2}{256\pi^5} dx_1 dx_2 d\cos\theta d\phi d\psi \\ & \times \begin{pmatrix} -Y'' s_\theta c_\psi + Z''(c_\theta c_\phi c_\psi - s_\phi s_\psi) \\ Y'' s_\theta s_\psi + Z''(-c_\theta c_\phi s_\psi - s_\phi c_\psi) \\ Y'' c_\theta + Z'' s_\theta c_\phi \end{pmatrix} , \end{aligned} \quad (4.74)$$

where functions X'' , Y'' , and Z'' are given by

$$X'' = \left(\frac{|g'_1|^2}{16} + \frac{|g'_2|^2}{16} + |g'_3|^2 + |g'_4|^2 \right) \alpha_1(x_1, x_2) + (|g'_5|^2 + |g'_6|^2) \alpha_2(x_1, x_2) , \quad (4.75)$$

$$Y'' = \left(\frac{|g'_1|^2}{16} - \frac{|g'_2|^2}{16} + |g'_3|^2 - |g'_4|^2 \right) \alpha_1(x_1, x_2) + (|g'_5|^2 - |g'_6|^2) \beta_1(x_1, x_2) , \quad (4.76)$$

$$Z'' = (|g'_5|^2 - |g'_6|^2) \gamma_1(x_1, x_2) , \quad (4.77)$$

where α_{1-2} , β_1 , and γ_1 are the same functions that we defined in $\tau^+ \rightarrow \mu^+ \mu^+ \mu^-$ calculation. X'' , Y'' , and Z'' can be extracted by asymmetric integrations as before, but we cannot obtain information on CP violation in this case.

Notice that the above three cases exhaust all possibilities in the three body decay of τ to e and/or μ as long as we neglect the electron and muon masses compared to the τ

mass. Namely, the formula for other cases can be obtained by appropriate replacements of e and/or μ .

The formulae for LFV decays with τ^- can be obtained in a similar substitution as the $\tau \rightarrow \mu\gamma$ case. Using appropriate angles of τ^- decay in Frame 3 and τ^+ decay in Frame 2, dR_b gets an extra minus sign in eqs.(4.55), (4.67), and (4.74).

4.4 $\tau \rightarrow \mu\nu\bar{\nu}\gamma$ process and background suppressions

In this section, we consider the background processes for the $\tau \rightarrow \mu\gamma$ search, and we show that the measurement of angular distributions is useful in identifying the background process. In the muon decay, the physical background can be suppressed if we use polarized muons [62]. In the following, we show a similar suppression mechanism holds for τ decay if we use the spin correlation.

One of the main background for the $\tau \rightarrow \mu\gamma$ search comes from the kinematical endpoint region of the $\tau \rightarrow \mu\nu\bar{\nu}\gamma$ process where two neutrinos carry out a little energy at the rest frame of τ . In the following, we assume that τ^+ decays into $\mu^+\nu\bar{\nu}\gamma$ and τ^- decays through one of hadronic and leptonic decay processes. For the τ^- decay, the differential branching ratio and the spin dependence term are given in eqs.(4.28)–(4.36). For $\tau^+ \rightarrow \mu^+\nu\bar{\nu}\gamma$, these quantities are given by

$$dB^{\text{B.G.}} = \frac{1}{\Gamma} \frac{G_F^2 m_\tau^5 \alpha}{3 \times 2^{11} \pi^5} dx dy dz d\Omega_\mu \sin z \frac{\beta_\mu}{y} F, \quad (4.78)$$

$$dR_b^{\text{B.G.}} = \frac{1}{\Gamma} \frac{G_F^2 m_\tau^5 \alpha}{3 \times 2^{11} \pi^5} dx dy dz d\Omega_\mu \sin z \frac{\beta_\mu}{y} \times (-\beta_\mu G + H \cos z) \begin{pmatrix} \sin \theta_\mu \cos \phi_\mu \\ \sin \theta_\mu \sin \phi_\mu \\ \cos \theta_\mu \end{pmatrix}, \quad (4.79)$$

where x and y are the muon and photon energies normalized by $m_\tau/2$, respectively, and (θ_μ, ϕ_μ) is the polar coordinate of the unit vector of the muon momentum direction, all defined in the rest frame of τ^+ (Frame 2). $\beta_\mu = \sqrt{1 - 4r/x^2}$ with $r \equiv m_\mu^2/m_\tau^2$. The

angle z is defined by $z \equiv \pi - \theta_{\mu\gamma}$, where $\theta_{\mu\gamma}$ is the angle between the muon and photon momentum in the same frame. These quantities can be obtained by a simple replacement from the formula of the differential decay width for the radiative muon decay presented in Ref. [63]. For completeness, the functions F , G , and H are given in Appendix D.

The background comes from the kinematical region near $x = 1 + r$ and $y = 1 - r$, at which the branching fraction vanishes. However, with finite detector resolutions, this kinematical region gives physical backgrounds. If we take the signal region as $1 + r - \delta x \leq x \leq 1 + r$ and $1 - r - \delta y \leq y \leq 1 - r$, the leading terms of the branching ratio and spin dependence term expanded in terms of r , δx , and δy , after integrating over z , are given by

$$dB^{\text{B.G.}} \simeq \frac{1}{\Gamma} \frac{G_{\text{F}}^2 m_{\tau}^5 \alpha}{3 \times 2^{11} \pi^5} d\Omega_{\mu} \left(\delta x^4 \delta y^2 + \frac{8}{3} \delta x^3 \delta y^3 \right), \quad (4.80)$$

$$dR_b^{\text{B.G.}} \simeq \frac{1}{\Gamma} \frac{G_{\text{F}}^2 m_{\tau}^5 \alpha}{3 \times 2^{11} \pi^5} d\Omega_{\mu} \left(-\delta x^4 \delta y^2 + \frac{8}{3} \delta x^3 \delta y^3 \right) \begin{pmatrix} \sin \theta_{\mu} \cos \phi_{\mu} \\ \sin \theta_{\mu} \sin \phi_{\mu} \\ \cos \theta_{\mu} \end{pmatrix}. \quad (4.81)$$

Then after integrating over ϕ_{μ} , ϕ_{π} , ϕ_{τ} , and θ_{τ} , the differential cross section for $e^+e^- \rightarrow \tau^+\tau^- \rightarrow \mu^+\nu\bar{\nu}\gamma + \pi^-\nu$ is given by

$$\begin{aligned} d\sigma(e^+e^- \rightarrow \tau^+\tau^- \rightarrow \mu^+\nu\bar{\nu}\gamma + \pi^-\nu) \\ = \sigma(e^+e^- \rightarrow \tau^+\tau^-) B(\tau^- \rightarrow \pi^-\nu) \left(\frac{G_{\text{F}}^2 m_{\tau}^5 \alpha}{3 \times 2^9 \pi^4} / \Gamma \right) \frac{d \cos \theta_{\mu}}{2} \frac{d \cos \theta_{\pi}}{2} \\ \times \left\{ \left(\delta x^4 \delta y^2 + \frac{8}{3} \delta x^3 \delta y^3 \right) - \frac{s - 2m_{\tau}^2}{s + 2m_{\tau}^2} \left(-\delta x^4 \delta y^2 + \frac{8}{3} \delta x^3 \delta y^3 \right) \cos \theta_{\mu} \cos \theta_{\pi} \right\}. \end{aligned} \quad (4.82)$$

If the photon energy resolution is worse than the muon energy resolution, the term $\delta x^4 \delta y^2$ is small compared to $(8/3)\delta x^3 \delta y^3$. In such a case, the angular distribution is similar to the $A_R^{\tau} = 0$, $A_L^{\tau} \neq 0$ case of the $\tau \rightarrow \mu\gamma$ angular distribution. See eqs.(4.25), (4.26), and (4.42). This feature is useful for the background suppressions for $\tau^+ \rightarrow \mu_R^+ \gamma$ search because signal and background processes have different angular correlation. For $\tau^+ \rightarrow \mu_L^+ \gamma$ search,

the signal to background ratio is almost the same even if we take into account angular correlation.

A similar background suppression works for $\tau \rightarrow e\gamma$ case because eqs.(4.80) and (4.81) do not include the mass of the muon explicitly.

4.5 Summary and Discussion

In this chapter, we have calculated the differential cross sections of $e^+e^- \rightarrow \tau^+\tau^- \rightarrow f_B f_A$ processes, where one of τ 's decays through LFV processes. Using spin correlations of $\tau^+\tau^-$, we show that the P odd asymmetry of $\tau \rightarrow \mu\gamma$ and $\tau \rightarrow e\gamma$ and P and T asymmetries of three body LFV decays of τ can be obtained by angular correlations. These P and T odd quantities are important to identify a model of new physics responsible for LFV processes.

We have also considered the background suppression of the $\tau \rightarrow \mu\gamma$ and $\tau \rightarrow e\gamma$ search by the angular distributions. We see that the analysis of the angular distributions are useful for the $\tau^+ \rightarrow \mu_R^+\gamma$ ($\tau^- \rightarrow \mu_L^-\gamma$) and $\tau^+ \rightarrow e_R^+\gamma$ ($\tau^- \rightarrow e_L^-\gamma$) searches.

We would like to give a rough estimate on the number of $\tau^+\tau^-$ pairs needed for the asymmetry measurement at the B-factory energy. As an example, we take $\tau \rightarrow \mu\gamma$ process for LFV decay and $\tau \rightarrow \pi\nu$, $\rho\nu$, and $a_1(\rightarrow \pi^\pm\pi^\mp\pi^\mp)\nu$ for the opposite side τ decay. For $\tau \rightarrow \pi\nu$, we use the angular distribution in eq.(4.42). In $\tau \rightarrow \rho\nu$ and $\tau \rightarrow a_1\nu$, we have to look at the angular distribution of two or three pions in addition to the $\cos\theta_\mu$ and $\cos\theta_V$ distributions in order to use the information on the ρ and a_1 polarizations. With help of optimized observable quantities defined in ref. [64], the statistical errors for the determination of the parameter A_P with N signal events are $3.4/\sqrt{N}$, $4.6/\sqrt{N}$, and $9.5/\sqrt{N}$ for $\tau \rightarrow \pi\nu$, $\tau \rightarrow \rho\nu$, and $\tau \rightarrow a_1\nu$, respectively. The combined error is then given by

$$\sigma_{A_P} = \frac{1}{\sqrt{2N_\tau B_{\tau \rightarrow \mu\gamma}}} \left(\frac{\epsilon_\pi B_\pi}{3.4^2} + \frac{\epsilon_\rho B_\rho}{4.6^2} + \frac{\epsilon_{a_1} B_{a_1}}{9.5^2} \right)^{-1/2}, \quad (4.83)$$

where ϵ_π , ϵ_ρ , and ϵ_{a_1} are the signal selection efficiencies for these modes, and $B_{\tau \rightarrow \mu\gamma}$, B_π ,

B_ρ , and B_{a_1} are the τ decay branching ratios, namely $B_{\tau \rightarrow \mu\gamma} = B(\tau \rightarrow \mu\gamma)$, $B_\pi = B(\tau \rightarrow \pi\nu) = 0.11$, $B_\rho = B(\tau \rightarrow \rho\nu) = 0.25$, and $B_{a_1} = B(\tau \rightarrow a_1\nu \rightarrow \pi^\pm\pi^\mp\pi^\mp\nu) = 0.09$. N_τ is the total number of τ pair. If we assume the $B(\tau \rightarrow \mu\gamma)$ is 1×10^{-6} , which is just below the current experimental bound [35], and the signal selection efficiency is 10–20%, $(2.5 - 5) \times 10^8$ $\tau^+\tau^-$ pairs are required in order to distinguish $A_P = +1$ and -1 at 3σ level. This number means that the on-going B-factory experiments could provide useful information on LFV interaction if the $B(\tau \rightarrow \mu\gamma)$ is close to the current experimental bound.

In this chapter, we only consider τ decay. We can obtain similar information in muon decay experiments if initial muons are polarized. Although highly polarized muons are available experimentally, a special setup for production and transportation of a muon beam is necessary for actual experiment. The advantage of the τ case is that we can extract the information on τ spins by looking at the decay distribution of the other side of τ decay so that we do not need a special requirement for experimental setup.

Chapter 5

Nucleus dependence of muon-electron conversion ratio

We complete the calculation of the $\mu - e$ conversion rate in the nuclei with wide range of atomic numbers by the method of Czarnecki *et al.* We take into account all the operators for the $\mu - e$ transition. With results of this chapter, we can calculate the $\mu - e$ conversion branching ratio in any models for each nucleus. The results of our calculation indicate a tendency that the conversion branching ratio is larger in the nuclei with moderate atomic number than that in the light or heavy nuclei.

5.1 Calculation of conversion rate

In this section, we present a method of the conversion rate calculation. We solve the Dirac equations for the muon and electron in the initial and final state, respectively, and obtain transition amplitudes by integrating the overlap of the both wave functions.

We start the calculation with the most general gauge invariant interaction Lagrangian

which contribute to the $\mu - e$ transition in nuclei as follows:

$$\begin{aligned} \mathcal{L}_{\text{int}} = & -\frac{4G_{\text{F}}}{\sqrt{2}} \{m_{\mu}A_{R\bar{\mu}}\sigma^{\mu\nu}P_{L}eF_{\mu\nu} + m_{\mu}A_{L\bar{\mu}}\sigma^{\mu\nu}P_{R}eF_{\mu\nu} + h.c.\} \\ & -\frac{G_{\text{F}}}{\sqrt{2}} \sum_{q=u,d,s} \left[\begin{aligned} & (g_{LS(q)}\bar{e}P_{R\mu} + g_{RS(q)}\bar{e}P_{L\mu}) \bar{q}q \\ & + (g_{LP(q)}\bar{e}P_{R\mu} + g_{RP(q)}\bar{e}P_{L\mu}) \bar{q}\gamma_5q \\ & + (g_{LV(q)}\bar{e}\gamma^{\mu}P_{L\mu} + g_{RV(q)}\bar{e}\gamma^{\mu}P_{R\mu}) \bar{q}\gamma_{\mu}q \\ & + (g_{LA(q)}\bar{e}\gamma^{\mu}P_{L\mu} + g_{RA(q)}\bar{e}\gamma^{\mu}P_{R\mu}) \bar{q}\gamma_{\mu}\gamma_5q \\ & + \frac{1}{2} (g_{LT(q)}\bar{e}\sigma^{\mu\nu}P_{R\mu} + g_{RT(q)}\bar{e}\sigma^{\mu\nu}P_{L\mu}) \bar{q}\sigma_{\mu\nu}q + h.c. \end{aligned} \right], \quad (5.1) \end{aligned}$$

where G_{F} and m_{μ} are the Fermi constant and the muon mass, respectively, and $A_{L,R}$ and g 's are all dimensionless coupling constants for the corresponding operators. The size of each coupling constant depends on the interaction of the new physics in which the lepton flavor conservation is violated. We use these interaction terms as a perturbation and take the initial and final states to be eigenstates of the QED Hamiltonian.

In the $\mu - e$ conversion process, the initial state is the $1s$ state of the muonic atom and the converted electron escapes from the electric field with the energy of the order of the muon mass. Both the wave functions in the initial and final state can be obtained by solving the Dirac equations in the electric field of the nucleus. The Dirac equation in the central force system is given by [65]

$$W\psi = \left[-i\gamma_5\sigma_r \left(\frac{\partial}{\partial r} + \frac{1}{r} - \frac{\beta}{r}K \right) + V(r) + \beta \right] \psi, \quad (5.2)$$

$$\gamma_5 = \begin{pmatrix} 0 & 1 \\ 1 & 0 \end{pmatrix}, \quad \beta = \begin{pmatrix} 1 & 0 \\ 0 & -1 \end{pmatrix}, \quad \sigma_r = \begin{pmatrix} \boldsymbol{\sigma} \cdot \mathbf{r} & 0 \\ 0 & \boldsymbol{\sigma} \cdot \mathbf{r} \end{pmatrix},$$

$$K = \begin{pmatrix} \boldsymbol{\sigma} \cdot \mathbf{l} + 1 & 0 \\ 0 & -(\boldsymbol{\sigma} \cdot \mathbf{l} + 1) \end{pmatrix}, \quad (5.3)$$

where W and $V(r)$ are the energy and potential in the unit of the reduced mass, respectively, and $\boldsymbol{\sigma}$ and \mathbf{l} are the Pauli matrices and the orbital angular momentum $-i\mathbf{r} \times \nabla$,

respectively. Since the operator K and the z -component of the total angular momentum j_z commute with this Hamiltonian, two eigenvalues of these operators, $-\kappa$ and μ , represent the quantum numbers which describe the wave functions of this system as follows:

$$\psi = \psi_\kappa^\mu = \begin{pmatrix} g(r)\chi_\kappa^\mu(\theta, \phi) \\ if(r)\chi_{-\kappa}^\mu(\theta, \phi) \end{pmatrix}, \quad (5.4)$$

where χ_κ^μ is the normalized eigenfunction of $(\boldsymbol{\sigma} \cdot \mathbf{l} + 1)$ and j_z such as

$$(\boldsymbol{\sigma} \cdot \mathbf{l} + 1)\chi_\kappa^\mu = -\kappa\chi_\kappa^\mu, \quad j_z\chi_\kappa^\mu = \mu\chi_\kappa^\mu, \quad \int_{-1}^1 d\cos\theta \int_0^{2\pi} d\phi \chi_\kappa^{\mu*}\chi_{\kappa'}^{\mu'} = \delta_{\mu\mu'}\delta_{\kappa\kappa'}. \quad (5.5)$$

With the notation of $u_1(r) = rg(r)$ and $u_2(r) = rf(r)$, the Dirac equation for the radial function is given by

$$\frac{d}{dr} \begin{pmatrix} u_1 \\ u_2 \end{pmatrix} = \begin{pmatrix} -\kappa/r & W - V + 1 \\ -(W - V - 1) & \kappa/r \end{pmatrix} \begin{pmatrix} u_1 \\ u_2 \end{pmatrix}. \quad (5.6)$$

For the initial state, the $1s$ state corresponds to the quantum numbers of $\mu = \pm 1/2$ and $\kappa = -1$. We take a normalization of

$$\int d^3x \psi_{1s}^{(\mu)*}(\mathbf{x})\psi_{1s}^{(\mu)}(\mathbf{x}) = 1, \quad (5.7)$$

which means that the wave function describes the state that one muon is trapped in $1s$ orbit of the nuclei. The normalization for the final electron is taken to be

$$\int d^3x \psi_{\kappa, W}^{\mu(e)*}(\mathbf{x})\psi_{\kappa', W'}^{\mu'(e)}(\mathbf{x}) = \delta_{\mu\mu'}\delta_{\kappa\kappa'}2\pi\delta(W - W'), \quad (5.8)$$

which describes the state that one electron is emitted per unit time. With this normalization, the conversion rate ω_{conv} is simply written by the square of the amplitude M , $\omega_{\text{conv}} = |M|^2$, with final state sum and spin average of the initial muon. The amplitude M is obtained from the effective Lagrangian in eq.(5.1) just by replacing the fields with

the wave functions as follows:

$$\begin{aligned}
M = & \frac{4G_F}{\sqrt{2}} \int d^3x \left\{ m_\mu A_R^* \bar{\psi}_{\kappa,W}^{\mu(e)} \sigma^{\alpha\beta} P_R \psi_{1s}^{(\mu)} F_{\alpha\beta} + m_\mu A_L^* \bar{\psi}_{\kappa,W}^{\mu(e)} \sigma^{\alpha\beta} P_L \psi_{1s}^{(\mu)} F_{\alpha\beta} \right\} \\
& + \frac{G_F}{\sqrt{2}} \sum_{q=u,d,s} \int d^3x \left[\left(g_{LS(q)} \bar{\psi}_{\kappa,W}^{\mu(e)} P_R \psi_{1s}^{(\mu)} + g_{RS(q)} \bar{\psi}_{\kappa,W}^{\mu(e)} P_L \psi_{1s}^{(\mu)} \right) \langle N' | \bar{q} q | N \rangle \right. \\
& + \left(g_{LP(q)} \bar{\psi}_{\kappa,W}^{\mu(e)} P_R \psi_{1s}^{(\mu)} + g_{RP(q)} \bar{\psi}_{\kappa,W}^{\mu(e)} P_L \psi_{1s}^{(\mu)} \right) \langle N' | \bar{q} \gamma_5 q | N \rangle \\
& + \left(g_{LV(q)} \bar{\psi}_{\kappa,W}^{\mu(e)} \gamma^\alpha P_L \psi_{1s}^{(\mu)} + g_{RV(q)} \bar{\psi}_{\kappa,W}^{\mu(e)} \gamma^\alpha P_R \psi_{1s}^{(\mu)} \right) \langle N' | \bar{q} \gamma_\alpha q | N \rangle \\
& + \left(g_{LA(q)} \bar{\psi}_{\kappa,W}^{\mu(e)} \gamma^\alpha P_L \psi_{1s}^{(\mu)} + g_{RA(q)} \bar{\psi}_{\kappa,W}^{\mu(e)} \gamma^\alpha P_R \psi_{1s}^{(\mu)} \right) \langle N' | \bar{q} \gamma_\alpha \gamma_5 q | N \rangle \\
& \left. + \frac{1}{2} \left(g_{LT(q)} \bar{\psi}_{\kappa,W}^{\mu(e)} \sigma^{\alpha\beta} P_R \psi_{1s}^{(\mu)} + g_{RT(q)} \bar{\psi}_{\kappa,W}^{\mu(e)} \sigma^{\alpha\beta} P_L \psi_{1s}^{(\mu)} \right) \langle N' | \bar{q} \sigma_{\alpha\beta} q | N \rangle \right], \tag{5.9}
\end{aligned}$$

where $\langle N' |$ and $|N\rangle$ are the final and initial states of the nucleus, respectively. With the notation of eq.(5.4), the muon wave function $\psi_{1s}^{(\mu)}$ is written as follows:

$$\psi_{1s}^{(\mu)}(r, \theta, \phi) = \begin{pmatrix} g_\mu^-(r) \chi_{-1}^{\pm 1/2}(\theta, \phi) \\ i f_\mu^-(r) \chi_1^{\pm 1/2}(\theta, \phi) \end{pmatrix}, \tag{5.10}$$

where upper index $(-)$ of g_μ and f_μ represents the corresponding eigenvalue of κ . By the angular momentum conservation, the electron final states are restricted to following two states for each muon spin.

$$\psi_{\kappa,W}^{\mu(e)}(r, \theta, \phi) = \begin{pmatrix} g_e^-(r) \chi_{-1}^{\pm 1/2}(\theta, \phi) \\ i f_e^-(r) \chi_1^{\pm 1/2}(\theta, \phi) \end{pmatrix}, \quad \begin{pmatrix} g_e^+(r) \chi_1^{\pm 1/2}(\theta, \phi) \\ i f_e^+(r) \chi_{-1}^{\pm 1/2}(\theta, \phi) \end{pmatrix}. \tag{5.11}$$

Neglecting the electron mass, we can find $g_e^+ = i f_e^-$ and $i f_e^+ = g_e^-$.

For the coherent conversion processes in which the final state of the nucleus is the same as initial one, the matrix elements of $\langle N | \bar{q} \gamma_5 q | N \rangle$, $\langle N | \bar{q} \gamma_\alpha \gamma_5 q | N \rangle$, and $\langle N | \bar{q} \sigma_{\alpha\beta} q | N \rangle$ identically vanish. Hereafter, we concentrate on the coherent conversion processes since the fraction of coherent process is generally larger than the non-coherent one by a factor of the mass number of the target nuclei approximately. The non-vanishing matrix elements

$\langle N|\bar{q}q|N\rangle$ and $\langle N|\bar{q}\gamma_\alpha q|N\rangle$ can be expressed by the proton and neutron density ($\rho^{(p)}$ and $\rho^{(n)}$) in nuclei as follows:

$$\langle N|\bar{q}q|N\rangle = Zc_p^{(q)}\rho^{(p)} + (A-Z)c_n^{(q)}\rho^{(n)}, \quad (5.12)$$

$$\langle N|\bar{q}\gamma^0 q|N\rangle = \begin{cases} 2Z\rho^{(p)} + (A-Z)\rho^{(n)} & \text{for } q = u \\ Z\rho^{(p)} + 2(A-Z)\rho^{(n)} & \text{for } q = d \\ 0 & \text{for } q = s \end{cases}, \quad (5.13)$$

$$\langle N|\bar{q}\gamma^i q|N\rangle = 0 \quad (i = 1, 2, 3). \quad (5.14)$$

Here we define coefficients $c_{p,n}^{(q)}$ for scalar operators which are evaluated to be $c_p^{(u)} = c_n^{(d)} = 5.1$, $c_p^{(d)} = c_n^{(u)} = 4.3$, and $c_p^{(s)} = c_n^{(s)} = 2.5$ by Kosmas *et al.* [66]. The normalization for the density functions is

$$\int_0^\infty 4\pi r^2 \rho^{(p,n)}(r) = 1. \quad (5.15)$$

The final formula of the conversion rate can be obtained with the above density functions and the wave functions in eq.(5.10-5.11) as follows:

$$\begin{aligned} \omega_{\text{conv}} = G_F^2 & \left| \frac{4}{\sqrt{2}} m_\mu (A_R^* + A_L^*) \int_0^\infty dr r^2 (-E(r)) (g_e^- f_\mu^- + f_e^- g_\mu^-) \right. \\ & + \frac{1}{2\sqrt{2}} \int_0^\infty dr r^2 (\tilde{g}_{LS}^{(p)} + \tilde{g}_{RS}^{(p)}) Z \rho^{(p)} (g_e^- g_\mu^- - f_e^- f_\mu^-) \\ & + \frac{1}{2\sqrt{2}} \int_0^\infty dr r^2 (\tilde{g}_{LS}^{(n)} + \tilde{g}_{RS}^{(n)}) (A-Z) \rho^{(n)} (g_e^- g_\mu^- - f_e^- f_\mu^-) \\ & + \frac{1}{2\sqrt{2}} \int_0^\infty dr r^2 (\tilde{g}_{LV}^{(p)} + \tilde{g}_{RV}^{(p)}) Z \rho^{(p)} (g_e^- g_\mu^- + f_e^- f_\mu^-) \\ & \left. + \frac{1}{2\sqrt{2}} \int_0^\infty dr r^2 (\tilde{g}_{LV}^{(n)} + \tilde{g}_{RV}^{(n)}) (A-Z) \rho^{(n)} (g_e^- g_\mu^- + f_e^- f_\mu^-) \right|^2 \\ & + \left(A_R \rightarrow -A_R, \tilde{g}_{LS}^{(p,n)} \rightarrow -\tilde{g}_{LS}^{(p,n)}, \tilde{g}_{LV}^{(p,n)} \rightarrow -\tilde{g}_{LV}^{(p,n)} \right), \quad (5.16) \end{aligned}$$

where $E(r)$ is the electric field strength and the coupling constants \tilde{g} 's are defined as

$$\tilde{g}_{LS,RS}^{(p,n)} = \sum_q c_{p,n}^{(q)} g_{LS,RS}^{(q)}, \quad (5.17)$$

$$\tilde{g}_{LV,RV}^{(p)} = 2g_{LV,RV}^{(u)} + g_{LV,RV}^{(d)} , \quad (5.18)$$

$$\tilde{g}_{LV,RV}^{(n)} = g_{LV,RV}^{(u)} + 2g_{LV,RV}^{(d)} . \quad (5.19)$$

5.2 Nucleus dependence of conversion rate

Now we calculate the conversion rate numerically by using eq.(5.16). We use the two- and three-parameter Fermi model, the three-parameter Gaussian model, and the Fourier-Bessel expansion for the proton (charge) densities where the values of the parameters are listed in ref. [67]. From the proton density function, we can calculate the electric field strength in eq.(5.16) and potential in the Dirac equation (5.2) for the muon and electron by solving the Maxwell's equation as follows:

$$E(r) = \frac{Ze}{r^2} \int_0^r r'^2 \rho^{(p)}(r') dr' , \quad (5.20)$$

$$V(r) = -e \int_r^\infty E(r') dr' , \quad (5.21)$$

where $e (> 0)$ is the positron charge. Next, with the above electric potential, we can calculate the muon and electron wave functions by solving the Dirac equation (5.2). In the calculation of the electron wave function, we take that the energy of the electron is equal to the muon mass minus the binding energy. We ignore the recoil of the nucleus which is of the order of m_μ^2/M_N , where M_N is the nucleus mass, and that is negligible compared to the muon mass. After that we can estimate the conversion rate by substituting the obtained wave functions with the normalization of eq.(5.7) and eq.(5.8) into eq.(5.16) and executing the overlap integrals.

As an example, we show the muon and electron wave functions in Ti nucleus in Figure 5.1 and Figure 5.2. We can see that $u_2(\equiv r f_\mu^-)$ have a non-vanishing value in Figure 5.1. Although it is very small compared to the upper component u_1 , the effect for the conversion rate is not negligible as pointed out in ref. [51]. In Figure 5.2, the electron wave functions look like the plane wave solution i.e. $u_1 \propto \sin(m_\mu r)$ and

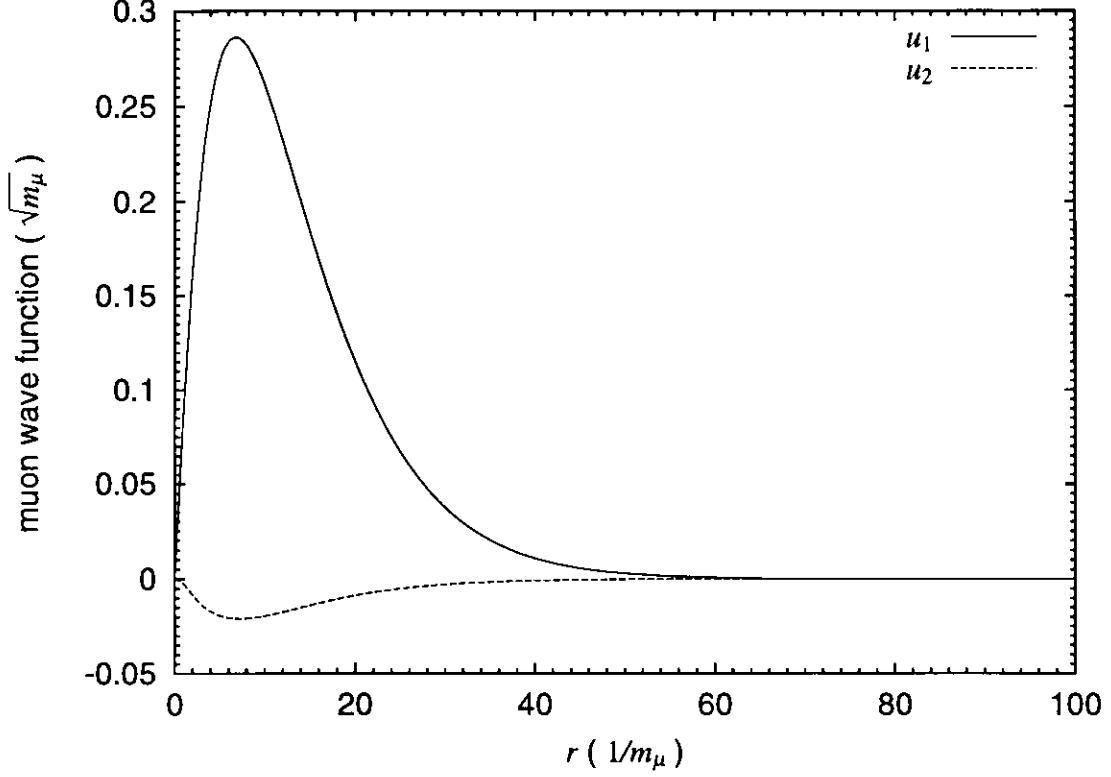


Figure 5.1: The normalized muon wave function in Ti nucleus is plotted. The solid line and dashed line represent $u_1(\equiv r g_\mu^-)$ and $u_2(\equiv r f_\mu^-)$ components, respectively. The horizontal axis is the distance between the nucleus and the muon in the unit of $1/m_\mu$. The unit for the wave function is taken to be $\sqrt{m_\mu}$.

$u_2 \propto (\cos(m_\mu r) - \sin(m_\mu r)/m_\mu r)$. However, it is also pointed out by Shanker [51] that the Coulomb distortion effect becomes extremely important in heavy nuclei.

Now we perform the evaluation of the overlap integrals defined as follows:

$$P = \frac{4}{\sqrt{2}} m_\mu \int_0^\infty dr r^2 (-E(r)) (g_e^- f_\mu^- + f_e^- g_\mu^-), \quad (5.22)$$

$$S^{(p)} = \frac{1}{2\sqrt{2}} \int_0^\infty dr r^2 Z \rho^{(p)} (g_e^- g_\mu^- - f_e^- f_\mu^-), \quad (5.23)$$

$$S^{(n)} = \frac{1}{2\sqrt{2}} \int_0^\infty dr r^2 (A - Z) \rho^{(n)} (g_e^- g_\mu^- - f_e^- f_\mu^-), \quad (5.24)$$

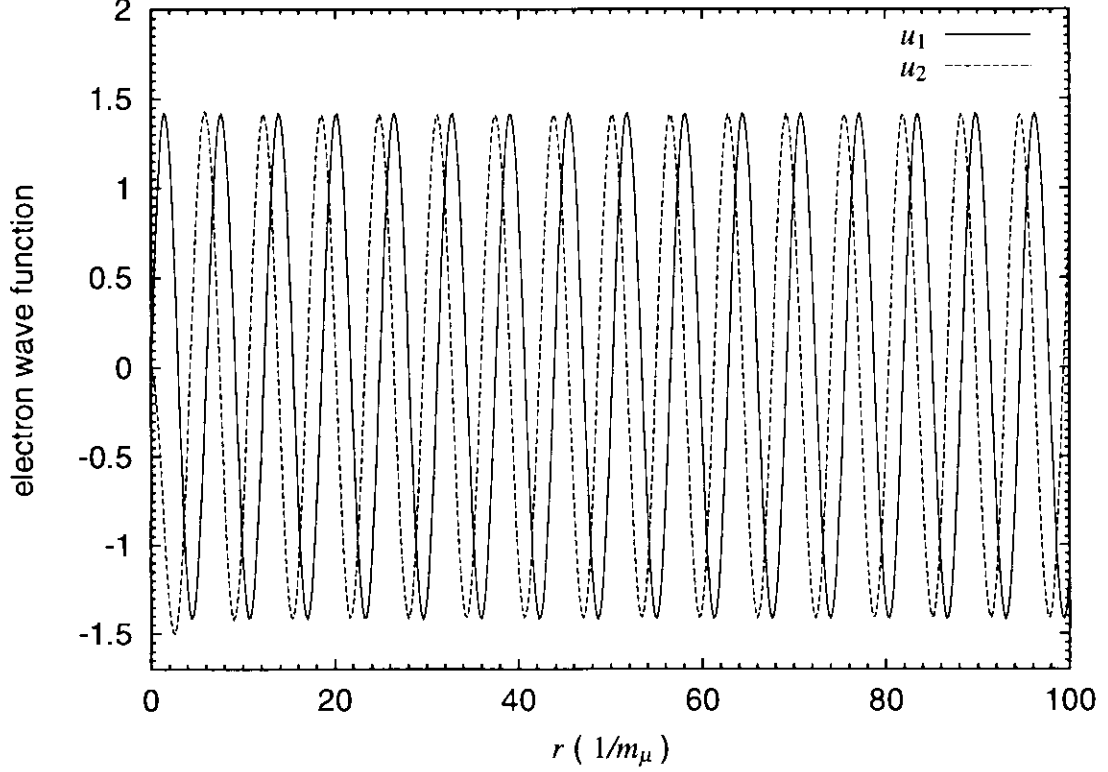


Figure 5.2: The normalized electron wave function in Ti nucleus is plotted. The solid line and dashed line represent $u_1(\equiv r g_e^-)$ and $u_2(\equiv r f_e^-)$ components, respectively. The horizontal axis is the distance between the nucleus and the electron in the unit of $1/m_\mu$.

$$V^{(p)} = \frac{1}{2\sqrt{2}} \int_0^\infty dr r^2 Z \rho^{(p)} (g_e^- g_\mu^- + f_e^- f_\mu^-), \quad (5.25)$$

$$V^{(n)} = \frac{1}{2\sqrt{2}} \int_0^\infty dr r^2 (A - Z) \rho^{(n)} (g_e^- g_\mu^- + f_e^- f_\mu^-). \quad (5.26)$$

With the quantities defined above, the conversion rate in eq.(5.16) is simply expressed as

$$\begin{aligned} \omega_{\text{conv}} = & G_F^2 \left| (A_R^* + A_L^*)P + (\tilde{g}_{LS}^{(p)} + \tilde{g}_{RS}^{(p)})S^{(p)} + (\tilde{g}_{LS}^{(n)} + \tilde{g}_{RS}^{(n)})S^{(n)} \right. \\ & \left. + (\tilde{g}_{LV}^{(p)} + \tilde{g}_{RV}^{(p)})V^{(p)} + (\tilde{g}_{LV}^{(n)} + \tilde{g}_{RV}^{(n)})V^{(n)} \right|^2 \\ & + \left(A_R \rightarrow -A_R, \tilde{g}_{LS}^{(p,n)} \rightarrow -\tilde{g}_{LS}^{(p,n)}, \tilde{g}_{LV}^{(p,n)} \rightarrow -\tilde{g}_{LV}^{(p,n)} \right). \end{aligned} \quad (5.27)$$

The Z dependences of each variable P , $S^{(p,n)}$ and $V^{(p,n)}$ are shown in Figure 5.3 and Table 5.1. With the values in Table 5.1, we can calculate the conversion rate in any high energy models. Here we use the neutron density functions ρ_n listed in ref. [68] which are obtained from the data of πN scattering experiments. Since the values listed in ref. [68] are available only for the selected 19 nuclei, we use the same density as the proton one when the neutron data is lacked in Figure 5.3. Both the values obtained from the data of ref. [68] and in the case of $\rho_n = \rho_p$ are listed in Table 5.1. The neutron and proton density are almost the same for light nuclei because of the isospin symmetry and the fact of $Z \sim N$. Even in the heavy nuclei, the differences are only within 5% in the radius parameter R_p and R_n of the two-parameter Fermi model in ref. [68]. However, we can see in Table 5.1 that the differences in the overlap integrals become more than 20% in heavy nuclei. It shows that the overlap integrals are very sensitive to the input parameters of the nucleon densities.

Figure 5.3 shows that the values are increasing function of Z for the light nuclei and saturate or decrease for the heavy nuclei. This property comes from somewhat accidental suppression of the electron-nucleon form factor at the energy of m_μ as seen below. When we adopt an approximation of the average muon wave function and the plane wave for the electron wave function as done by Weinberg-Feinberg [50], the formula for the overlap integrals are proportional to $\langle\phi_\mu\rangle Z F_p$, where F_p is the form factor defined by

$$F_p = \int_0^\infty dr 4\pi r^2 \rho^{(p)}(r) \frac{\sin m_\mu r}{m_\mu r}, \quad (5.28)$$

and $\langle\phi_\mu\rangle$ is the average value of the muon wave function in the nucleus calculated to be

$$\langle\phi_\mu\rangle^2 = \int_0^\infty dr 4\pi r^2 (g_\mu^2 + f_\mu^2) \rho^{(p)} = \frac{4m_\mu^3 \alpha^3 Z_{\text{eff}}^4}{Z}. \quad (5.29)$$

The last expression is the standard definition of Z_{eff} . With Z_{eff} , the overlap integrals are proportional to $Z_{\text{eff}}^2 Z^{1/2} F_p$. Z_{eff} is the effective charge which the muon in the 1s state feels. For the heavy nuclei, the muon does not see the whole charge of the nuclei Z since the muon wave function enter into the inside of the charge distribution of the nuclei. Z_{eff} thus does not increase linearly with respect to Z as shown in Figure 5.4. However, since Z_{eff}

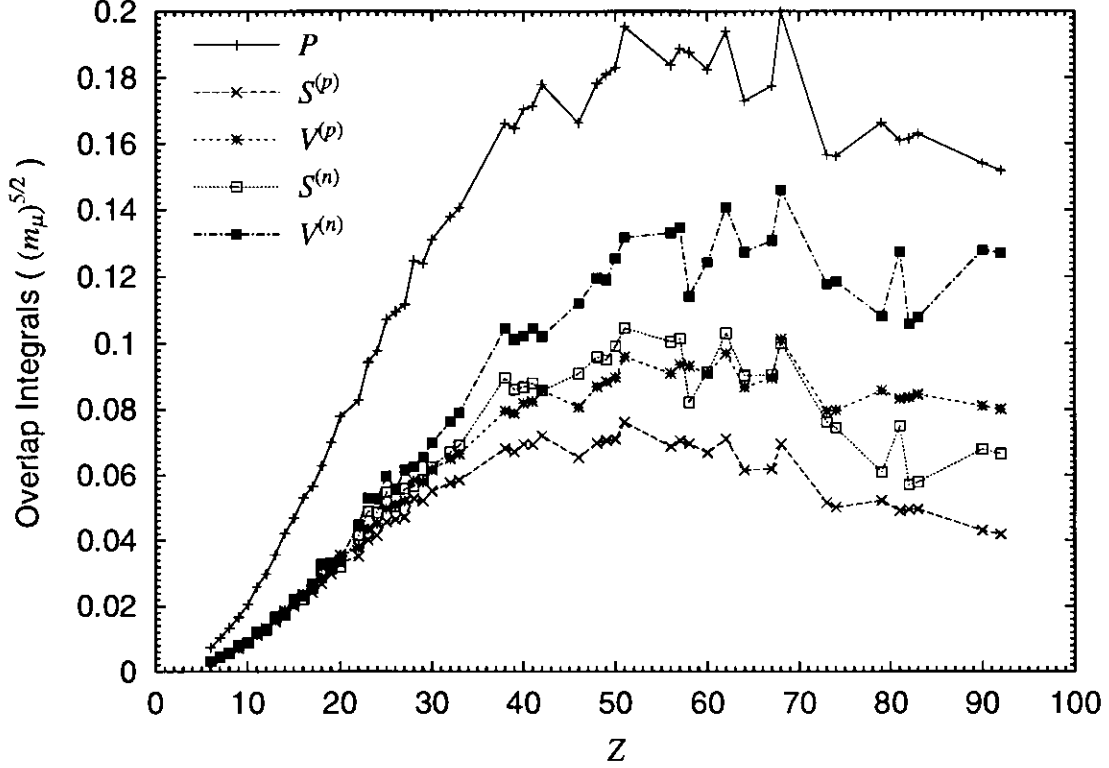


Figure 5.3: The Z dependence of the overlap integrals are plotted.

is still an increasing function, the saturating property of the overlap integral should be understood by properties of the form factor F_p . Figure 5.5 shows the decreasing property of F_p . As mentioned before, these small values for the heavy nuclei are an accidental result caused by a small factor of $\langle \sin(m_\mu r) \rangle$ where $\langle \dots \rangle$ is the mean value in the nuclei. This is also the reason of the sensitivity to the input parameters of the nucleon distributions in heavy nuclei.

As an illustration, we show the Z dependence of the $\mu - e$ conversion to muon capture ratio in a special case that A_L and A_R are much larger than the other coefficients. Now we define following quantity R_Z .

$$\frac{\omega_{\text{conv}}}{\omega_{\text{capt}}} = 384\pi^2 (|A_R|^2 + |A_L|^2) R_Z, \quad (5.30)$$

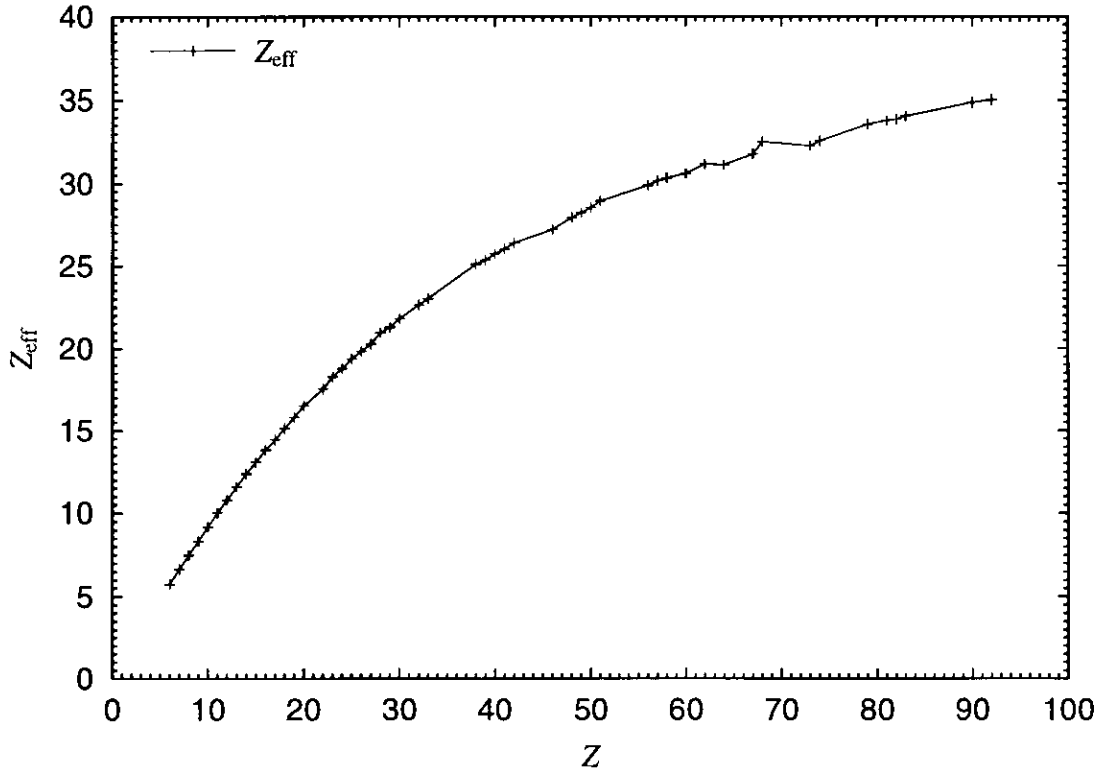


Figure 5.4: The Z dependence of Z_{eff} is plotted.

where ω_{capt} is the muon capture rate and $384\pi^2(|A_R|^2 + |A_L|^2)$ is nothing but the $\mu \rightarrow e\gamma$ decay branching ratio. The quantity R_Z is calculated to be

$$R_Z = \frac{G_F^2 P^2}{192\pi^2 \omega_{\text{capt}}}, \quad (5.31)$$

and shown in Figure 5.6. Here we use the experimental values for the capture rate [69]. We can see that R_Z varies in the range of 0.002 to 0.006 and moderate number of Z like $30 \lesssim Z \lesssim 60$ is preferred for the experiments. The maximum value is 0.00545 for Sr ($Z = 38$).

Now we comment on the comparison with the previous calculation. In the Weinberg-Feinberg calculation, they ignored the relativistic effects, the Coulomb distortion, and the binding energy of the muon [50]. The approximate capture rates and form factors are used

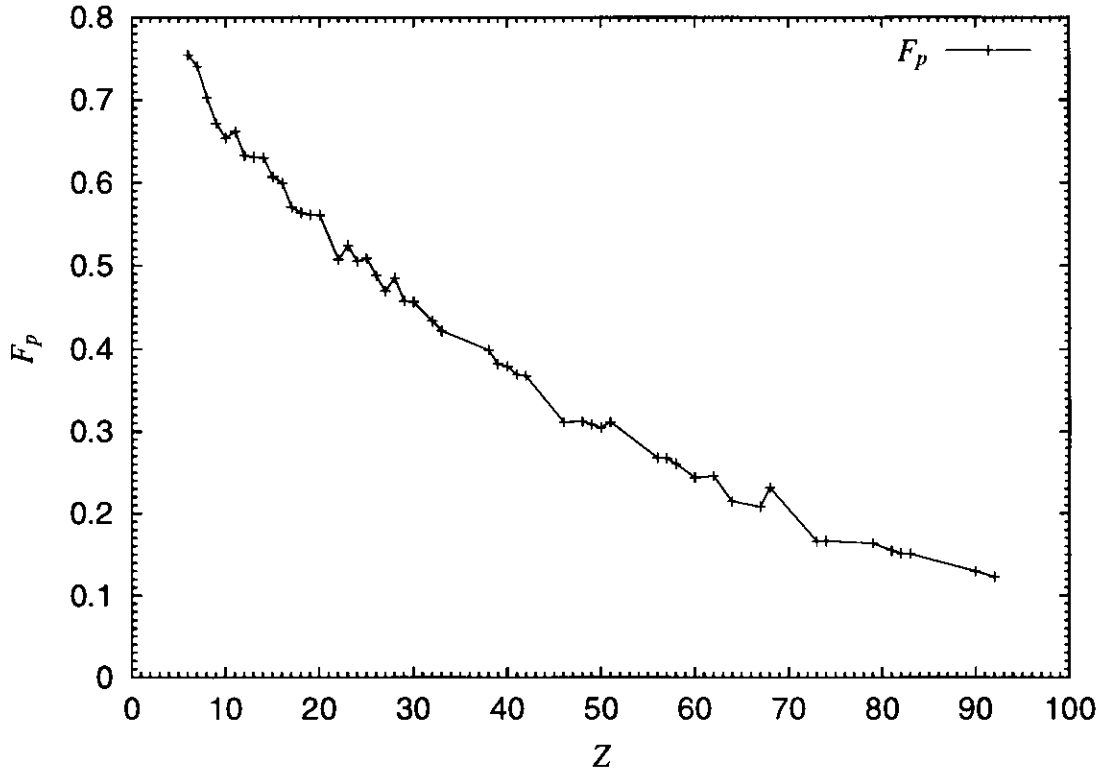


Figure 5.5: The Z dependence of the form factor F_p is plotted.

for the numerical evaluation. By replacing the approximate values with the experimental one, we can obtain a similar behavior to our results shown in Figure 5.6 (long dashed line). Shanker gave correction factors for the Weinberg-Feinberg formula [51]. We also re-evaluated the correction factors by using the updated proton density functions instead of the approximate formula used in Shanker's calculation. The correction gives positive contributions to the R_Z^{WF} (dashed line in Figure 5.6). Another calculation is further done by Czarnecki *et al.* in which the correction to R_Z^{WF} is negative by a correct treatment for the photonic dipole operators in Al, Ti, and Pb nuclei [52]. We can reproduce their results within a good accuracy (See three boxes in Figure 5.6). However, our results conflict with the calculation by Kosmas in which the conversion ratio have a monotonically increasing

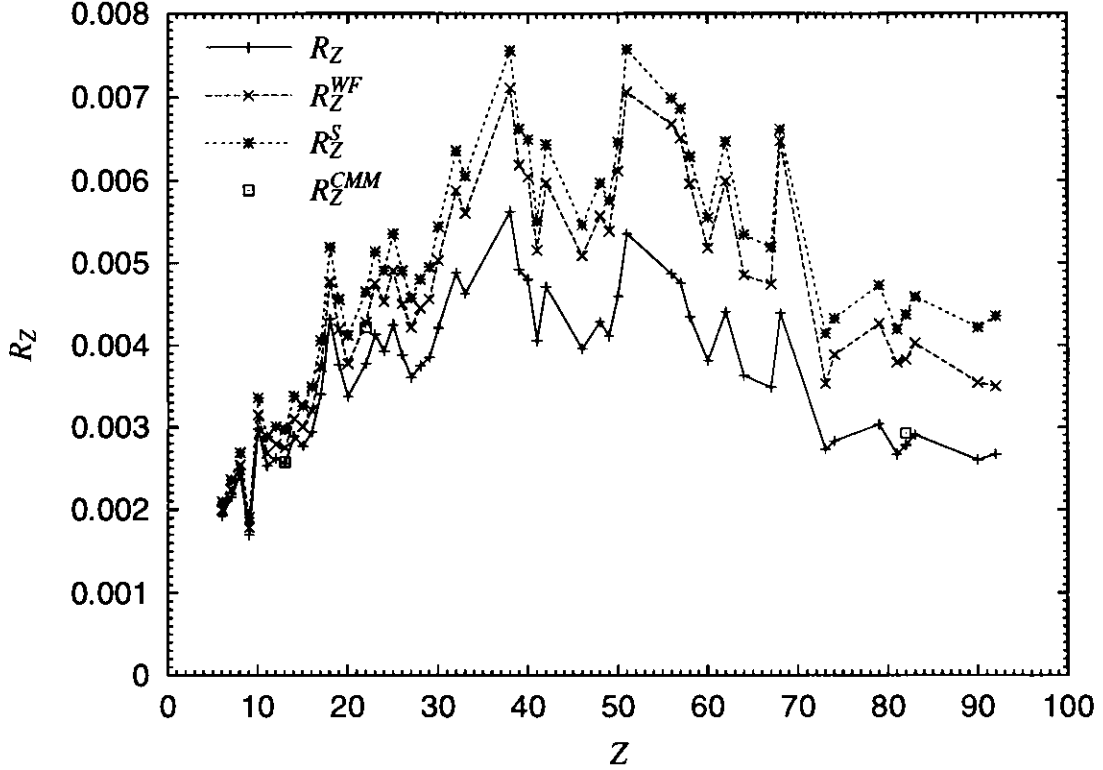


Figure 5.6: The Z dependence of the $\mu - e$ conversion branching ratio divided by the $\mu \rightarrow e\gamma$ decay branching ratio is plotted. R_Z , R_Z^{WF} , R_Z^S , and R_Z^{CMM} represent the results of our calculation, the Weinberg-Feinberg formula, the Shanker evaluation, and Czarnecki *et al.* calculation, respectively.

property with respect to Z [53]. In his analysis, the essential point is that the binding energy cannot be neglected in heavy nuclei and the value of the form factor F_p at the energy of m_μ minus the binding energy ϵ_b is much greater than that at the energy of m_μ for heavy nuclei. Although we could verify this fact, the problem is that the author ignores the Coulomb distortion effect on the electron wave function. Originally $F_p(m_\mu)$ is used as an approximation for the overlap integral of the charge distribution function $\rho^{(p)}$ and the electron wave function in the Coulomb force g_e^- with the energy of $m_\mu - \epsilon_b$. However, this approximation breaks in the heavy nuclei by two reasons. One is the binding energy

effect which is considered in the Kosmas calculation and the other is that the Coulomb distortion effect which is also important for large Z . Both effects are included in the Shanker's correction factors of C_3 which makes the conversion ratio suppress in contrast to the case of considering only the binding energy effect. It follows that solving the Dirac equation for the electron in the Coulomb force is indeed necessary to obtain the correct conversion rates in heavy nuclei, as is done in our calculation.

5.3 Calculation in typical cases

Now we evaluate the conversion ratio in three typical cases of the parameters A and g in the effective Lagrangian of eq.(5.1), and discuss the possibility of the model distinction.

In Figure 5.3, each overlap integrals have different Z dependences especially in heavy nuclei. For example, the scalar ($S^{(p,n)}$) and the vector ($V^{(p,n)}$) type integrals are almost the same values in light nuclei ($Z \lesssim 30$), whereas the ratios of the scalar type integral over the vector type one are enhanced by a factor of more than 1.5 in heavy nuclei. These differences come from the relativistic effects of the muon wave functions which are significant in heavy nuclei. In the limit of ignoring the relativistic effects, namely we ignore the small component of the wave function f_μ^- , the overlap integrals in eqs.(5.23) and (5.25) [eqs.(5.24) and (5.26)] are exactly the same.

Figure 5.7 shows the three typical Z dependence of the $\mu - e$ conversion ratio $B_{\mu e} \equiv \omega_{\text{conv}}/\omega_{\text{capt}}$, where the values are normalized by the conversion ratio in Ti nuclei. The first case (solid line) is that the conversion occurs dominantly through the photonic dipole operator $A_{L,R}$ which is already evaluated in the previous section. This is often the case in SUSY models, especially in SO(10) SUSY GUT models because of the m_τ/m_μ enhancement [22] and in SUSY models with right-handed neutrinos [25]. The long dashed line represents the case of the scalar operator domination. In particular, we take non-vanishing values only for $g_{RS(d)}$ and $g_{LS(d)}$. Such kind of parameter sets are realized in SUSY models with R-parity violation [70]. The third one (dashed line) is for the case of the vector operator domination. This case also appears in SUSY models with R-parity

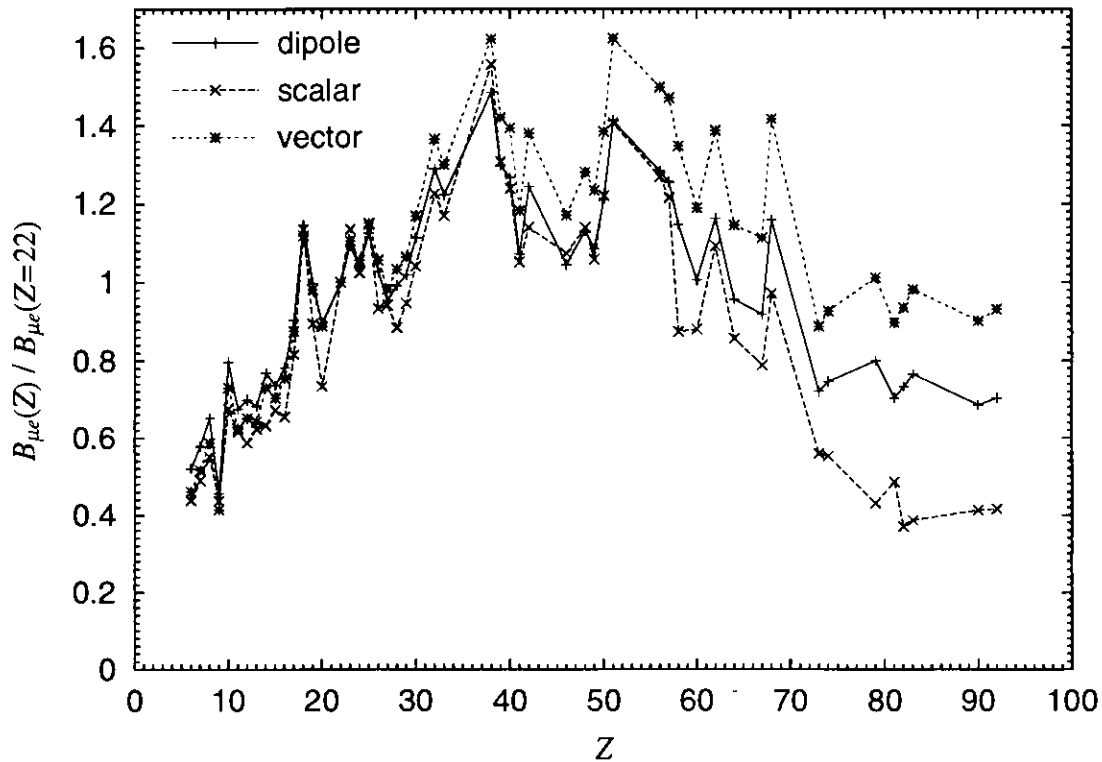


Figure 5.7: The Z dependences of the typical models are plotted. The solid, the long dashed, and the dashed line represent the cases that the photonic dipole, scalar, and vector operator dominates, respectively. We normalize the values by the conversion ratio in Ti nuclei ($Z = 22$).

violation and in a special parameter range of SU(5) SUSY GUT models where the dipole operators $A_{L,R}$ are very suppressed [23]. We take $g_{RV(u)} = -2g_{RV(d)}$ which is the relation of the photon exchange diagrams.

We can see the large differences of the conversion ratio in heavy nuclei in Figure 5.7. This property of the different Z dependences indicates the possibility of distinguishing the models of physics beyond the standard model through several experiments with different targets.

The calculation for the typical models such as SUSY-GUT and SUSY with right-

handed neutrinos is also an important work now. Figure 5.8 is the conversion ratio in Ti nuclei in SU(5) SUSY GUT. Comparing with Figure 2.3 in Chapter 2, the parameter region where the cancellation occurs is different with that of the $\mu \rightarrow e\gamma$ decay. Also, in the $\mu - e$ conversion process, the cancellation point changes when we differ the $\tan\beta$. Figure 5.9 shows the conversion ratio in MSSM with right-handed neutrinos and the masses of the right-handed neutrinos are taken to be $M_N = 10^{14}$ GeV, and the neutrino masses and mixing parameters are chosen so as to account for solar neutrino anomaly by the large angle MSW solution and $U_{MNS}^{e3} = 0.1$. In this model, the difference between the $\mu \rightarrow e\gamma$ decay and the $\mu - e$ conversion is remarkable. In the case of $\tan\beta = 10$, we can see the cancellation point which does not appear in Figure 2.5. This cancellation occurs between the dipole and the vector operators. In the large $\tan\beta$ region, this cancellation disappears because of the $\tan\beta$ enhancements of the dipole operators.

5.4 Summary

We calculated the coherent $\mu - e$ conversion rate in a model independent way. This calculation is important not only for the choice of the target in $\mu - e$ conversion experiments, also for the extraction of information on new physics by comparing the conversion rate among several experiments running with different targets.

In our calculation, we solve the Dirac equations for the muon and electron wave functions in the Coulomb force of the target nuclei. This treatment is especially important for the heavy nuclei where relativistic and Coulomb distortion effects on the wave functions are large.

The numerical results of the overlap integrals for various nuclei are obtained and listed in Table 5.1, so that we can calculate the conversion ratio in general models of physics beyond the standard model.

Z	A	P	$S^{(p)}$	$V^{(p)}$	$S^{(n)}$	$V^{(n)}$	$S^{(n)} _{\rho_p=\rho_n}$	$V^{(n)} _{\rho_p=\rho_n}$
6	12	0.0073	0.0031	0.0031			0.0031	0.0031
7	14	0.0103	0.0044	0.0045			0.0044	0.0045
8	16	0.0133	0.0057	0.0058			0.0057	0.0058
9	19	0.0166	0.0071	0.0073	0.0080	0.0082	0.0079	0.0081
10	20	0.0205	0.0088	0.0090			0.0088	0.0090
11	23	0.0260	0.0111	0.0114	0.0119	0.0122	0.0121	0.0125
12	24	0.0299	0.0128	0.0132	0.0126	0.0131	0.0128	0.0132
13	27	0.0357	0.0153	0.0159	0.0163	0.0169	0.0165	0.0171
14	28	0.0421	0.0181	0.0188	0.0173	0.0180	0.0181	0.0188
15	31	0.0467	0.0200	0.0209			0.0213	0.0223
16	32	0.0529	0.0227	0.0238	0.0221	0.0232	0.0227	0.0238
17	35	0.0564	0.0241	0.0254			0.0256	0.0269
18	40	0.0628	0.0268	0.0284	0.0310	0.0330	0.0328	0.0347
19	39	0.0699	0.0299	0.0317			0.0314	0.0334
20	40	0.0778	0.0333	0.0355	0.0319	0.0341	0.0333	0.0355
22	48	0.0828	0.0351	0.0379			0.0415	0.0448
23	51	0.0942	0.0401	0.0434			0.0488	0.0528
24	52	0.0977	0.0415	0.0451			0.0484	0.0526
25	55	0.1071	0.0456	0.0496			0.0547	0.0596
26	56	0.1095	0.0464	0.0508	0.0503	0.0555	0.0535	0.0586
27	59	0.1116	0.0470	0.0519			0.0558	0.0615
28	58	0.1248	0.0527	0.0583			0.0565	0.0625
29	63	0.1237	0.0520	0.0579	0.0585	0.0653	0.0610	0.0678
30	64	0.1311	0.0550	0.0615			0.0624	0.0697
32	72	0.1379	0.0575	0.0650	0.0670	0.0763	0.0719	0.0812
33	75	0.1405	0.0584	0.0664	0.0689	0.0791	0.0743	0.0845
38	88	0.1662	0.0680	0.0795			0.0895	0.1046
39	89	0.1647	0.0671	0.0789			0.0860	0.1011
40	90	0.1704	0.0694	0.0818			0.0867	0.1023
41	93	0.1713	0.0693	0.0824			0.0879	0.1046
42	92	0.1779	0.0720	0.0858			0.0857	0.1022
46	110	0.1662	0.0653	0.0806			0.0908	0.1121
48	114	0.1782	0.0698	0.0868			0.0959	0.1194
49	115	0.1809	0.0705	0.0884			0.0950	0.1190
50	120	0.1830	0.0709	0.0896			0.0992	0.1254

Table 5.1: The Z dependence of the overlap integrals in the unit of $m_\mu^{5/2}$ are listed. We use the neutron distributions in ref. [68] in the calculation of $S^{(n)}$ and $V^{(n)}$ and the same quantities calculated with $\rho_n = \rho_p$ are listed in the last two columns.

Z	A	P	$S^{(p)}$	$V^{(p)}$	$S^{(n)}$	$V^{(n)}$	$S^{(n)} _{\rho_p=\rho_n}$	$V^{(n)} _{\rho_p=\rho_n}$
51	121	0.1953	0.0761	0.0959			0.1045	0.1316
56	138	0.1837	0.0687	0.0909			0.1005	0.1331
57	139	0.1886	0.0705	0.0935			0.1014	0.1345
58	140	0.1875	0.0696	0.0931	0.0821	0.1141	0.0984	0.1316
60	142	0.1823	0.0668	0.0908			0.0913	0.1241
62	152	0.1939	0.0710	0.0970			0.1030	0.1408
64	158	0.1730	0.0614	0.0866			0.0902	0.1273
67	165	0.1774	0.0618	0.0894			0.0904	0.1308
68	166	0.1999	0.0695	0.1013			0.1002	0.1459
73	181	0.1566	0.0515	0.0796			0.0762	0.1177
74	184	0.1562	0.0501	0.0797			0.0744	0.1185
79	197	0.1663	0.0522	0.0857	0.0608	0.1081	0.0779	0.1280
81	205	0.1609	0.0489	0.0832			0.0749	0.1274
82	207	0.1614	0.0493	0.0836	0.0569	0.1058	0.0752	0.1274
83	209	0.1629	0.0494	0.0845	0.0578	0.1078	0.0750	0.1283
90	232	0.1541	0.0430	0.0810			0.0678	0.1278
92	238	0.1519	0.0418	0.0801			0.0664	0.1271

Table 5.1: (Continued).

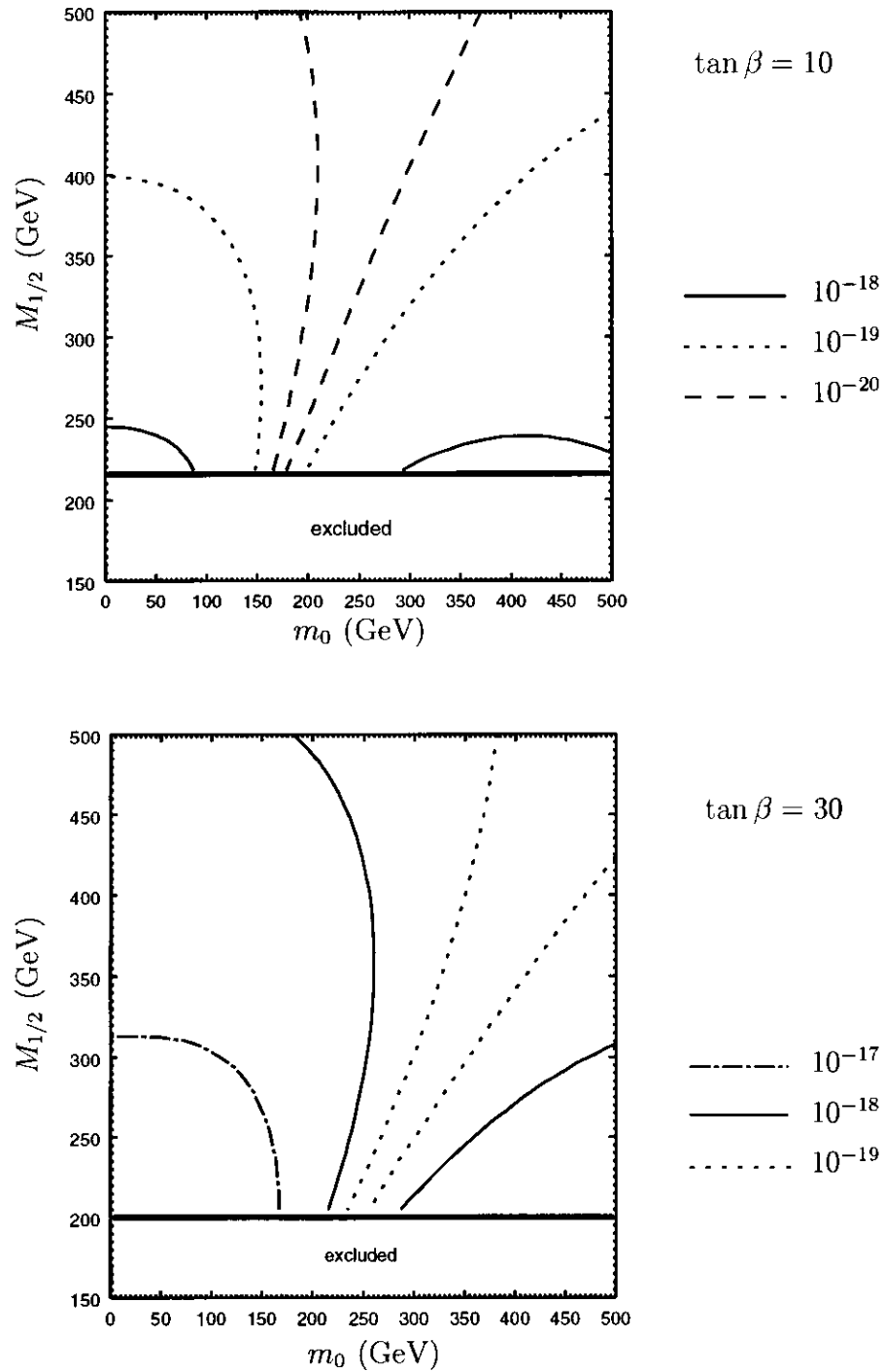


Figure 5.8: The $\mu - e$ conversion ratio in Ti nuclei is plotted in SU(5) SUSY GUT model.

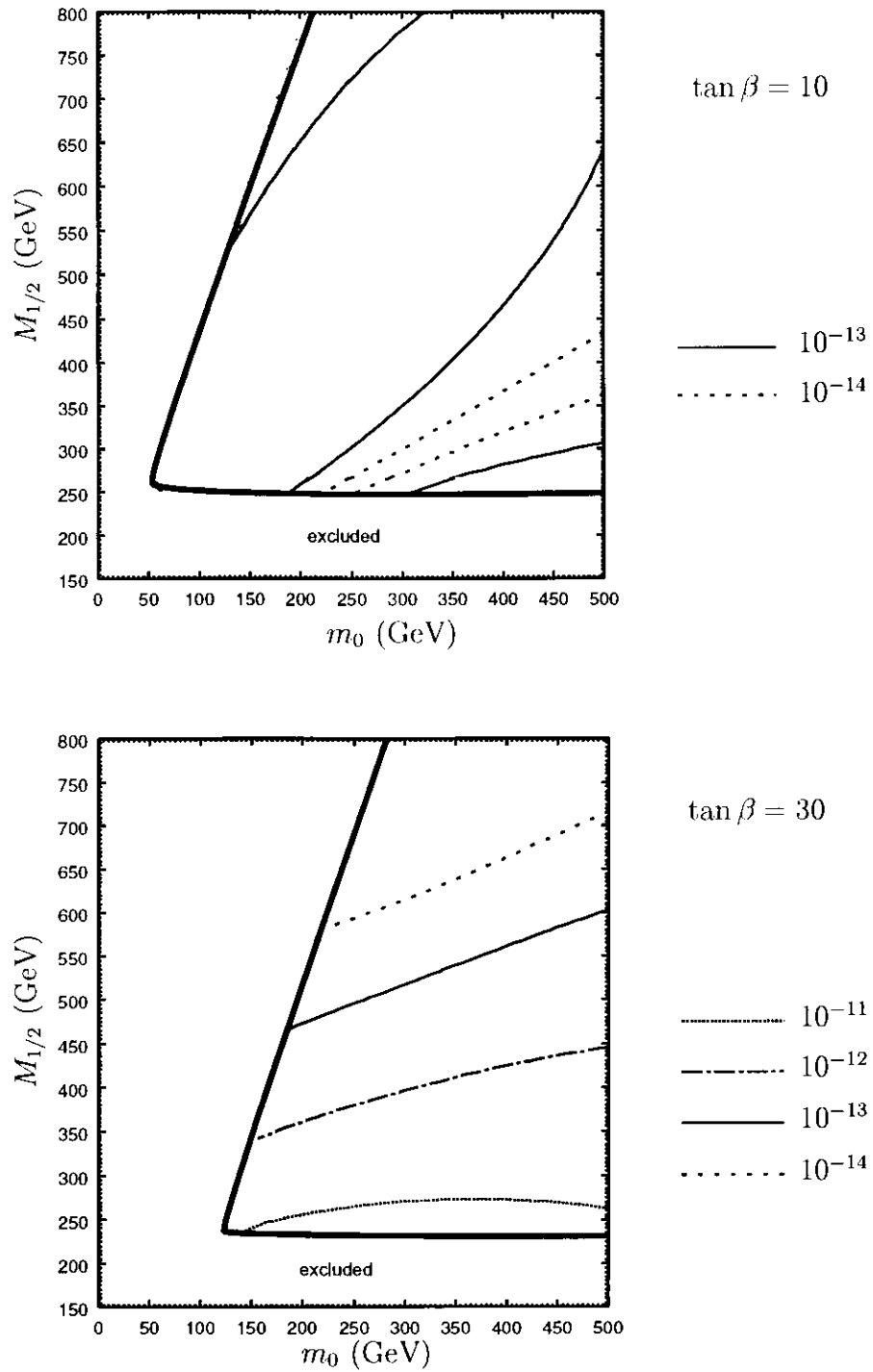


Figure 5.9: The $\mu - e$ conversion ratio in Ti nuclei is plotted in MSSM with right-handed neutrinos. The masses of the right-handed neutrinos are taken to be 10^{14} GeV.

Chapter 6

Conclusions

We have investigated LFV from the both sides i.e. the calculation based on the models and the extraction of information on new physics by means of the detailed studies of the LFV processes.

We pointed out that LFV give an effective constraint on the parameters of the models with extra-dimensions. The non-vanishing neutrino mass and mixing needs the existence of the right-handed neutrinos, but naive introduction of the right-handed neutrino does not provide tiny neutrino masses in the RS model. Grossman and Neubert then proposed the existence of right-handed neutrinos which live in bulk and couple to the lepton doublets and we saw that this model lead to small Dirac neutrino mass terms. The neutrino mass and mixing causes LFV. The KK modes of the right-handed neutrinos enhance the branching ratio of these processes. We calculated the $B(\mu \rightarrow e\gamma)$, $B(\tau \rightarrow \mu\gamma)$ and $B(\tau \rightarrow e\gamma)$ and found that $B(\mu \rightarrow e\gamma)$ gives severe constraints on the neutrino Yukawa couplings $\hat{y}_{i\alpha}$ and/or the Higgs mass parameter v_0 in the five dimensional theory.

As an analysis of the LFV processes, we defined P-odd and T-odd quantities in τ decays which have important information on new physics. Using spin correlations of $\tau^+\tau^-$, we show that the P odd asymmetry of $\tau \rightarrow \mu\gamma$ and $\tau \rightarrow e\gamma$ and P and T asymmetries of three body LFV decays of τ can be obtained by angular correlations. These P and T odd quantities are important to identify a model of new physics responsible for LFV processes.

We have also considered the background suppression of the $\tau \rightarrow \mu\gamma$ and $\tau \rightarrow e\gamma$

search by the angular distributions. We see that the analysis of the angular distributions is useful for the $\tau^+ \rightarrow \mu_R^+ \gamma$ ($\tau^- \rightarrow \mu_L^- \gamma$) and $\tau^+ \rightarrow e_R^+ \gamma$ ($\tau^- \rightarrow e_L^- \gamma$) searches.

We can obtain similar information in muon decay experiments if initial muons are polarized. Although highly polarized muons are available experimentally, a special setup for production and transportation of a muon beam is necessary for actual experiment. The advantage of the τ case is that we can extract the information on τ spins by looking at the decay distribution of the other side of τ decay so that we do not need a special requirement for experimental setup.

The $\mu - e$ conversion in nuclei is another important process of LFV. We calculated the coherent $\mu - e$ conversion rate in a model independent way. This calculation is important not only for the choice of the target in $\mu - e$ conversion experiments, also for the extraction of information on new physics by comparing the conversion rate among several experiments running with different targets.

In our calculation, we solve the Dirac equations for the muon and electron wave functions in the Coulomb force of the target nuclei. This treatment is especially important for the heavy nuclei where relativistic and Coulomb distortion effects on the wave functions are large.

Acknowledgments

I would like to greatly thank Prof. Yasuhiro Okada. During the three years of the doctor course, he and I often discussed physics and he always gave us a good advice and a useful knowledge. Thanks to him, I could spend happy days and proceed my ability of physics. I am very influenced by him, especially, at the point of his attitude toward physics. I am proud of being his student in the graduate university.

I express my gratitude to Prof. Junji Hisano and Prof. Mihoko Nojiri for giving a chance to make a computational program of the phenomenology in the supersymmetric model, in spite of the delay of the collaboration. Obtaining this big set of the programs enlarges my field of studies. Prof. Hisano is a person who informed me about the invitation of graduate students in the Graduate University for Advanced Studies at KEK. After entering the graduate university, I often ask questions to him on physics and he always answers carefully. Prof. Nojiri gave me an education on the collider physics of the supersymmetric models.

I am grateful to Dr. Toru Goto for the useful discussions. He often checked my computational programs whether the results coincide with that from his programs when I asked.

I also express my gratitude to Prof. Kaoru Hagiwara for his great lectures of supersymmetric theory and of the collider physics, from which I learned the importance of using a definite notation and many useful techniques.

I wish to thank Prof. Nobuyuki Ishibashi, Prof. Satoshi Iso, and Prof. Yoshihisa Kitazawa for the teaching of string theory. Besides the formal lectures, Prof. Kitazawa and

Prof. Ishibashi attended to the informal weekly seminars for the students as advisers. I could learn the basics of string theory in the seminars.

I wish to thank Dr. Takayuki Hirayama, Dr. Masafumi Koike, Dr. Yukihiro Mimura, Dr. Kin-ya Oda, and Dr. Nobuchika Okada who are postdocs at KEK and my collaborators in the works on the extra-dimension, the mu-e conversion, flavor symmetry, neutrino masses, and GUT models, respectively. These works are accomplished by the discussions in many times through which I learned a lot of knowledge and the way of studies.

I wish to thank people in the KEK Theory Group. They welcome discussions with students. Especially I often discuss physics with Dr. Masashi Hayakawa, Dr. Shingo Kiyoura, Dr. Ken-ichi Okumura, and Prof. Makoto Natsuume.

Finally, I would like to thank my wife Yumi Kitano for her daily support to my research activities. Our marriage is one of the major factors of the progress in my studies. I also would like to thank my parents Kimio Kitano and Haruko Kitano for their support for a long time. Now, sincerely, I would like to dedicate this thesis to my wife and parents.

The present study was supported by the JSPS Research Fellowships for Young Scientists.

Appendix A

The Minimal Supersymmetric Standard Model

A.1 Notation

We use the following notation.

$$\eta_{\mu\nu} = \begin{pmatrix} 1 & & & \\ & -1 & & \\ & & -1 & \\ & & & -1 \end{pmatrix}. \quad (\text{A.1})$$

$$\sigma^1 = \begin{pmatrix} 0 & 1 \\ 1 & 0 \end{pmatrix}, \quad \sigma^2 = \begin{pmatrix} 0 & -i \\ i & 0 \end{pmatrix}, \quad \sigma^3 = \begin{pmatrix} 1 & 0 \\ 0 & -1 \end{pmatrix}. \quad (\text{A.2})$$

$$\gamma^0 = \begin{pmatrix} 0 & 1 \\ 1 & 0 \end{pmatrix}, \quad \gamma^i = \begin{pmatrix} 0 & \sigma^i \\ -\sigma^i & 0 \end{pmatrix}, \quad \gamma_5 = i\gamma^0\gamma^1\gamma^2\gamma^3 = \begin{pmatrix} -1 & 0 \\ 0 & 1 \end{pmatrix}. \quad (\text{A.3})$$

$$P_L = \frac{1 - \gamma_5}{2}, \quad P_R = \frac{1 + \gamma_5}{2}. \quad (\text{A.4})$$

$$\epsilon_{0123} = 1, \quad \epsilon^{0123} = -1. \quad (\text{A.5})$$

$$\sigma^{\mu\nu} = \frac{i}{2} [\gamma^\mu, \gamma^\nu]. \quad (\text{A.6})$$

A.2 SUSY Lagrangian

The SUSY Lagrangian is given as follows:

$$\begin{aligned}
\mathcal{L}_{\text{SUSY}} = & -\frac{1}{4}F_{\mu\nu}^a F^{a\mu\nu} + \frac{i}{2}\bar{\lambda}_M^a \gamma_\mu (D_{\text{adj}}^\mu \lambda_M)^a + (D_\mu \phi)_i^\dagger (D^\mu \phi)_i + i\bar{\psi}_i \gamma_\mu (D^\mu \psi)_i \\
& + \sqrt{2}g (\phi_i^* \bar{\lambda}_m^a T_{ij}^a P_L \psi_j + \bar{\psi}_i P_R \lambda_M^a T_{ij}^a \phi_j) \\
& + \frac{1}{2} \frac{\partial^2 W}{\partial \phi_i \partial \phi_j} \bar{\psi}_i^c P_L \psi_j + \frac{1}{2} \frac{\partial^2 W^*}{\partial \phi_i^* \partial \phi_j^*} \bar{\psi}_j P_R \psi_i^c \\
& - \frac{1}{2} g^2 (\phi_i^* T_{ij}^a \phi_j)^2 - \left| \frac{\partial W}{\partial \phi_i} \right|^2, \tag{A.7}
\end{aligned}$$

where i, j are the gauge index depend on the representation of matter fields ϕ and ψ , and a is the gauge index of the adjoint representation. The fields ϕ and ψ are the boson and fermion fields which belong to the same representation of the gauge group. g and T^a are the gauge coupling constants and the generator of the gauge group, respectively. The Majorana field λ_M is the superpartner of the gauge fields called gaugino. This field is a adjoint representation of the gauge group and the covariant derivative D_{adj}^μ is given by

$$(D_{\text{adj}}^\mu)^{ab} = \delta^{ab} \partial^\mu - g f_{abc} A^{c\mu}. \tag{A.8}$$

The covariant derivative for the matter fields are given by

$$(D^\mu)_{ij} = \delta_{ij} \partial^\mu - ig T_{ij}^a A^{a\mu}. \tag{A.9}$$

The superpotential W in eq.(A.7) is arbitrary holomorphic functions of ϕ . The charge conjugation ϕ^c is defined by

$$\psi^c = C \bar{\psi}^T, \quad C = i\gamma^2 \gamma^0. \tag{A.10}$$

A.3 Particle content

The particle content of the MSSM is given in Table A.1. where R is the R -parity. With this superfields, the renormalizable superpotential is written as follows:

$$W_{\text{MSSM}} = \mu H_1 \cdot H_2 + f_e^{ij} H_1 \cdot E_j^c L_i + f_d^{ij} H_1 \cdot D_j^c Q_i + f_u^{ij} H_2 \cdot U_j^c Q_i, \tag{A.11}$$

	SU(3) _C	SU(2) _L	U(1) _Y	R
Q	3	2	+1/6	–
U^c	$\bar{\mathbf{3}}$	1	–2/3	–
D^c	3	1	+1/3	–
L	1	2	–1/2	–
E^c	1	1	+1	–
H_1	1	2	–1/2	+
H_2	1	2	+1/2	+

Table A.1: The particle content of the MSSM.

where ‘ \cdot ’ represents the contraction of the SU(2)_L index by $\epsilon_{ij} = i\sigma^2$. The Yukawa coupling constants f_e , f_d , and f_u can be related to the masses and mixing of the fermions as follows:

$$f_e^{ij} = \frac{-\sqrt{2}m_e^i}{v \cos \beta} \delta_{ij}, \quad f_d^{ij} = \frac{-\sqrt{2}m_d^i}{v \cos \beta} \delta_{ij}, \quad f_u^{ij} = \frac{\sqrt{2}V_{\text{CKM}}^{ji}m_u^j}{v \sin \beta}. \quad (\text{A.12})$$

Here m_e^i , m_d^i , and m_u^i are the masses of the fermions in each generation, and V_{CKM} is the CKM matrix. The vacuum expectation value v and the angle β are defined as

$$\langle H_1 \rangle = \begin{pmatrix} v_1 \\ 0 \end{pmatrix}, \quad \langle H_2 \rangle = \begin{pmatrix} 0 \\ v_2 \end{pmatrix}, \quad v = \sqrt{2(v_1^2 + v_2^2)}, \quad \tan \beta = \frac{v_2}{v_1}. \quad (\text{A.13})$$

A.4 Soft SUSY breaking terms

The soft SUSY breaking terms are given as follows:

$$\begin{aligned} \mathcal{L}_{\text{soft}} = & - \left(B\mu H_1 \cdot H_2 + A_e^{ij} H_1 \cdot \tilde{e}_j^c \tilde{l}_i + A_d^{ij} H_1 \cdot \tilde{d}_j^c \tilde{q}_i + A_u^{ij} H_2 \cdot \tilde{u}_j^c \tilde{q}_i + \text{h.c.} \right) \\ & - (\tilde{m}_{\tilde{q}}^2)_{ij} \tilde{q}_i^\dagger \tilde{q}_j - (\tilde{m}_{\tilde{u}^c}^2)_{ij} \tilde{u}_i^{c\dagger} \tilde{u}_j^c - (\tilde{m}_{\tilde{d}^c}^2)_{ij} \tilde{d}_i^{c\dagger} \tilde{d}_j^c \\ & - (\tilde{m}_{\tilde{l}}^2)_{ij} \tilde{l}_i^\dagger \tilde{l}_j - (\tilde{m}_{\tilde{e}^c}^2)_{ij} \tilde{e}_i^{c\dagger} \tilde{e}_j^c \\ & - (\tilde{m}_{H_1}^2) H_1^\dagger H_1 - (\tilde{m}_{H_2}^2) H_2^\dagger H_2 \\ & - \frac{1}{2} M_1 \tilde{B}^0 \tilde{B}^0 - \frac{1}{2} M_2 \tilde{W}^i \tilde{W}^i - \frac{1}{2} M_3 \tilde{g}^a \tilde{g}^a. \end{aligned} \quad (\text{A.14})$$

A.5 Renormalization group equations

The renormalization group equations (RGEs) for the Yukawa coupling constants are given as follows:

$$(4\pi)^2 \frac{d}{dt} f_e^{ij} = f_e^{ij} \gamma_{H_1}^{H_1} + f_e^{ik} \gamma_{e_k^c}^{e_j^c} + f_e^{kj} \gamma_{l_k}^{l_i}, \quad (\text{A.15})$$

$$(4\pi)^2 \frac{d}{dt} f_d^{ij} = f_d^{ij} \gamma_{H_1}^{H_1} + f_d^{ik} \gamma_{d_k^c}^{d_j^c} + f_d^{kj} \gamma_{q_k}^{q_i}, \quad (\text{A.16})$$

$$(4\pi)^2 \frac{d}{dt} f_u^{ij} = f_u^{ij} \gamma_{H_2}^{H_2} + f_u^{ik} \gamma_{u_k^c}^{u_j^c} + f_u^{kj} \gamma_{q_k}^{q_i}, \quad (\text{A.17})$$

where

$$\gamma_{H_1}^{H_1} = f_e^{kl*} f_e^{kl} + 3 f_d^{kl*} f_d^{kl} - \frac{1}{2} g_Y^2 - \frac{3}{2} g_2^2, \quad (\text{A.18})$$

$$\gamma_{e_k^c}^{e_j^c} = 2 f_e^{lk*} f_e^{lj} - 2 g_Y^2 \delta_{kj}, \quad (\text{A.19})$$

$$\gamma_{l_k}^{l_i} = f_e^{kl*} f_e^{il} - \frac{1}{2} g_Y^2 \delta_{ki} - \frac{3}{2} g_2^2 \delta_{ki}, \quad (\text{A.20})$$

$$\gamma_{d_k^c}^{d_j^c} = 2 f_d^{lk*} f_d^{lj} - \frac{2}{9} g_Y^2 \delta_{kj} - \frac{8}{3} g_3^2 \delta_{kj}, \quad (\text{A.21})$$

$$\gamma_{q_k}^{q_i} = f_d^{kl*} f_d^{il} + f_u^{kl*} f_u^{il} - \frac{1}{18} g_Y^2 \delta_{ki} - \frac{3}{2} g_2^2 \delta_{ki} - \frac{8}{3} g_3^2 \delta_{ki}. \quad (\text{A.22})$$

The RGEs for the gauge coupling constants g_Y , g_2 , and g_3 corresponding to the gauge group of $U(1)_Y$, $SU(2)_L$, and $SU(3)_C$ are given by

$$(4\pi)^2 \frac{d}{dt} g_Y = 11 g_Y^3, \quad (\text{A.23})$$

$$(4\pi)^2 \frac{d}{dt} g_2 = g_2^3, \quad (\text{A.24})$$

$$(4\pi)^2 \frac{d}{dt} g_3 = -3 g_3^3. \quad (\text{A.25})$$

The RGEs for the gaugino masses are given by

$$(4\pi)^2 \frac{d}{dt} M_1 = 22g_Y^2 M_1 , \quad (\text{A.26})$$

$$(4\pi)^2 \frac{d}{dt} M_2 = 2g_2^2 M_2 , \quad (\text{A.27})$$

$$(4\pi)^2 \frac{d}{dt} M_3 = -6g_3^2 M_3 . \quad (\text{A.28})$$

The RGEs for the A-terms are given as follows:

$$(4\pi)^2 \frac{d}{dt} A_e^{ij} = A_e^{ij} \gamma_{H_1}^{H_1} + A_e^{ik} \gamma_{e_k^c}^{e_j^c} + A_e^{kj} \gamma_{l_k}^{l_i} + 2f_e^{ij} \tilde{\gamma}_{H_1}^{H_1} + 2f_e^{ik} \tilde{\gamma}_{e_k^c}^{e_j^c} + 2f_e^{kj} \tilde{\gamma}_{l_k}^{l_i} , \quad (\text{A.29})$$

$$(4\pi)^2 \frac{d}{dt} A_d^{ij} = A_d^{ij} \gamma_{H_1}^{H_1} + A_d^{ik} \gamma_{d_k^c}^{d_j^c} + A_d^{kj} \gamma_{q_k}^{q_i} + 2f_d^{ij} \tilde{\gamma}_{H_1}^{H_1} + 2f_d^{ik} \tilde{\gamma}_{d_k^c}^{d_j^c} + 2f_d^{kj} \tilde{\gamma}_{q_k}^{q_i} , \quad (\text{A.30})$$

$$(4\pi)^2 \frac{d}{dt} A_u^{ij} = A_u^{ij} \gamma_{H_2}^{H_2} + A_u^{ik} \gamma_{u_k^c}^{u_j^c} + A_u^{kj} \gamma_{q_k}^{q_i} + 2f_u^{ij} \tilde{\gamma}_{H_2}^{H_2} + 2f_u^{ik} \tilde{\gamma}_{u_k^c}^{u_j^c} + 2f_u^{kj} \tilde{\gamma}_{q_k}^{q_i} , \quad (\text{A.31})$$

where

$$\tilde{\gamma}_{H_1}^{H_1} = f_e^{kl*} A_e^{kl} + 3f_d^{kl*} A_d^{kl} - \frac{1}{2}g_Y^2 M_1 - \frac{3}{2}g_2^2 M_2 , \quad (\text{A.32})$$

$$\tilde{\gamma}_{e_k^c}^{e_j^c} = 2f_e^{lk*} A_e^{lj} - 2g_Y^2 M_1 \delta_{kj} , \quad (\text{A.33})$$

$$\tilde{\gamma}_{l_k}^{l_i} = f_e^{kl*} A_e^{il} - \frac{1}{2}g_Y^2 M_1 \delta_{ki} - \frac{3}{2}g_2^2 M_2 \delta_{ki} , \quad (\text{A.34})$$

$$\tilde{\gamma}_{d_k^c}^{d_j^c} = 2f_d^{lk*} A_d^{lj} - \frac{2}{9}g_Y^2 M_1 \delta_{kj} - \frac{8}{3}g_3^2 M_3 \delta_{kj} , \quad (\text{A.35})$$

$$\tilde{\gamma}_{q_k}^{q_i} = f_d^{kl*} A_d^{il} + f_u^{kl*} A_u^{il} - \frac{1}{18}g_Y^2 M_1 \delta_{ki} - \frac{3}{2}g_2^2 M_2 \delta_{ki} - \frac{8}{3}g_3^2 M_3 \delta_{ki} . \quad (\text{A.36})$$

The RGE for the scalar soft mass terms are given as follows:

$$(4\pi)^2 \frac{d}{dt} (\tilde{m}_l^2)_{ij} = (\tilde{m}_l^2)_{ik} \gamma_{l_k}^{l_j} + (\tilde{m}_l^2)_{kj} \gamma_{l_i}^{l_k} + 2\tilde{\gamma}_{l_i}^{l_j} - g_Y^2 S \delta_{ij} , \quad (\text{A.37})$$

$$(4\pi)^2 \frac{d}{dt} (\tilde{m}_{\tilde{e}^c}^2)_{ij} = (\tilde{m}_{\tilde{e}^c}^2)_{ik} \gamma_{e_k^c}^{e_j^c} + (\tilde{m}_{\tilde{e}^c}^2)_{kj} \gamma_{e_i^c}^{e_k^c} + 2\tilde{\gamma}_{e_i^c}^{e_j^c} + 2g_Y^2 S \delta_{ij} , \quad (\text{A.38})$$

$$(4\pi)^2 \frac{d}{dt} (\tilde{m}_{\tilde{q}}^2)_{ij} = (\tilde{m}_{\tilde{q}}^2)_{ik} \gamma_{q_k}^{q_j} + (\tilde{m}_{\tilde{q}}^2)_{kj} \gamma_{q_i}^{q_k} + 2\tilde{\gamma}_{q_i}^{q_j} + \frac{1}{3} g_Y^2 S \delta_{ij} , \quad (\text{A.39})$$

$$(4\pi)^2 \frac{d}{dt} (\tilde{m}_{\tilde{u}^c}^2)_{ij} = (\tilde{m}_{\tilde{u}^c}^2)_{ik} \gamma_{u_k^c}^{u_j^c} + (\tilde{m}_{\tilde{u}^c}^2)_{kj} \gamma_{u_i^c}^{u_k^c} + 2\tilde{\gamma}_{u_i^c}^{u_j^c} - \frac{4}{3} g_Y^2 S \delta_{ij} , \quad (\text{A.40})$$

$$(4\pi)^2 \frac{d}{dt} (\tilde{m}_{\tilde{d}^c}^2)_{ij} = (\tilde{m}_{\tilde{d}^c}^2)_{ik} \gamma_{d_k^c}^{d_j^c} + (\tilde{m}_{\tilde{d}^c}^2)_{kj} \gamma_{d_i^c}^{d_k^c} + 2\tilde{\gamma}_{d_i^c}^{d_j^c} + \frac{2}{3} g_Y^2 S \delta_{ij} , \quad (\text{A.41})$$

$$(4\pi)^2 \frac{d}{dt} \tilde{m}_{H_1}^2 = 2\tilde{m}_{H_1}^2 \gamma_{H_1}^{H_1} + 2\tilde{\gamma}_{H_1}^{H_1} - g_Y^2 S , \quad (\text{A.42})$$

$$(4\pi)^2 \frac{d}{dt} \tilde{m}_{H_2}^2 = 2\tilde{m}_{H_2}^2 \gamma_{H_2}^{H_2} + 2\tilde{\gamma}_{H_2}^{H_2} + g_Y^2 S , \quad (\text{A.43})$$

where

$$S = (\tilde{m}_{\tilde{q}}^2)_{kk} - 2(\tilde{m}_{\tilde{u}^c}^2)_{kk} + (\tilde{m}_{\tilde{d}^c}^2)_{kk} - (\tilde{m}_{\tilde{l}}^2)_{kk} + (\tilde{m}_{\tilde{e}^c}^2)_{kk} - \tilde{m}_{H_1}^2 + \tilde{m}_{H_2}^2 , \quad (\text{A.44})$$

$$\begin{aligned} \tilde{\gamma}_{\tilde{l}_i}^{l_j} &= f_e^{ik*} f_e^{jl} (\tilde{m}_{\tilde{e}^c}^2)_{lk} + f_e^{ik*} f_e^{jk} \tilde{m}_{H_1}^2 + A_e^{ik*} A_e^{jk} \\ &\quad - g_Y^2 |M_1|^2 \delta_{ij} - 3g_2^2 |M_2|^2 \delta_{ij} + \frac{1}{2} g_Y^2 (\tilde{m}_{\tilde{l}}^2)_{ij} + \frac{3}{2} g_2^2 (\tilde{m}_{\tilde{l}}^2)_{ij} , \end{aligned} \quad (\text{A.45})$$

$$\begin{aligned} \tilde{\gamma}_{e_i^c}^{e_j^c} &= 2f_e^{ki*} f_e^{lj} (\tilde{m}_{\tilde{l}}^2)_{lk} + 2f_e^{ki*} f_e^{kj} \tilde{m}_{H_1}^2 + 2A_e^{ki*} A_e^{kj} \\ &\quad - 4g_Y^2 |M_1|^2 \delta_{ij} + 2g_Y^2 (\tilde{m}_{\tilde{e}^c}^2)_{ij} , \end{aligned} \quad (\text{A.46})$$

$$\begin{aligned} \tilde{\gamma}_{q_i}^{q_j} &= f_u^{ik*} f_u^{jl} (\tilde{m}_{\tilde{u}^c}^2)_{lk} + f_u^{ik*} f_u^{jk} \tilde{m}_{H_2}^2 + f_d^{ik*} f_d^{jl} (\tilde{m}_{\tilde{d}^c}^2)_{lk} + f_d^{ik*} f_d^{jk} \tilde{m}_{H_1}^2 \\ &\quad + A_u^{ik*} A_u^{jk} + A_d^{ik*} A_d^{jk} \\ &\quad - \frac{1}{9} g_Y^2 |M_1|^2 \delta_{ij} - 3g_2^2 |M_2|^2 \delta_{ij} - \frac{16}{3} g_3^2 |M_3|^2 \delta_{ij} \\ &\quad + \frac{1}{18} g_Y^2 (\tilde{m}_{\tilde{q}}^2)_{ij} + \frac{3}{2} g_2^2 (\tilde{m}_{\tilde{q}}^2)_{ij} + \frac{8}{3} g_3^2 (\tilde{m}_{\tilde{q}}^2)_{ij} , \end{aligned} \quad (\text{A.47})$$

$$\begin{aligned}\tilde{\gamma}_{u_c^c}^{u_c^c} &= 2f_u^{ki*} f_u^{lj} (\tilde{m}_q^2)_{lk} + 2f_u^{ki*} f_u^{kj} \tilde{m}_{H_2}^2 + 2A_u^{ki*} A_u^{kj} \\ &\quad - \frac{16}{9} g_Y^2 |M_1|^2 \delta_{ij} - \frac{16}{3} g_3^2 |M_3|^2 \delta_{ij} + \frac{8}{9} g_Y^2 (\tilde{m}_{u^c}^2)_{ij} + \frac{8}{3} g_3^2 (\tilde{m}_{u^c}^2)_{ij} ,\end{aligned}\quad (\text{A.48})$$

$$\begin{aligned}\tilde{\gamma}_{d_c^c}^{d_c^c} &= 2f_d^{ki*} f_d^{lj} (\tilde{m}_q^2)_{lk} + 2f_d^{ki*} f_d^{kj} \tilde{m}_{H_1}^2 + 2A_d^{ki*} A_d^{kj} \\ &\quad - \frac{4}{9} g_Y^2 |M_1|^2 \delta_{ij} - \frac{16}{3} g_3^2 |M_3|^2 \delta_{ij} + \frac{2}{9} g_Y^2 (\tilde{m}_{d^c}^2)_{ij} + \frac{8}{3} g_3^2 (\tilde{m}_{d^c}^2)_{ij} ,\end{aligned}\quad (\text{A.49})$$

$$\begin{aligned}\tilde{\gamma}_{H_1}^{H_1} &= f_e^{ij*} f_e^{ik} (\tilde{m}_{e^c}^2)_{kj} + f_e^{ik*} f_e^{jk} (\tilde{m}_l^2)_{ji} + 3f_d^{ij*} f_d^{ik} (\tilde{m}_{d^c}^2)_{kj} + 3f_d^{ik*} f_d^{jk} (\tilde{m}_q^2)_{ji} \\ &\quad + A_e^{ij*} A_e^{ij} + 3A_d^{ij*} A_d^{ij} \\ &\quad - g_Y^2 |M_1|^2 - 3g_2^2 |M_2|^2 + \frac{1}{2} g_Y^2 \tilde{m}_{H_1}^2 + \frac{3}{2} g_2^2 \tilde{m}_{H_1}^2 ,\end{aligned}\quad (\text{A.50})$$

$$\begin{aligned}\tilde{\gamma}_{H_2}^{H_2} &= +3f_u^{ij*} f_u^{ik} (\tilde{m}_{u^c}^2)_{kj} + 3f_u^{ik*} f_u^{jk} (\tilde{m}_q^2)_{ji} + 3A_u^{ij*} A_u^{ij} \\ &\quad - g_Y^2 |M_1|^2 - 3g_2^2 |M_2|^2 + \frac{1}{2} g_Y^2 \tilde{m}_{H_1}^2 + \frac{3}{2} g_2^2 \tilde{m}_{H_1}^2 .\end{aligned}\quad (\text{A.51})$$

The RGE for the μ and B parameters are given by

$$(4\pi)^2 \frac{d}{dt} \mu = \mu (\gamma_{H_1}^{H_1} + \gamma_{H_2}^{H_2}) ,\quad (\text{A.52})$$

$$(4\pi)^2 \frac{d}{dt} (B\mu) = B\mu (\gamma_{H_1}^{H_1} + \gamma_{H_2}^{H_2}) + 2\mu (\tilde{\gamma}_{H_1}^{H_1} + \tilde{\gamma}_{H_2}^{H_2}) .\quad (\text{A.53})$$

A.6 The mass matrices

The mass matrices of the charginos and neutralinos are defined by

$$\mathcal{L}_{\text{chargino}} = -(\bar{W}^+, \bar{H}_2^+) M_C P_L \begin{pmatrix} \bar{W}^- \\ \bar{H}_1^- \end{pmatrix} + \text{h.c.} ,\quad (\text{A.54})$$

$$\mathcal{L}_{\text{neutralino}} = -\frac{1}{2} (\bar{B}^0, \bar{W}^0, \bar{H}_1^0, \bar{H}_2^0) M_N \begin{pmatrix} \tilde{B}^0 \\ \tilde{W}^0 \\ \tilde{H}_1^0 \\ \tilde{H}_2^0 \end{pmatrix} .\quad (\text{A.55})$$

The matrices are given by

$$M_C = \begin{pmatrix} M_2 & -g_2 v_1 \\ -g_2 v_2 & \mu \end{pmatrix}, \quad (\text{A.56})$$

$$M_N = \begin{pmatrix} M_1 & 0 & g_Y v_1/\sqrt{2} & -g_Y v_2/\sqrt{2} \\ 0 & M_2 & -g_2 v_1/\sqrt{2} & g_2 v_2/\sqrt{2} \\ g_Y v_1/\sqrt{2} & -g_2 v_1/\sqrt{2} & 0 & -\mu \\ -g_Y v_2/\sqrt{2} & g_2 v_2/\sqrt{2} & -\mu & 0 \end{pmatrix}. \quad (\text{A.57})$$

We define unitary and complex orthogonal matrices which diagonalize the above two matrices as follows:

$$O_R M_C O_L^\dagger = M_C^{\text{diagonal}}, \quad (\text{A.58})$$

$$O_N M_N O_N^T = M_N^{\text{diagonal}}. \quad (\text{A.59})$$

The mass matrix for the sfermions are defined as

$$\mathcal{L}_{\text{slepton}} = -(\tilde{e}_i^*, \tilde{e}_i^c) M_e^2 \begin{pmatrix} \tilde{e}_j \\ \tilde{e}_j^c \end{pmatrix}, \quad (\text{A.60})$$

$$\mathcal{L}_{\text{sneutrino}} = -\tilde{\nu}_i^* M_\nu^2 \tilde{\nu}_j, \quad (\text{A.61})$$

$$\mathcal{L}_{\text{sup}} = -(\tilde{u}_i^*, \tilde{u}_i^c) M_u^2 \begin{pmatrix} \tilde{u}_j \\ \tilde{u}_j^c \end{pmatrix}, \quad (\text{A.62})$$

$$\mathcal{L}_{\text{sdown}} = -(\tilde{d}_i^*, \tilde{d}_i^c) M_d^2 \begin{pmatrix} \tilde{d}_j \\ \tilde{d}_j^c \end{pmatrix}. \quad (\text{A.63})$$

Each components for the mass matrices are given as follows:

$$(M_e^2)_{ij} = (\tilde{m}_i^2)_{ij} + f_e^{ik*} f_e^{jk} |v_1|^2 + \frac{1}{2}(|v_2|^2 - |v_1|^2) \left(-\frac{1}{2}g_2^2 + \frac{1}{2}g_Y^2\right) \delta_{ij}, \quad (\text{A.64})$$

$$(M_e^2)_{i+3, j+3} = (\tilde{m}_{e^c}^2)_{ji} + f_e^{kj*} f_e^{ki} |v_1|^2 + \frac{1}{2}(|v_2|^2 - |v_1|^2) (-g_Y^2) \delta_{ij}, \quad (\text{A.65})$$

$$(M_e^2)_{i, j+3} = (M_e^2)_{j+3, i}^* = A_e^{ij*} v_1^* + \mu f_e^{ij*} v_2, \quad (\text{A.66})$$

$$(M_{\bar{\nu}}^2)_{ij} = (\tilde{m}_{\bar{\nu}}^2)_{ij} + \frac{1}{2}(|v_2|^2 - |v_1|^2)\left(\frac{1}{2}g_2^2 + \frac{1}{2}g_Y^2\right)\delta_{ij} , \quad (\text{A.67})$$

$$(M_{\bar{u}}^2)_{ij} = (\tilde{m}_{\bar{u}}^2)_{ij} + f_u^{ik*} f_u^{jk} |v_2|^2 + \frac{1}{2}(|v_2|^2 - |v_1|^2)\left(\frac{1}{2}g_2^2 - \frac{1}{6}g_Y^2\right)\delta_{ij} , \quad (\text{A.68})$$

$$(M_{\bar{u}}^2)_{i+3,j+3} = (\tilde{m}_{\bar{u}^c}^2)_{ji} + f_u^{kj*} f_u^{ki} |v_2|^2 + \frac{1}{2}(|v_2|^2 - |v_1|^2) \frac{2}{3}g_Y^2 \delta_{ij} , \quad (\text{A.69})$$

$$(M_{\bar{u}}^2)_{i,j+3} = (M_{\bar{u}}^2)_{j+3,i}^* = -A_u^{ij*} v_2^* - \mu f_u^{ij*} v_1 , \quad (\text{A.70})$$

$$(M_d^2)_{ij} = (\tilde{m}_d^2)_{ij} + f_d^{ik*} f_d^{jk} |v_1|^2 + \frac{1}{2}(|v_2|^2 - |v_1|^2)\left(-\frac{1}{2}g_2^2 - \frac{1}{6}g_Y^2\right)\delta_{ij} , \quad (\text{A.71})$$

$$(M_d^2)_{i+3,j+3} = (\tilde{m}_{d^c}^2)_{ji} + f_d^{kj*} f_d^{ki} |v_1|^2 + \frac{1}{2}(|v_2|^2 - |v_1|^2)\left(-\frac{1}{3}g_Y^2\right)\delta_{ij} , \quad (\text{A.72})$$

$$(M_d^2)_{i,j+3} = (M_d^2)_{j+3,i}^* = A_d^{ij*} v_1^* + \mu f_d^{ij*} v_2 . \quad (\text{A.73})$$

We define the unitary matrices which diagonalize the sfermion mass matrices as follows:

$$U_{\bar{e}} M_{\bar{e}}^2 U_{\bar{e}}^\dagger = (M_{\bar{e}}^2)^{\text{diagonal}} , \quad (\text{A.74})$$

$$U_{\bar{\nu}} M_{\bar{\nu}}^2 U_{\bar{\nu}}^\dagger = (M_{\bar{\nu}}^2)^{\text{diagonal}} , \quad (\text{A.75})$$

$$U_{\bar{u}} M_{\bar{u}}^2 U_{\bar{u}}^\dagger = (M_{\bar{u}}^2)^{\text{diagonal}} , \quad (\text{A.76})$$

$$U_d M_d^2 U_d^\dagger = (M_d^2)^{\text{diagonal}} . \quad (\text{A.77})$$

We also define the unitary matrices which diagonalize the fermion mass matrices as follows:

$$U_e^L (-f_e^{ij} v_1) U_e^{R\dagger} = m_e^i \delta_{ij} , \quad (\text{A.78})$$

$$U_d^L (-f_d^{ij} v_1) U_d^{R\dagger} = m_d^i \delta_{ij} , \quad (\text{A.79})$$

$$U_u^L (f_u^{ij} v_2) U_u^{R\dagger} = m_u^i \delta_{ij} . \quad (\text{A.80})$$

In the convention of eq.(A.12), the above unitary matrices are simply the unit matrices except for $U_u^L = V_{\text{CKM}}^*$.

A.7 The vertices

We write down the interaction terms in the Lagrangian which are often used in the calculation.

- Neutralino-fermion-sfermion

$$\mathcal{L} = \bar{\chi}_A^0 \left(N_{iAX}^{R(f)} P_R + N_{iAX}^{L(f)} P_L \right) f_i \tilde{f}_X^\dagger + \text{h.c.} , \quad (\text{A.81})$$

where i , A , and X are the indices of the mass eigenstates of the fermions, neutralinos, and sfermions, respectively. The coupling constants are given as follows:

$$\begin{aligned} N_{iAX}^{R(e)} &= \sqrt{2} g_Y (U_{\bar{e}})_{X,3+k} (O_N)_{A,1}^* (U_e^R)_{i,k}^* \\ &\quad + f_e^{kl*} (U_{\bar{e}})_{X,k} (O_N)_{A,3}^* (U_e^R)_{il}^* , \end{aligned} \quad (\text{A.82})$$

$$\begin{aligned} N_{iAX}^{L(e)} &= -\frac{1}{\sqrt{2}} g_2 (U_{\bar{e}})_{X,k} (O_N)_{A,2}^* (U_e^L)_{i,k}^* \\ &\quad - \frac{1}{\sqrt{2}} g_Y (U_{\bar{e}})_{X,k} (O_N)_{A,1}^* (U_e^L)_{i,k}^* \\ &\quad + f_e^{kl*} (U_{\bar{e}})_{X,3+l} (O_N)_{A,3}^* (U_e^L)_{ik}^* , \end{aligned} \quad (\text{A.83})$$

$$N_{iAX}^{R(\nu)} = 0 , \quad (\text{A.84})$$

$$\begin{aligned} N_{iAX}^{L(\nu)} &= \frac{1}{\sqrt{2}} g_2 (U_{\bar{\nu}})_{X,i} (O_N)_{A,2}^* \\ &\quad - \frac{1}{\sqrt{2}} g_Y (U_{\bar{\nu}})_{X,i} (O_N)_{A,1}^* , \end{aligned} \quad (\text{A.85})$$

$$\begin{aligned} N_{iAX}^{R(u)} &= -\frac{2\sqrt{2}}{3} g_Y (U_{\bar{u}})_{X,3+k} (O_N)_{A,1}^* (U_u^R)_{i,k}^* \\ &\quad - f_u^{kl*} (U_{\bar{u}})_{X,k} (O_N)_{A,4}^* (U_u^R)_{il}^* , \end{aligned} \quad (\text{A.86})$$

$$\begin{aligned}
N_{iAX}^{L(u)} &= \frac{1}{\sqrt{2}} g_2 (U_{\bar{u}})_{X,k} (O_N)_{A,2}^* (U_u^L)_{i,k}^* \\
&\quad + \frac{2\sqrt{2}}{6} g_Y (U_{\bar{u}})_{X,k} (O_N)_{A,1}^* (U_u^L)_{i,k}^* \\
&\quad - f_u^{kl*} (U_{\bar{u}})_{X,3+l} (O_N)_{A,4}^* (U_u^L)_{ik}^* ,
\end{aligned} \tag{A.87}$$

$$\begin{aligned}
N_{iAX}^{R(d)} &= \frac{\sqrt{2}}{3} g_Y (U_{\bar{d}})_{X,3+k} (O_N)_{A,1}^* (U_d^R)_{i,k}^* \\
&\quad + f_d^{kl*} (U_{\bar{d}})_{X,k} (O_N)_{A,3}^* (U_d^R)_{il}^* ,
\end{aligned} \tag{A.88}$$

$$\begin{aligned}
N_{iAX}^{L(d)} &= -\frac{1}{\sqrt{2}} g_2 (U_{\bar{d}})_{X,k} (O_N)_{A,2}^* (U_d^L)_{i,k}^* \\
&\quad + \frac{\sqrt{2}}{6} g_Y (U_{\bar{d}})_{X,k} (O_N)_{A,1}^* (U_d^L)_{i,k}^* \\
&\quad + f_d^{kl*} (U_{\bar{d}})_{X,3+l} (O_N)_{A,3}^* (U_d^L)_{ik}^* .
\end{aligned} \tag{A.89}$$

- Chargino-fermion-sfermion

$$\begin{aligned}
\mathcal{L} &= \bar{\chi}_A^- \left(C_{iAX}^{R(e)} P_R + C_{iAX}^{L(e)} P_L \right) e_i \tilde{\nu}_X^* \\
&\quad + \bar{\chi}_A^+ \left(C_{iAX}^{R(\nu)} P_R + C_{iAX}^{L(\nu)} P_L \right) \nu_i \tilde{e}_X^* \\
&\quad + \bar{\chi}_A^- \left(C_{iAX}^{R(d)} P_R + C_{iAX}^{L(d)} P_L \right) d_i \tilde{u}_X^* \\
&\quad + \bar{\chi}_A^+ \left(C_{iAX}^{R(u)} P_R + C_{iAX}^{L(u)} P_L \right) u_i \tilde{d}_X^* + \text{h.c.} ,
\end{aligned} \tag{A.90}$$

where

$$C_{iAX}^{R(e)} = -f_e^{kl*} (U_{\bar{\nu}})_{X,k} (O_L)_{A,2} (U_e^R)_{i,l}^* , \tag{A.91}$$

$$C_{iAX}^{L(e)} = g_2 (U_{\bar{\nu}})_{X,k} (O_R)_{A,1} (U_e^L)_{i,k}^* , \tag{A.92}$$

$$C_{iAX}^{R(\nu)} = 0 , \tag{A.93}$$

$$C_{iAX}^{L(\nu)} = g_2(U_{\bar{e}})_{X,i}(O_L)_{A,1} - f_e^{ik}(U_{\bar{e}})_{X,3+k}(O_L)_{A,2} , \quad (\text{A.94})$$

$$C_{iAX}^{R(d)} = -f_d^{kl*}(U_{\bar{u}})_{X,k}(O_L)_{A,2}(U_d^R)_{i,l}^* , \quad (\text{A.95})$$

$$C_{iAX}^{L(d)} = g_2(U_{\bar{u}})_{X,k}(O_R)_{A,1}(U_d^L)_{i,k}^* + f_u^{kl}(U_{\bar{u}})_{X,3+l}(O_R)_{A,2}(U_d^L)_{i,k}^* , \quad (\text{A.96})$$

$$C_{iAX}^{R(u)} = f_u^{kl*}(U_{\bar{d}})_{X,k}(O_L)_{A,1}(U_u^R)_{i,l}^* , \quad (\text{A.97})$$

$$C_{iAX}^{L(u)} = g_2(U_{\bar{d}})_{X,k}(O_L)_{A,1}(U_u^L)_{i,k}^* - f_d^{kl}(U_{\bar{d}})_{X,3+l}(O_L)_{A,2}(U_u^L)_{i,k}^* , \quad (\text{A.98})$$

- Neutralino-neutralino- Z^0

$$\mathcal{L} = \bar{\chi}_A^0 \gamma^\mu \left(z_{AB}^{L(n)} P_L + z_{AB}^{R(n)} P_R \right) \tilde{\chi}_B^0 Z_\mu^0 , \quad (\text{A.99})$$

where

$$z_{AB}^{L(n)} = \frac{1}{4} \sqrt{g_2^2 + g_Y^2} \left[(O_N)_{A,3}^* (O_N)_{B,3} - (O_N)_{A,4}^* (O_N)_{B,4} \right] , \quad (\text{A.100})$$

$$z_{AB}^{R(n)} = -z_{BA}^{L(n)} \quad (\text{A.101})$$

- Neutralino-chargino-W

$$\mathcal{L} = \bar{\chi}_A^0 \gamma^\mu \left(w_{AB}^{L(\chi)} P_L + w_{AB}^{R(\chi)} P_R \right) \tilde{\chi}_B^- W^+ + \text{h.c.} , \quad (\text{A.102})$$

where

$$w_{AB}^{L(\chi)} = g_2(O_N)_{A,2}^* (O_L)_{B,1}^* + \frac{g_2}{\sqrt{2}} (O_N)_{A,3}^* (O_L)_{B,2}^* , \quad (\text{A.103})$$

$$w_{AB}^{R(\chi)} = g_2(O_N)_{A,2}^* (O_R)_{B,1}^* - \frac{g_2}{\sqrt{2}} (O_N)_{A,3}^* (O_R)_{B,2}^* , \quad (\text{A.104})$$

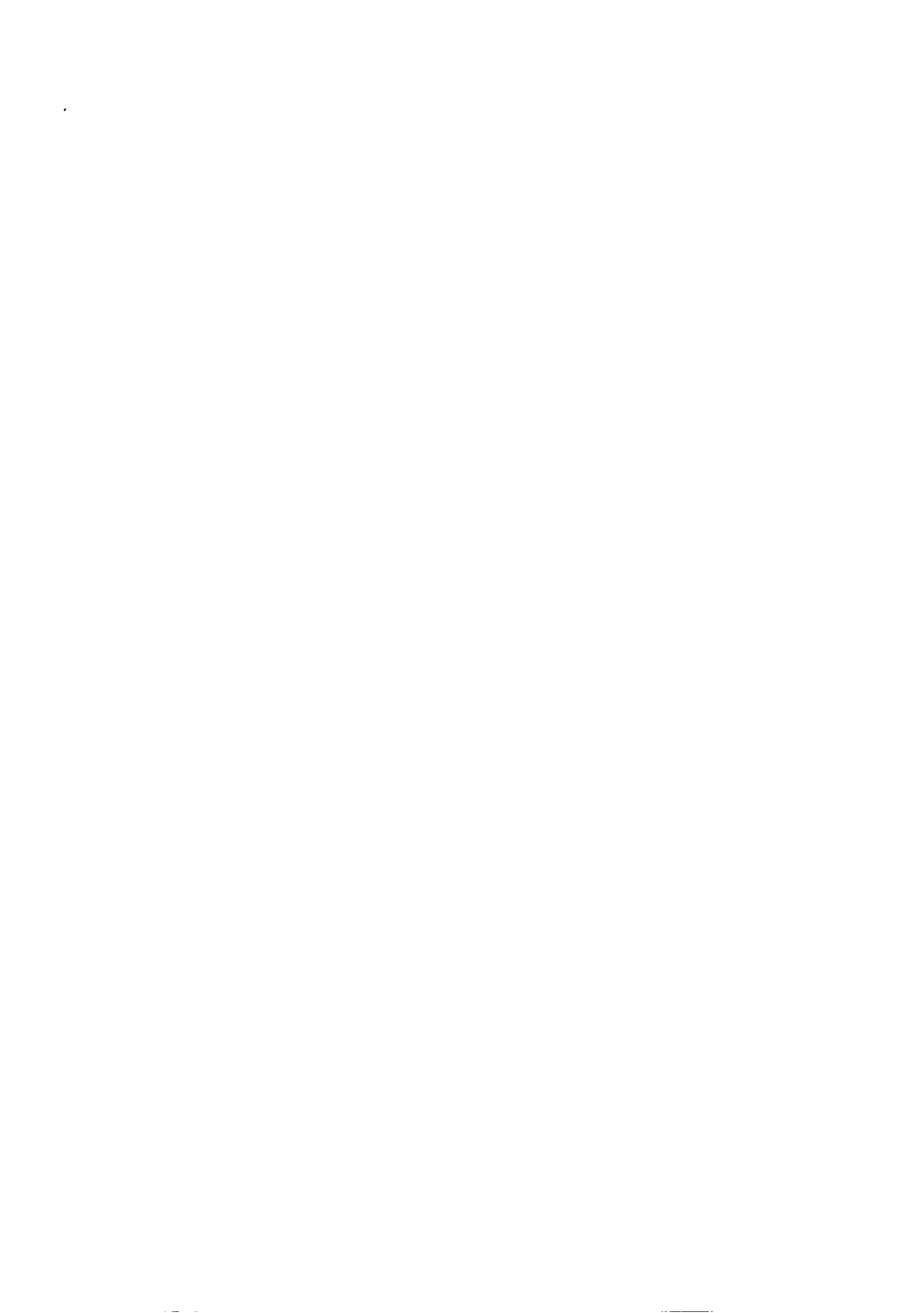
- Chargino-chargino- Z^0

$$\mathcal{L} = \bar{\chi}_A^- \gamma^\mu \left(z_{AB}^{L(c)} P_L + z_{AB}^{R(c)} P_R \right) \tilde{\chi}_B^- Z_\mu^0, \quad (\text{A.105})$$

where

$$\begin{aligned} z_{AB}^{L(c)} &= -\frac{g_2^2}{\sqrt{g_2^2 + g_Y^2}} (O_L)_{A,1} (O_L)_{B,1}^* \\ &\quad + \left(\frac{1}{2} \frac{g_Y^2}{\sqrt{g_2^2 + g_Y^2}} - \frac{1}{2} \frac{g_2^2}{\sqrt{g_2^2 + g_Y^2}} \right) (O_L)_{A,2} (O_L)_{B,2}^*, \end{aligned} \quad (\text{A.106})$$

$$\begin{aligned} z_{AB}^{R(c)} &= -\frac{g_2^2}{\sqrt{g_2^2 + g_Y^2}} (O_R)_{A,1} (O_R)_{B,1}^* \\ &\quad + \left(\frac{1}{2} \frac{g_Y^2}{\sqrt{g_2^2 + g_Y^2}} - \frac{1}{2} \frac{g_2^2}{\sqrt{g_2^2 + g_Y^2}} \right) (O_R)_{A,2} (O_R)_{B,2}^*. \end{aligned} \quad (\text{A.107})$$



Appendix B

The minimal SU(5) SUSY GUT

The superpotential of the minimal SU(5) SUSY GUT is given by

$$\begin{aligned}
 W = & \frac{1}{8} \epsilon_{abcde} (\tilde{y}_u)_{ij} T_i^{ab} T_j^{cd} H^e + (\tilde{y}_d)_{ij} \bar{F}_{ja} T_i^{ab} \bar{H}_b \\
 & + m_H H \bar{H} + \frac{1}{2} m_\Sigma \Sigma_b^a \Sigma_a^b + \frac{1}{3} \lambda_\Sigma \Sigma_b^a \Sigma_c^b \Sigma_a^c + \lambda_H H^a \Sigma_a^b \bar{H}_b ,
 \end{aligned} \tag{B.1}$$

where \bar{F} and T are the matter fields of $\bar{\mathbf{5}}$ and $\mathbf{10}$ representations, respectively, and H , \bar{H} , and Σ are the Higgs fields of $\mathbf{5}$, $\bar{\mathbf{5}}$, and $\mathbf{24}$ representation. In the basis where the matrix \tilde{y}_u is diagonal, the matter fields and the Higgs fields in the MSSM are embedded in the \bar{F} , T , H , and \bar{H} fields as follows:

$$T_i^{\hat{a}\hat{b}} = \epsilon^{\hat{a}\hat{b}\hat{c}} (U_R^u)_{ij} U_{\hat{c},j}^c , \tag{B.2}$$

$$T_i^{\hat{a},\beta+3} = -(U_L^u)^*_{ij} Q_j^{\hat{a},\beta} , \tag{B.3}$$

$$T_i^{\alpha+3,\beta+3} = -\epsilon^{\alpha\beta} (U_L^{u*} U_L^{dT} U_R^e)_{ij} E_j^c , \tag{B.4}$$

$$\bar{F}_{\hat{a},i} = (U_L^{eT} U_R^d)_{ij} D_{\hat{a},j}^c , \tag{B.5}$$

$$\bar{F}_{\alpha+3,i} = -\epsilon_{\alpha\beta} L_i^\beta , \tag{B.6}$$

$$H^{\alpha+3} = H_2^\alpha , \tag{B.7}$$

$$\bar{H}_{\alpha+3} = -\epsilon_{\alpha\beta} H_1^\beta, \quad (\text{B.8})$$

where $\hat{a}, \hat{b}, \hat{c} = 1, 2, 3$, $\alpha, \beta = 1, 2$, and $i, j = 1, 2, 3$ corresponding to $SU(3)_C$, $SU(2)_L$, and the generations, respectively. The remained part of H and \bar{H} is called colored Higgs field:

$$H^{\hat{a}} = H_C^{\hat{a}}, \quad \bar{H}_{\hat{a}} = \bar{H}_{C\hat{a}}. \quad (\text{B.9})$$

In the basis in eq.(A.12), the terms in superpotential (B.1) are decomposed as follows:

$$\begin{aligned} W = & f_u^{ij} H_2 \cdot U_j^c Q_i - f_u^{ij} E_i^c U_j^c H_C - \frac{1}{2} (f_u V_{\text{CKM}})_{ij} Q_i Q_j H_C \\ & + f_d^{ij} H_1 \cdot L_j E_i^c + f_d^{ij} H_1 \cdot Q_i D_j^c \\ & + (V_{\text{CKM}} f_d)_{ij} U_i^c D_j^c \bar{H}_C + f_d^{ij} L_j \cdot Q_i \bar{H}_C + (\text{Higgs sector}). \end{aligned} \quad (\text{B.10})$$

The soft SUSY breaking terms are given as follows:

$$\begin{aligned} \mathcal{L}_{\text{soft}} = & \left(-\frac{1}{8} \tilde{A}_u^{ij} \epsilon_{abcde} \tilde{T}_i^{ab} \tilde{T}_j^{cd} H^e - \tilde{A}_d^{ij} \tilde{F}_{ja} \tilde{T}_i^{ab} \bar{H}_b + \text{h.c.} \right) \\ & - \frac{1}{2} (\tilde{m}_T^2)_{ij} \tilde{T}_i^{ab*} \tilde{T}_j^{ab} - (\tilde{m}_F^2)_{ij} \tilde{F}_{ai}^* \tilde{F}_{aj} - \tilde{m}_H^2 H^{a*} H^a - \tilde{m}_{\bar{H}}^2 \bar{H}_a^* \bar{H}_a \\ & - \frac{1}{2} M_5 \bar{g}^A g^A \\ & - \left(B_H m_H H^a \bar{H}_a + \frac{1}{2} B_\Sigma m_\Sigma \Sigma_b^a \Sigma_a^b + \text{h.c.} \right) \\ & - \left(\frac{1}{3} A_\Sigma \Sigma_b^a \Sigma_c^b \Sigma_a^c + A_H H^a \Sigma_a^b \bar{H}_b + \text{h.c.} \right) \\ & - \tilde{m}_\Sigma^2 \Sigma_b^{a*} \Sigma_b^a. \end{aligned} \quad (\text{B.11})$$

The RGEs for the coupling constants are given as follows:

- gauge coupling constant

$$(4\pi)^2 \frac{d}{dt} g_5 = -3g_5^3. \quad (\text{B.12})$$

- Yukawa coupling constants

$$(4\pi)^2 \frac{d}{dt} (\tilde{y}_u)_{ij} = (\tilde{y}_u)_{ij} \gamma_H^H + (\tilde{y}_u)_{kj} \gamma_{T_k}^{T_i} + (\tilde{y}_u)_{ik} \gamma_{T_k}^{T_j}, \quad (\text{B.13})$$

$$(4\pi)^2 \frac{d}{dt} (\tilde{y}_d)_{ij} = (\tilde{y}_d)_{ij} \gamma_{\tilde{H}}^{\tilde{H}} + (\tilde{y}_d)_{kj} \gamma_{T_k}^{T_i} + (\tilde{y}_d)_{ik} \gamma_{\tilde{F}_k}^{\tilde{F}_j}, \quad (\text{B.14})$$

$$(4\pi)^2 \frac{d}{dt} \lambda_{\Sigma} = 3\lambda_{\Sigma} \gamma_{\Sigma}^{\Sigma}, \quad (\text{B.15})$$

$$(4\pi)^2 \frac{d}{dt} \lambda_H = \lambda_H (\gamma_{\tilde{H}}^{\tilde{H}} + \gamma_H^H + \gamma_{\Sigma}^{\Sigma}), \quad (\text{B.16})$$

where

$$\gamma_H^H = 3(\tilde{y}_u)_{kl}^* (\tilde{y}_u)_{kl} + \frac{12}{5} |\lambda_H|^2 - \frac{24}{5} g_5^2, \quad (\text{B.17})$$

$$\gamma_{T_k}^{T_i} = 3(\tilde{y}_u)_{kl}^* (\tilde{y}_u)_{il} + 2(\tilde{y}_d)_{kl}^* (\tilde{y}_d)_{il} - \frac{36}{5} g_5^2 \delta_{ki}, \quad (\text{B.18})$$

$$\gamma_{\tilde{H}}^{\tilde{H}} = 4(\tilde{y}_d)_{kl}^* (\tilde{y}_d)_{kl} + \frac{12}{5} |\lambda_H|^2 - \frac{24}{5} g_5^2, \quad (\text{B.19})$$

$$\gamma_{\tilde{F}_k}^{\tilde{F}_j} = 4(\tilde{y}_d)_{ik}^* (\tilde{y}_d)_{lj} - \frac{24}{5} g_5^2 \delta_{kj}, \quad (\text{B.20})$$

$$\gamma_{\Sigma}^{\Sigma} = \frac{21}{40} |\lambda_{\Sigma}|^2 + \frac{1}{2} |\lambda_H|^2 - 10g_5^2. \quad (\text{B.21})$$

- mass parameters

$$(4\pi)^2 \frac{d}{dt} m_H = m_H (\gamma_{\tilde{H}}^{\tilde{H}} + \gamma_H^H + \gamma_{\Sigma}^{\Sigma}), \quad (\text{B.22})$$

$$(4\pi)^2 \frac{d}{dt} m_{\Sigma} = 2m_{\Sigma} \gamma_{\Sigma}^{\Sigma}, \quad (\text{B.23})$$

- gaugino mass

$$(4\pi)^2 \frac{d}{dt} M_5 = -6g_5^2 M_5 . \quad (\text{B.24})$$

- A-terms

$$(4\pi)^2 \frac{d}{dt} \tilde{A}_u^{ij} = \tilde{A}_u^{ij} \gamma_H^H + \tilde{A}_u^{kj} \gamma_{T_k}^{T_i} + \tilde{A}_u^{ik} \gamma_{T_k}^{T_j} \\ + 2\tilde{y}_u^{ij} \tilde{\gamma}_H^H + 2\tilde{y}_u^{kj} \tilde{\gamma}_{T_k}^{T_i} + 2\tilde{y}_u^{ik} \tilde{\gamma}_{T_k}^{T_j} , \quad (\text{B.25})$$

$$(4\pi)^2 \frac{d}{dt} \tilde{A}_d^{ij} = \tilde{A}_d^{ij} \gamma_{\bar{H}}^{\bar{H}} + \tilde{A}_d^{kj} \gamma_{T_k}^{T_i} + \tilde{A}_d^{ik} \gamma_{\bar{F}_k}^{\bar{F}_j} \\ + 2\tilde{y}_d^{ij} \tilde{\gamma}_{\bar{H}}^{\bar{H}} + 2\tilde{y}_d^{kj} \tilde{\gamma}_{T_k}^{T_i} + 2\tilde{y}_d^{ik} \tilde{\gamma}_{\bar{F}_k}^{\bar{F}_j} , \quad (\text{B.26})$$

$$(4\pi)^2 \frac{d}{dt} A_\Sigma = 3A_\Sigma \gamma_\Sigma^\Sigma + 6\lambda_\Sigma \tilde{\gamma}_\Sigma^\Sigma , \quad (\text{B.27})$$

$$(4\pi)^2 \frac{d}{dt} A_H = A_H (\gamma_{\bar{H}}^{\bar{H}} + \gamma_H^H + \gamma_\Sigma^\Sigma) + 2\lambda_H (\tilde{\gamma}_{\bar{H}}^{\bar{H}} + \tilde{\gamma}_H^H + \tilde{\gamma}_\Sigma^\Sigma) , \quad (\text{B.28})$$

where

$$\tilde{\gamma}_H^H = 3(\tilde{y}_u)_{kl}^* \tilde{A}_u^{kl} + \frac{12}{5} \lambda_H^* A_H - \frac{24}{5} g_5^2 M_5 , \quad (\text{B.29})$$

$$\tilde{\gamma}_{T_k}^{T_i} = 3(\tilde{y}_u)_{kl}^* \tilde{A}_u^{il} + 2(\tilde{y}_d)_{kl}^* \tilde{A}_d^{il} - \frac{36}{5} g_5^2 \delta_{ki} , \quad (\text{B.30})$$

$$\tilde{\gamma}_{\bar{H}}^{\bar{H}} = 4(\tilde{y}_d)_{kl}^* \tilde{A}_d^{kl} + \frac{12}{5} \lambda_H^* A_H - \frac{24}{5} g_5^2 M_5 , \quad (\text{B.31})$$

$$\tilde{\gamma}_{\bar{F}_k}^{\bar{F}_j} = 4(\tilde{y}_d)_{lk}^* \tilde{A}_d^{lj} - \frac{24}{5} g_5^2 M_5 \delta_{kj} , \quad (\text{B.32})$$

$$\tilde{\gamma}_\Sigma^\Sigma = \frac{21}{40} \lambda_\Sigma^* A_\Sigma + \frac{1}{2} \lambda_H^* A_H - 10g_5^2 M_5 . \quad (\text{B.33})$$

- B-terms

$$(4\pi)^2 \frac{d}{dt} B_H = 2(\tilde{\gamma}_H^H + \tilde{\gamma}_{\bar{H}}^{\bar{H}}) , \quad (\text{B.34})$$

$$(4\pi)^2 \frac{d}{dt} B_\Sigma = 4\tilde{\gamma}_\Sigma^\Sigma . \quad (\text{B.35})$$

- soft mass terms

$$(4\pi)^2 \frac{d}{dt} (\tilde{m}_T^2)_{ij} = (\tilde{m}_T^2)_{kj} \gamma_{T_i}^{T_k} + (\tilde{m}_T^2)_{ik} \gamma_{T_k}^{T_j} + 2\tilde{\gamma}_{T_i}^{T_j} , \quad (\text{B.36})$$

$$(4\pi)^2 \frac{d}{dt} (\tilde{m}_{\bar{F}}^2)_{ij} = (\tilde{m}_{\bar{F}}^2)_{kj} \gamma_{\bar{F}_i}^{\bar{F}_k} + (\tilde{m}_{\bar{F}}^2)_{ik} \gamma_{\bar{F}_k}^{\bar{F}_j} + 2\tilde{\gamma}_{\bar{F}_i}^{\bar{F}_j} , \quad (\text{B.37})$$

$$(4\pi)^2 \frac{d}{dt} \tilde{m}_H^2 = 2\tilde{m}_H^2 \gamma_H^H + 2\tilde{\gamma}_H^H , \quad (\text{B.38})$$

$$(4\pi)^2 \frac{d}{dt} \tilde{m}_{\bar{H}}^2 = 2\tilde{m}_{\bar{H}}^2 \gamma_{\bar{H}}^{\bar{H}} + 2\tilde{\gamma}_{\bar{H}}^{\bar{H}} , \quad (\text{B.39})$$

$$(4\pi)^2 \frac{d}{dt} \tilde{m}_\Sigma^2 = 2\tilde{m}_\Sigma^2 \gamma_\Sigma^\Sigma + 2\tilde{\gamma}_\Sigma^\Sigma , \quad (\text{B.40})$$

where

$$\begin{aligned} \tilde{\gamma}_{T_i}^{T_j} = & 3(\tilde{y}_u)_ik^* (\tilde{y}_u)_{jl} (\tilde{m}_T^2)_{lk} + 3(\tilde{y}_u)_ik^* (\tilde{y}_u)_{jk} \tilde{m}_H^2 \\ & + 2(\tilde{y}_d)_ik^* (\tilde{y}_d)_{jl} (\tilde{m}_{\bar{F}}^2)_{lk} + 2(\tilde{y}_d)_ik^* (\tilde{y}_d)_{jk} \tilde{m}_{\bar{H}}^2 \\ & + 3\tilde{A}_u^{ik*} \tilde{A}_u^{jk} + 2\tilde{A}_d^{ik*} \tilde{A}_d^{jk} \\ & - \frac{72}{5} g_5^2 |M_5|^2 \delta_{ij} + \frac{36}{5} g_5^2 (\tilde{m}_T^2)_{ij} , \end{aligned} \quad (\text{B.41})$$

$$\begin{aligned}
\tilde{\tilde{\gamma}}_{\tilde{F}_i}^{\tilde{F}_j} &= 4(\tilde{y}_d)_{ki}^*(\tilde{y}_d)_{lj}(\tilde{m}_T^2)_{lk} + 4(\tilde{y}_d)_{ki}^*(\tilde{y}_d)_{kj}\tilde{m}_H^2 \\
&\quad + 4\tilde{A}_d^{ki*}\tilde{A}_d^{kj} \\
&\quad - \frac{48}{5}g_5^2|M_5|^2\delta_{ij} + \frac{24}{5}g_5^2(\tilde{m}_F^2)_{ij} ,
\end{aligned} \tag{B.42}$$

$$\begin{aligned}
\tilde{\tilde{\gamma}}_H^H &= 4(\tilde{y}_u)_{ik}^*(\tilde{y}_u)_{il}(\tilde{m}_T^2)_{lk} + 4(\tilde{y}_d)_{ki}^*(\tilde{y}_d)_{li}(\tilde{m}_T^2)_{lk} + \frac{12}{5}|\lambda_H|^2(\tilde{m}_H^2 + \tilde{m}_\Sigma^2) \\
&\quad + 3\tilde{A}_u^{kl*}\tilde{A}_u^{kl} + \frac{12}{5}|A_H|^2 \\
&\quad - \frac{48}{5}g_5^2|M_5|^2 + \frac{24}{5}g_5^2\tilde{m}_H^2 ,
\end{aligned} \tag{B.43}$$

$$\begin{aligned}
\tilde{\tilde{\gamma}}_H^{\tilde{H}} &= 4(\tilde{y}_d)_{ik}^*(\tilde{y}_d)_{il}(\tilde{m}_F^2)_{lk} + 4(\tilde{y}_d)_{ki}^*(\tilde{y}_d)_{li}(\tilde{m}_T^2)_{lk} + \frac{12}{5}|\lambda_H|^2(\tilde{m}_H^2 + \tilde{m}_\Sigma^2) \\
&\quad + 4\tilde{A}_d^{kl*}\tilde{A}_d^{kl} + \frac{12}{5}|A_H|^2 \\
&\quad - \frac{48}{5}g_5^2|M_5|^2 + \frac{24}{5}g_5^2\tilde{m}_H^2 ,
\end{aligned} \tag{B.44}$$

$$\begin{aligned}
\tilde{\tilde{\gamma}}_\Sigma^\Sigma &= \frac{42}{40}|\lambda_\Sigma|^2\tilde{m}_\Sigma^2 + \frac{1}{2}|\lambda_H|^2(\tilde{m}_H^2 + \tilde{m}_H^2) + \frac{21}{40}|A_\Sigma|^2 + \frac{1}{2}|A_H|^2 \\
&\quad - 20g_5^2|M_5|^2 + 10g_5^2\tilde{m}_\Sigma^2 .
\end{aligned} \tag{B.45}$$

Appendix C

The derivation of the general formulae for the spin correlation

In this appendix, we derive the eq.(4.1) from the amplitude in eq.(4.8).

By using the completeness relation of the fermion spinors, the amplitude squared is deformed to

$$\begin{aligned}
& \left| \bar{A}(\not{p}_A + m_\tau) \gamma^\mu (\not{p}_B - m_\tau) B \right|^2 \\
&= \left| \sum_{\lambda_1=\pm} \sum_{\lambda_2=\pm} \bar{A} u(\mathbf{p}_A, \lambda_1) \bar{u}(\mathbf{p}_A, \lambda_1) \gamma^\mu v(\mathbf{p}_B, \lambda_2) \bar{v}(\mathbf{p}_B, \lambda_2) B \right|^2 \\
&= \sum_{\lambda_1=\pm} \sum_{\lambda_2=\pm} \sum_{\lambda'_1=\pm} \sum_{\lambda'_2=\pm} (\bar{A} u(\mathbf{p}_A, \lambda_1) \bar{u}(\mathbf{p}_A, \lambda'_1) A) \\
&\quad \times (\bar{u}(\mathbf{p}_A, \lambda_1) \gamma^\mu v(\mathbf{p}_B, \lambda_2) \bar{v}(\mathbf{p}_B, \lambda'_2) \gamma^\nu u(\mathbf{p}_A, \lambda'_1)) (\bar{B} v(\mathbf{p}_B, \lambda'_2) \bar{v}(\mathbf{p}_B, \lambda_2) B) , \quad (C.1)
\end{aligned}$$

where λ 's are the spin eigenvalues. The spin summation can be performed by using the Bouchiat-Michel formulae as follows [60, 71]:

$$\begin{aligned}
& \left| \bar{A}(\not{p}_A + m_\tau) \gamma^\mu (\not{p}_B - m_\tau) B \right|^2 \\
&= \alpha^{D-} \text{Tr} [(\not{p}_A + m_\tau) \gamma^\mu (\not{p}_B - m_\tau) \gamma^\nu] \alpha^{D+} \\
&\quad + \alpha^{D-} \text{Tr} [(\not{p}_A + m_\tau) \gamma^\mu \gamma_5 \not{\beta}_B (\not{p}_B - m_\tau) \gamma^\nu] \rho_b^{D+} \\
&\quad + \rho_a^{D-} \text{Tr} [\gamma_5 \not{\beta}_A (\not{p}_A + m_\tau) \gamma^\mu (\not{p}_B - m_\tau) \gamma^\nu] \alpha^{D+} \\
&\quad + \rho_a^{D-} \text{Tr} [\gamma_5 \not{\beta}_A (\not{p}_A + m_\tau) \gamma^\mu \gamma_5 \not{\beta}_B (\not{p}_B - m_\tau) \gamma^\nu] \rho_b^{D+} , \quad (C.2)
\end{aligned}$$

where

$$\alpha^{D-} = \frac{1}{2} \{ \bar{A} (\not{p}_A + m_\tau) A \} , \quad \alpha^{D+} = \frac{1}{2} \{ \bar{B} (\not{p}_B - m_\tau) B \} , \quad (\text{C.3})$$

$$\rho_a^{D-} = \frac{1}{2} \{ \bar{A} \gamma_5 \beta_A^a (\not{p}_A + m_\tau) A \} , \quad \rho_b^{D+} = \frac{1}{2} \{ \bar{B} \gamma_5 \beta_B^b (\not{p}_B - m_\tau) B \} , \quad (\text{C.4})$$

where $(s_A^a)^\mu$ and $(s_B^b)^\nu$ are four vectors which satisfy the following equations:

$$p_A \cdot s_A^a = p_B \cdot s_B^b = 0, \quad (\text{C.5})$$

$$s_A^a \cdot s_A^b = s_B^a \cdot s_B^b = -\delta^{ab} , \quad (\text{C.6})$$

$$\sum_{a=1}^3 (s_A^a)_\mu (s_A^a)_\nu = -g_{\mu\nu} + \frac{p_{A\mu} p_{A\nu}}{m_\tau^2} , \quad \sum_{b=1}^3 (s_B^b)_\mu (s_B^b)_\nu = -g_{\mu\nu} + \frac{p_{B\mu} p_{B\nu}}{m_\tau^2} . \quad (\text{C.7})$$

The second and third terms in eq.(C.2) vanish because the production parts are anti-symmetric on μ and ν indices while the square of the electromagnetic current from e^+e^- collision is symmetric on μ and ν indices. Explicit calculation gives

$$\text{Tr} [(\not{p}_A + m_\tau) \gamma^\mu \gamma_5 \beta_B^b (\not{p}_B - m_\tau) \gamma^\nu] = 4i m_\tau \epsilon^{\mu\nu\rho\sigma} p_{B\rho} (s_B^b)_\sigma + 4i m_\tau \epsilon^{\mu\nu\rho\sigma} p_{A\rho} (s_B^b)_\sigma \quad (\text{C.8})$$

$$\text{Tr} [\gamma_5 \beta_A^a (\not{p}_A + m_\tau) \gamma^\mu (\not{p}_B - m_\tau) \gamma^\nu] = 4i m_\tau \epsilon^{\mu\nu\rho\sigma} p_{B\rho} (s_A^a)_\sigma + 4i m_\tau \epsilon^{\mu\nu\rho\sigma} p_{A\rho} (s_A^a)_\sigma . \quad (\text{C.9})$$

$$\begin{aligned} \sum_{\text{spin}} |\bar{v}_{e^+} \gamma_\mu u_{e^-}|^2 &= \text{Tr} [\not{p}_{e^+} \gamma_\mu \not{p}_{e^-} \gamma_\nu] \\ &= 4p_{e^+\mu} p_{e^-\nu} + 4p_{e^+\nu} p_{e^-\mu} - 4g_{\mu\nu} p_{e^+} \cdot p_{e^-} . \end{aligned} \quad (\text{C.10})$$

Using the narrow width approximation,

$$\left| \frac{1}{q^2 - (m - \frac{i\Gamma}{2})^2} \right|^2 \simeq \frac{\pi}{m\Gamma} \delta(q^2 - m^2) , \quad (\text{C.11})$$

the first and last terms in eq.(C.2) give formula (4.1) after the phase space integral.

Appendix D

The kinematical functions in LFV τ decays

In this appendix, we list the kinematical functions used in the formulae of branching ratios in Chapter 4.

The functions α_{1-5} , β_{1-2} , and γ_{1-4} in the $\tau^+ \rightarrow \mu^+\mu^+\mu^-$ and $\tau^+ \rightarrow \mu^-e^+e^+$ decay calculations are given as follows. These functions are the same as those used in $\mu^+ \rightarrow e^+e^+e^-$ decay [49]. x_1 and x_2 are given by $x_1 = 2E_1/m_\tau$ and $x_2 = 2E_2/m_\tau$.

$$\alpha_1(x_1, x_2) = 8(2 - x_1 - x_2)(x_1 + x_2 - 1) , \quad (\text{D.1})$$

$$\alpha_2(x_1, x_2) = 2 \{ x_1(1 - x_1) + x_2(1 - x_2) \} , \quad (\text{D.2})$$

$$\alpha_3(x_1, x_2) = 8 \left\{ \frac{2x_2^2 - 2x_2 + 1}{1 - x_1} + \frac{2x_1^2 - 2x_1 + 1}{1 - x_2} \right\} , \quad (\text{D.3})$$

$$\alpha_4(x_1, x_2) = 32(x_1 + x_2 - 1) , \quad (\text{D.4})$$

$$\alpha_5(x_1, x_2) = 8(2 - x_1 - x_2) , \quad (\text{D.5})$$

$$\beta_1(x_1, x_2) = \frac{2(x_1 + x_2)(x_1^2 + x_2^2) - 6(x_1 + x_2)^2 + 12(x_1 + x_2) - 8}{2 - x_1 - x_2} \quad (\text{D.6})$$

$$\beta_2(x_1, x_2) = \frac{8}{(1-x_1)(1-x_2)(2-x_1-x_2)} \times \left\{ \begin{aligned} &2(x_1+x_2)(x_1^3+x_2^3) - 4(x_1+x_2)(2x_1^2+x_1x_2+2x_2^2) \\ &+(19x_1^2+30x_1x_2+19x_2^2) - 12(2x_1+2x_2-1) \end{aligned} \right\}, \quad (\text{D.7})$$

$$\gamma_1(x_1, x_2) = \frac{4\sqrt{(1-x_1)(1-x_2)(x_1+x_2-1)}(x_2-x_1)}{2-x_1-x_2}, \quad (\text{D.8})$$

$$\gamma_2(x_1, x_2) = 32\sqrt{\frac{x_1+x_2-1}{(1-x_1)(1-x_2)}} \frac{(x_1+x_2-1)(x_2-x_1)}{2-x_1-x_2}, \quad (\text{D.9})$$

$$\gamma_3(x_1, x_2) = 16\sqrt{\frac{x_1+x_2-1}{(1-x_1)(1-x_2)}} (x_1+x_2-1)(x_2-x_1), \quad (\text{D.10})$$

$$\gamma_4(x_1, x_2) = 8\sqrt{\frac{x_1+x_2-1}{(1-x_1)(1-x_2)}} (2-x_1-x_2)(x_2-x_1). \quad (\text{D.11})$$

The functions A_{1-7} , B_{1-4} , and C_{1-6} in the $\tau^+ \rightarrow \mu^+ e^+ e^-$ decay calculation are given by

$$A_1(x_1, x_2) = \frac{8(2-x_1-4x_2+2x_1x_2+2x_2^2)}{1-x_1}, \quad (\text{D.12})$$

$$A_2(x_1, x_2) = -8(x_1+x_2-1), \quad (\text{D.13})$$

$$A_3(x_2) = -8(1-x_2), \quad (\text{D.14})$$

$$A_4(x_1) = \frac{x_1(1-x_1)}{2}, \quad (\text{D.15})$$

$$A_5(x_1, x_2) = 2(2-x_1-x_2)(x_1+x_2-1), \quad (\text{D.16})$$

$$A_6(x_2) = 2x_2(1-x_2) , \quad (\text{D.17})$$

$$A_7(x_1, x_2) = -8(4 - 5x_1 + x_1^2 - 8x_2 + 4x_1x_2 + 4x_2^2) , \quad (\text{D.18})$$

$$A_8(x_1, x_2) = -4(1-x_1)(x_1 + 2x_2 - 2) , \quad (\text{D.19})$$

$$B_1(x_1, x_2) = \frac{-8}{(1-x_1)(2-x_1-x_2)} \times (-6 + 8x_1 - 3x_1^2 + 12x_2 - 11x_1x_2 + 2x_1^2x_2 - 8x_2^2 + 4x_1x_2^2 + 2x_2^3) , \quad (\text{D.20})$$

$$B_2(x_1, x_2) = \frac{-(1-x_1)(2-2x_1+x_1^2-2x_2+x_1x_2)}{2(2-x_1-x_2)} , \quad (\text{D.21})$$

$$B_3(x_1, x_2) = \frac{2(1-x_2)(2-2x_1-2x_2+x_1x_2+x_2^2)}{2-x_1-x_2} , \quad (\text{D.22})$$

$$B_4(x_1, x_2) = \frac{8}{2-x_1-x_2} \times \left(-10 + 16x_1 - 7x_1^2 + x_1^3 + 22x_2 - 23x_1x_2 + 5x_1^2x_2 - 16x_2^2 + 8x_1x_2^2 + 4x_2^3 \right) , \quad (\text{D.23})$$

$$B_5(x_1, x_2) = \frac{4(1-x_1)(2-4x_1+x_1^2-4x_2+3x_1x_2+2x_2^2)}{2-x_1-x_2} , \quad (\text{D.24})$$

$$C_1(x_1, x_2) = \frac{-16(x_1+x_2-1)\sqrt{(1-x_1)(1-x_2)(x_1+x_2-1)}}{(1-x_1)(2-x_1-x_2)} , \quad (\text{D.25})$$

$$C_2(x_1, x_2) = \frac{8(x_1+x_2-1)\sqrt{(1-x_1)(1-x_2)(x_1+x_2-1)}}{1-x_1} , \quad (\text{D.26})$$

$$C_3(x_1, x_2) = \frac{-8(1-x_2)\sqrt{(1-x_1)(1-x_2)(x_1+x_2-1)}}{1-x_1} , \quad (\text{D.27})$$

$$C_4(x_1, x_2) = \frac{(1-x_1) \sqrt{(1-x_1)(1-x_2)(x_1+x_2-1)}}{2-x_1-x_2}, \quad (\text{D.28})$$

$$C_5(x_1, x_2) = \frac{4(1-x_2) \sqrt{(1-x_1)(1-x_2)(x_1+x_2-1)}}{2-x_1-x_2}, \quad (\text{D.29})$$

$$C_6(x_1, x_2) = \frac{-16 \sqrt{(1-x_1)(1-x_2)(x_1+x_2-1)} (3-x_1-2x_2)}{2-x_1-x_2}, \quad (\text{D.30})$$

$$C_7(x_1, x_2) = 8 \sqrt{(1-x_1)(1-x_2)(x_1+x_2-1)}. \quad (\text{D.31})$$

Finally, the functions F , G , and H in the $\tau \rightarrow \mu\nu\bar{\nu}\gamma$ decay calculation are given by

$$F = F^{(0)} + rF^{(1)} + r^2F^{(2)}, \quad (\text{D.32})$$

$$G = G^{(0)} + rG^{(1)} + r^2G^{(2)}, \quad (\text{D.33})$$

$$H = H^{(0)} + rH^{(1)} + r^2H^{(2)}, \quad (\text{D.34})$$

where $F^{(0)-(2)}$, $G^{(0)-(2)}$, and $H^{(0)-(2)}$ are the functions of $x(\equiv 2E_\mu/m_\tau)$, $y(\equiv 2E_\gamma/m_\tau)$, $d(\equiv 1 + \beta_\mu \cos z)$ with $\beta_\mu = \sqrt{1 - 4r/x^2}$ ($r \equiv m_\mu^2/m_\tau^2$) and $z = \pi - \theta_{\mu\gamma}$. These functions are given by

$$\begin{aligned} F^{(0)}(x, y, d) = & \frac{-8(-3+2x+2y)(2x^2+2xy+y^2)}{d} \\ & + 8x \{x^2(2+4y) + y(-3+y+y^2) + x(-3+y+4y^2)\} \\ & - 2x^2y \{-6+y(5+2y) + 2x(4+3y)\} d \\ & + 2x^3y^2(2+y)d^2, \end{aligned} \quad (\text{D.35})$$

$$\begin{aligned} F^{(1)}(x, y, d) = & \frac{32(x+y)(-3+2x+2y)}{xd^2} + \frac{8\{6x^2+(6-5y)y-2x(4+y)\}}{d} \\ & - 8x\{-4-(-3+y)y+3x(1+y)\} + 6x^2y(2+y)d, \end{aligned} \quad (\text{D.36})$$

$$F^{(2)}(x, y, d) = \frac{-32(-4+3x+3y)}{xd^2} + \frac{48y}{d}, \quad (\text{D.37})$$

$$G^{(0)}(x, y, d) = \frac{-8x \{4x^2 + y(-1 + 2y) + x(-2 + 6y)\}}{d} + 4x^2 \{-2 + 3y + 4y^2 + x(4 + 6y)\} - 4x^3 y(2 + y)d, \quad (\text{D.38})$$

$$G^{(1)}(x, y, d) = \frac{32(-1 + 2x + 2y)}{d^2} + \frac{8x(6x - y)}{d} - 12x^2(2 + y), \quad (\text{D.39})$$

$$G^{(2)}(x, y, d) = \frac{-96}{d^2}, \quad (\text{D.40})$$

$$H^{(0)}(x, y, d) = \frac{-8y(x + y)(-1 + 2x + 2y)}{d} + 4xy \{2x^2 + 2y(1 + y) + x(-1 + 4y)\} - 2x^2 y^2(-1 + 4x + 2y)d + 2x^3 y^3 d^2, \quad (\text{D.41})$$

$$H^{(1)}(x, y, d) = \frac{32y(-1 + 2x + 2y)}{x d^2} - \frac{8y(-2 + x + 5y)}{d} - 4x(3x - 2y)y + 6x^2 y^2 d, \quad (\text{D.42})$$

$$H^{(2)}(x, y, d) = \frac{-96y}{x d^2} + \frac{48y}{d}. \quad (\text{D.43})$$

Bibliography

- [1] T. Kinoshita and W. B. Lindquist, Phys. Rev. Lett. **47**, 1573 (1981).
- [2] D. E. Groom *et al.* [Particle Data Group Collaboration], Eur. Phys. J. C **15**, 1 (2000).
- [3] S. L. Glashow, Nucl. Phys. **22**, 579 (1961);
S. Weinberg, Phys. Rev. Lett. **19**, 1264 (1967);
A. Salam, p. 367 of *Elementary Particle Theory*, ed. N. Svartholm (Almqvist and Wiksells, Stockholm, 1969).
- [4] The LEP Collaborations: ALEPH, DELPHI, L3, OPAL, LEP Electroweak Working Group, and the SLD Heavy Flavour and Electroweak Groups, CERN-EP-2000-016 annual report (15th February 2000).
- [5] B. Aubert *et al.* [BABAR Collaboration], Phys. Rev. Lett. **87**, 091801 (2001);
K. Abe *et al.* [Belle Collaboration], Phys. Rev. Lett. **87**, 091802 (2001).
- [6] N. Cabibbo, Phys. Rev. Lett. **10**, 531 (1963).
- [7] M. Kobayashi and T. Maskawa, Prog. Theor. Phys. **49**, 652 (1973).
- [8] For review, see H. P. Nilles, Phys. Rept. **110**, 1 (1984).
- [9] U. Amaldi, W. de Boer and H. Furstenau, Phys. Lett. B **260**, 447 (1991);
J. R. Ellis, S. Kelley and D. V. Nanopoulos, Phys. Lett. B **260**, 131 (1991);
P. Langacker and M. Luo, Phys. Rev. D **44**, 817 (1991).

- [10] H. Georgi and S. L. Glashow, *Phys. Rev. Lett.* **32**, 438 (1974).
- [11] N. Arkani-Hamed, S. Dimopoulos and G. Dvali, *Phys. Lett.* **B429**, 263 (1998);
I. Antoniadis, N. Arkani-Hamed, S. Dimopoulos and G. Dvali, *Phys. Lett.* **B436**, 257 (1998).
- [12] L. Randall and R. Sundrum, *Phys. Rev. Lett.* **83**, 3370 (1999).
- [13] V. A. Rubakov and M. E. Shaposhnikov, *Phys. Lett. B* **125**, 139 (1983);
N. Arkani-Hamed, S. Dimopoulos, N. Kaloper and R. Sundrum, *Phys. Lett. B* **480**, 193 (2000);
S. Kachru, M. Schulz and E. Silverstein, *Phys. Rev. D* **62**, 045021 (2000);
S. Hayakawa, T. Hirayama and R. Kitano, arXiv:hep-th/0108109.
- [14] N. Arkani-Hamed, S. Dimopoulos, G. Dvali and J. March-Russell, hep-ph/9811448.
- [15] Y. Grossman and M. Neubert, *Phys. Lett.* **B474**, 361 (2000).
- [16] For a textbook, see J. Polchinski, *String Theory*, (Cambridge University Press).
- [17] S. M. Bilenkii, S. T. Petcov and B. Pontecorvo, *Phys. Lett. B* **67**, 309 (1977);
S. T. Petcov, *Yad. Fiz.* **25**, 641 [*Sov. J. Nucl. Phys.* **25**, 340 (1977)].
- [18] T. P. Cheng and L. F. Li, *Phys. Rev. Lett.* **45**, 1908 (1980).
- [19] A. H. Chamseddine, R. Arnowitt and P. Nath, *Phys. Rev. Lett.* **49**, 970 (1982);
R. Barbieri, S. Ferrara and C. A. Savoy, *Phys. Lett.* **B119**, 343 (1982);
L. Hall, J. Lykken and S. Weinberg, *Phys. Rev.* **D27**, 2359 (1983).
- [20] L. J. Hall, V. A. Kostelecky and S. Raby, *Nucl. Phys.* **B267**, 415 (1986).
- [21] R. Barbieri and L. J. Hall, *Phys. Lett.* **B338**, 212 (1994);
N. Arkani-Hamed, H. Cheng and L. J. Hall, *Phys. Rev.* **D53**, 413 (1996).
- [22] R. Barbieri, L. Hall and A. Strumia, *Nucl. Phys.* **B445**, 219 (1995).

- [23] J. Hisano, T. Moroi, K. Tobe and M. Yamaguchi, Phys. Lett. **B391**, 341 (1997).
- [24] F. Borzumati and A. Masiero, Phys. Rev. Lett. **57**, 961 (1986);
J. Hisano, T. Moroi, K. Tobe, M. Yamaguchi and T. Yanagida, Phys. Lett. **B357**, 579 (1995);
J. Hisano, D. Nomura and T. Yanagida, Phys. Lett. **B437**, 351 (1998);
J. Hisano and D. Nomura, Phys. Rev. **D59**, 116005 (1999);
W. Buchmuller, D. Delepine and F. Vissani, Phys. Lett. **B459**, 171 (1999);
J. Ellis, M. E. Gomez, G. K. Leontaris, S. Lola and D. V. Nanopoulos, Eur. Phys. J. **C14**, 319 (2000);
W. Buchmuller, D. Delepine and L. T. Handoko, Nucl. Phys. **B576**, 445 (2000);
J. Sato, K. Tobe and T. Yanagida, Phys. Lett. B **498**, 189 (2001);
J. Sato and K. Tobe, Phys. Rev. D **63**, 116010 (2001).
- [25] J. Hisano, T. Moroi, K. Tobe and M. Yamaguchi, Phys. Rev. **D53**, 2442 (1996).
- [26] R. Kitano and K. Yamamoto, Phys. Rev. **D62**, 073007 (2000).
- [27] A. E. Faraggi and M. Pospelov, Phys. Lett. **B458**, 237 (1999).
- [28] R. Kitano, Phys. Lett. **B481**, 39 (2000).
- [29] M. L. Brooks *et al.* [MEGA Collaboration], Phys. Rev. Lett. **83**, 1521 (1999).
- [30] L. M. Barkov *et al.* research proposal to PSI.
- [31] M. Furusaka *et al.* [Joint Project team of JAERI and KEK Collaboration], KEK-REPORT-99-4.
- [32] P. Wintz, in Proceedings of the First International Symposium on Lepton and Baryon Number Violation, edited by H. V. Klapdor-Kleingrothaus and I. V. Krivosheina (Institute of Physics, Bristol/Philadelphia), p. 534 (1998).

- [33] M. Bachman *et al.* [MECO Collaboration], experimental proposal E940 to Brookhaven National Laboratory AGS (1997).
- [34] S. Ahmed *et al.* [CLEO Collaboration], Phys. Rev. **D 61**, 071101 (2000).
- [35] K. Abe *et al.* [Belle Collaboration], BELLE-CONF-0118.
- [36] R. Kitano and Y. Okada, Phys. Rev. D **63**, 113003 (2001).
- [37] Y. Tsai, Phys. Rev. **D4**, 2821 (1971);
S. Kawasaki, T. Shirafuji, and S. Y. Tsai, Prog. Theor. Phys. **49**, 1656 (1973);
S. Pi and A. I. Sanda, Phys. Rev. Lett. **36**, 1 (1976);
K. Fujikawa and N. Kawamoto, Phys. Rev. **D14**, 59 (1976);
A. Pais and S. B. Treiman, Phys. Rev. **D14**, 293 (1976);
T. Hagiwara, S. Pi and A. I. Sanda, Annals Phys. **106**, 134 (1977);
S. Pi and A. I. Sanda, Annals Phys. **106**, 171 (1977).
- [38] H. Kuhn and F. Wagner, Nucl. Phys. **B236**, 16 (1984);
C. A. Nelson, Phys. Rev. **D40**, 123 (1989); Phys. Rev. **D41**, 2805 (1990); Phys. Rev. **D53**, 5001 (1996);
W. Fetscher, Phys. Rev. **D42**, 1544 (1990);
W. Bernreuther, G. W. Botz, O. Nachtmann and P. Overmann, Z. Phys. **C52**, 567 (1991);
J. Bernabeu, N. Rius and A. Pich, Phys. Lett. **B257**, 219 (1991);
S. Goozovat and C. A. Nelson, Phys. Rev. **D44**, 2818 (1991);
G. Couture, Phys. Lett. **B272**, 404 (1991); Phys. Lett. **B305**, 306 (1993);
B. K. Bullock, K. Hagiwara and A. D. Martin, Phys. Lett. **B273**, 501 (1991);
R. Alemany, N. Rius, J. Bernabeu, J. J. Gomez-Cadenas and A. Pich, Nucl. Phys. **B379**, 3 (1992);
A. Aeppli and A. Soni, Phys. Rev. **D46**, 315 (1992);
P. Privitera, Phys. Lett. **B288**, 227 (1992);

- W. Bernreuther, O. Nachtmann and P. Overmann, Phys. Rev. **D48**, 78 (1993);
B. Ananthanarayan and S. D. Rindani, Phys. Rev. Lett. **73**, 1215 (1994); Phys. Rev. **D51**, 5996 (1995);
J. Bernabeu, G. A. Gonzalez-Sprinberg and J. Vidal, Phys. Lett. **B326**, 168 (1994);
C. A. Nelson, H. S. Friedman, S. Goozovat, J. A. Klein, L. R. Kneller, W. J. Perry and S. A. Ustin, Phys. Rev. **D50**, 4544 (1994);
Y. S. Tsai, Phys. Rev. **D51**, 3172 (1995);
J. Bernabeu, G. A. Gonzalez-Sprinberg, M. Tung and J. Vidal, Nucl. Phys. **B436**, 474 (1995).
- [39] R. Kitano, M. Koike, and Y. Okada, in preparation.
- [40] Y. Fukuda *et al.* [Super-Kamiokande Collaboration], Phys. Rev. Lett. **81**, 1562 (1998);
E. Kearns, a talk given in International Conference on High Energy Physics, Osaka, Japan, (2000).
- [41] T. Yanagida, in *Proceedings of the Workshop on Unified Theory and Baryon Number of the Universe*, edited by O. Sawada and A. Sugamoto (KEK, 1979) p.95;
M. Gell-Mann, P. Ramond, and R. Slansky, in *Supergravity*, edited by P. van Nieuwenhuizen and D. Freedman (North Holland, Amsterdam, 1979).
- [42] R. Barate *et al.* [ALEPH Collaboration], Phys. Lett. B **495**, 1 (2000);
M. Acciarri *et al.* [L3 Collaboration], Phys. Lett. B **495**, 18 (2000);
P. Abreu *et al.* [DELPHI Collaboration], Phys. Lett. B **499**, 23 (2001);
G. Abbiendi *et al.* [OPAL Collaboration], Phys. Lett. B **499**, 38 (2001).
- [43] Z. Maki, M. Nakagawa and S. Sakata, Prog. Theor. Phys. **28**, 870 (1962).
- [44] L. Wolfenstein, Phys. Rev. **D17**, 2369 (1978);
S.P. Mikheev and A.Y. Smirnov, Sov. J. Nucl. Phys. **42**, 913 (1985); Nuovo Cim. **9C**, 17 (1986).

- [45] M. Apollonio *et al.*, Phys. Lett. **B466**, 415 (1999).
- [46] S. Chang, J. Hisano, H. Nakano, N. Okada and M. Yamaguchi, Phys. Rev. D **62**, 084025 (2000).
- [47] H. Davoudiasl, J. L. Hewett and T. G. Rizzo, Phys. Lett. B **473**, 43 (2000).
- [48] A. Pomarol, Phys. Lett. B **486**, 153 (2000).
- [49] Y. Okada, K. Okumura and Y. Shimizu, Phys. Rev. **D61**, 094001 (2000).
- [50] S. Weinberg and G. Feinberg, Phys. Rev. Lett. **3** 111 (1959).
- [51] O. Shanker, Phys. Rev. D **20**, 1608 (1979).
- [52] A. Czarnecki, W. J. Marciano and K. Melnikov, arXiv:hep-ph/9801218.
- [53] T. S. Kosmas, arXiv:nucl-th/0108045.
- [54] K. Agashe and M. Graesser, Phys. Rev. D **61**, 075008 (2000).
- [55] I. Hinchliffe and F. E. Paige, Phys. Rev. D **63**, 115006 (2001).
- [56] J. Hisano, R. Kitano and M. M. Nojiri, in preparation.
- [57] T. Cheng and L. Li, Phys. Rev. **D16**, 1425 (1977);
T. P. Cheng and L. Li, Phys. Rev. Lett. **38**, 381 (1977);
J. D. Bjorken, K. Lane and S. Weinberg, Phys. Rev. **D16**, 1474 (1977);
B. W. Lee, S. Pakvasa, R. E. Shrock and H. Sugawara, Phys. Rev. Lett. **38**, 937 (1977);
B. W. Lee and R. E. Shrock, Phys. Rev. **D16**, 1444 (1977);
G. Altarelli, L. Baulieu, N. Cabibbo, L. Maiani and R. Petronzio, Nucl. Phys. **B125**, 285 (1977);
P. Langacker and D. London, Phys. Rev. **D38**, 886 (1988);

- P. Langacker and D. London, Phys. Rev. **D38**, 907 (1988);
A. Ilakovac, Nucl. Phys. Proc. Suppl. **76**, 193 (1999).
- [58] S. L. Glashow, J. Iliopoulos and L. Maiani, Phys. Rev. D **2**, 1285 (1970).
- [59] K. W. Edwards *et al.* [CLEO Collaboration], Phys. Rev. **D55**, 3919 (1997).
- [60] C. Bouchiat and L. Michel, Nucl. Phys. **5**, 416 (1958);
L. Michel, Suppl. Nuovo Cim. **14**, 95 (1959).
- [61] B. K. Bullock, K. Hagiwara and A. D. Martin, Nucl. Phys. **B395**, 499 (1993).
- [62] Y. Kuno and Y. Okada, Phys. Rev. Lett. **77**, 434 (1996).
- [63] Y. Kuno and Y. Okada, Rev. Mod. Phys. **73**, 151 (2001).
- [64] D. Atwood and A. Soni, Phys. Rev. **D 45**, 2405 (1992).
- [65] M. E. Rose, *Relativistic Electron Theory* (John Wiley, New York, 1961).
- [66] T. S. Kosmas, S. Kovalenko and I. Schmidt, Phys. Lett. B **511**, 203 (2001).
- [67] H. De Vries, C. W. De Jager, and C. De Vries, Atomic Data and Nuclear Data Tables **36**, 495 (1987).
- [68] C. Garcia-Recio, J. Nieves, and E. Oset, Nucl. Phys. **A547**, 473 (1992).
- [69] T. Suzuki, D. F. Measday and J. P. Roalsvig, Phys. Rev. C **35** (1987) 2212.
- [70] A. Faessler, T. S. Kosmas, S. Kovalenko and J. D. Vergados, Nucl. Phys. B **587**, 25 (2000);
A. de Gouvea, S. Lola and K. Tobe, Phys. Rev. D **63**, 035004 (2001).
- [71] For a review of spin formalism, see for instance,
H. E. Haber, hep-ph/9405376.